HRC-70-1

AD

A STUDY OF THE MECHANISM OF CHEMICAL REACTIVITY OF NITROGEN TETROXIDE WITH TITANIUM ALLOY

Contract No. NAS 8-30519
Control No. DCN 1-8-54-10278
The George C. Marshall Space Flight Center
National Aeronautics and Space Administration

FINAL REPORT
January 24, 1969 through March 31, 1970

HERCULES RESEARCH CENTER
HERCULES INCORPORATED
WILMINGTON, DELAWARE

A STUDY OF THE MECHANISM OF CHEMICAL REACTIVITY OF NITROGEN TETROXIDE WITH TITANIUM ALLOY

FINAL REPORT
January 24, 1969 through March 31, 1970

Sponsored by
The George C. Marshall Space Flight Center
National Aeronautics and Space Administration
Contract No. NAS 8-30519
Control No. DCN 1-8-54-10278

Prepared by:

A. Z. Conner, Project Leader
J. F. G. Clarke, Jr.
J. A. Gailey
A. A. Orr
W. D. Stone

June 15, 1970

Hercules Research Center
Hercules Incorporated
Wilmington, Delaware 19899

A STUDY OF THE MECHANISM OF CHEMICAL REACTIVITY OF NITROGEN TETROXIDE WITH TITANIUM ALLOY

Foreword

This is the final report prepared by the Hercules Research Center, Hercules Incorporated, under Contract No. NAS 8-30519, Control Number DCN 1-8-54-10278 (1F) for the George C. Marshall Space Flight Center of the National Aeronautics and Space Administration, and covering the period from January 24, 1969 through March 31, 1970. The work was administered under the technical direction of the Propulsion and Vehicle Engineering Laboratory, Materials Division, of the George C. Marshall Space Flight Center with Mr. W. A. Riehl acting as project manager. Scientific personnel that have participated in this program include:

Mr. A. Z. Conner, Project Leader

Mr. J. A. Gailey, Spectrophotometry and Computer Programming

Mr. A. A. Orr, Spectrophotometry

Dr. J. F. G. Clarke, Jr., Gas Chromatography

Mr. A. H. Betley, Corrosion Tests

Mr. W. D. Stone, Corrosion Tests

Dr. J. B. Arots, Corrosion Consultant

TABLE OF CONTENTS

Appendix

LIST OF FIGURES

ABSTRACT

This is the final report of this investigation. It summarizes two years of experimental work performed under Contract Nos. NAS 8-21207 and NAS 8-30519. The overall purpose of this work was to study the interactions between liquid dinitrogen tetroxide (N_2O_4) and 6Al 4V titanium alloy that lead to stress corrosion cracking (SCC). The study was almost exclusively focused on establishing the relationships between the chemical composition of N_2O_4 systems and SCC behavior. The specific objectives of the program were:

(1) To develop a standard SCC test capable of evaluating the SCC behavior of various types of N_2O_4.

(2) To develop qualitative and quantitative methods of analysis capable of determining significant compositional differences in various types of N_2O_4.

(3) To identify that constituent or component of N_2O_4 that induces or enhances SCC in 6Al 4V Ti alloy.

(4) To attempt to establish the possible presence of SCC inhibitors in certain types of N_2O_4 and to determine the concentration levels that are critical to their inhibitory action.

Essentially all of these objectives were achieved. The experimental accomplishments relative to the specific objectives of the program were as follows:

(1) A satisfactory SCC test was developed.

(2) Six new analytical methods for the analysis of liquid N_2O_4 systems were developed.

(3) A process was devised that was capable of reducing the total proton level of liquid N_2O_4 to below the analytical limit of detection, i.e., $\sim$10 ppm.

(4) Methods were developed by which the composition of liquid N_2O_4 systems could be adjusted with respect to the minor constituents, i.e., N_2O_3, HNO_3, HNO_2, H_2O, O_2.

(5) A major success was achieved in the development of spectrophotometric methods for the qualitative and quantitative characterization of liquid N_2O_4 systems. These methods required computer analysis of the complex digitized spectra in the visible and near-infrared regions.

(6) The spectrophotometric methods were used to study the composition of the proton-containing compounds in liquid N_2O_4. Changes of composition with the addition of H_2O, NO, and O_2 were measured and equilibrium constants for the system N_2O_4-NO-H_2O calculated. In order to relate measured equilibrium compositions at -10°C. with those actually present at the SCC test temperature, the effect of temperature on the equilibrium was determined.

(7) The above developments were used to establish basic correlations relating the composition of the N_2O_4 system with stress corrosion cracking behavior. The effects of trace organic impurities, dissolved O_2, and HNO_3 addition on SCC were first investigated. A definite interdependency between combined NO and proton level was established and the composition range between NO/HNO_3 ratios of 10/1 to 1/100 was tested for SCC behavior; a basic correlation curve was determined.

(8) Several experiments were performed in an effort to clarify certain aspects of the SCC mechanism. These included measurement of the change of dielectric constant, electrical conductivity, and dissipation factor with increasing NO content. A limited number of SCC tests related to surface passivation, brittle-film formation, and effect of applied potential were performed.

(9) A substantial experimental effort was made to study the thermal dissociation of NO_2 to form NO and O_2 at the SCC test temperature. A previously developed gas chromatography method for the determination of dissolved O_2 was employed. The work was unsuccessful due to the severe sampling problems encountered at elevated temperatures.

The data obtained from the above experimental program showed that a cracking N_2O_4 system contained N_2O_4, NO_2, HNO_3, and usually some dissolved O_2. Non-cracking N_2O_4 contained N_2O_4, NO_2, N_2O_3, HNO_3, HNO_2, and H_2O. Conversion of one system to another, and the complex equilibria involved are discussed in detail. Addition of O_2 to a reactive N_2O_4 system increased the rate and/or the extent of cracking but not in direct proportion to the O_2 concentration. However, the absence of dissolved O_2 did not prevent SCC. Cracking occurred in the presence of 20-7000 ppm. HNO_3; raising the HNO_3 level to 1-2% decreased the rate and/or the extent of cracking. Gaseous mixtures of NO_2 and O_2 did not cause SCC. The presence of as little as 50-150 ppm.

of organic impurity in liquid N_2O_4 can inhibit SCC. The effectiveness of inhibition is somewhat dependent on the structure of the organic compound.

The mechanism of the attack of N_2O_4 on the alloy was not definitely established. An oxidative, ionic attack mechanism based on the generation and reaction of NO_2^+ ions at freshly exposed alloy surfaces is postulated as consistent with the observed facts. The principal inhibitors of the SCC reaction have been shown to be the HNO_2/H_2O species that are generated whenever N_2O_3 and protons are present. These inhibitors operate effectively at very low concentrations; critical levels at 70°C. were found to be ∿20 ppm. HNO and ∿1 ppm. H_2O.

INTRODUCTION

Since 1965 the stress corrosion cracking of 6Al 4V titanium alloy in contact with liquid dinitrogen tetroxide (N_2O_4) has been studied by a number of investigators. The historical background of this problem as related to the Apollo program has recently been described (1). In July 1967, the George C. Marshall Space Flight Center awarded a contract (NAS 8-21207) to the Hercules Research Center, Hercules Incorporated, for a further study of the interaction of N_2O_4 with 6Al 4V titanium alloy. This contract differed from other related studies in that it was almost exclusively focused on establishing the chemical composition of reactive and nonreactive N_2O_4 to a previously unattained degree.

The original specific objectives of this program were:

(1) To identify that constituent or component of N_2O_4 that induces or enhances stress corrosion cracking (SCC) in 6 Al 4V Ti alloy.

(2) To develop qualitative and quantitative methods of analysis capable of determining significant differences in various types of N_2O_4.

(3) To attempt to establish the possible presence of stress corrosion inhibitors in certain types of N_2O_4 and to determine the concentration levels that are critical to their inhibitory action.

The general experimental program consisted of the following:

(1) Development of a standard stress corrosion cracking test of sufficient sensitivity and statistical reliability to permit the assessment of the corrosive nature of different types of N_2O_4.

(2) Preparation of a variety of types of N_2O_4 representing different reactivities with 6Al 4V titanium alloy and including:

a. Red-Reactive (RR) N_2O_4: Visually "red" material that induces SCC under standard test conditions.

b. Red-Nonreactive (RN) N_2O_4: Visually "red" material that does not induce SCC under standard test conditions.

c. Green N_2O_4: Visually "green" material representing the extremes of nitric oxide content of the MSC-PPD-2A specification, i.e., G4 N_2O_4 containing 0.4% and G8 N_2O_4 containing 0.8% NO.

(3) Analytical characterization of the above and other N_2O_4 compositions, particularly with respect to measurable differences correlatable with SCC. This characterization involved the development of new, sensitive, and precise methods for the determination of trace constituents of N_2O_4 systems.

(4) Application of the standard SCC test, analytical methods, and compositional adjustment techniques in an effort to establish the critical concentrations of NO and H_2O that must be added to reactive N_2O_4 in order to prevent SCC.

The majority of the specific experimental goals were achieved. A satisfactory stress corrosion cracking test was developed and found to give extremely consistent results. Six new analytical methods were developed that were capable of detecting and determining significant differences in the minor constituent composition of N_2O_4. These methods included:

(1) Combined nitric oxide (visible spectrophotometry).

(2) Total protons (NMR).

(3) Distribution of protonated species (near-infrared spectrophotometry).

(4) Dissolved oxygen (gas chromatography).

(5) Combined chlorine (x-ray fluorescence).

(6) Metallic impurities (atomic absorption).

Methods (1), (4), and (5) permitted analyses to be made at previously unattainable trace levels. Method (2) gave more definitive qualitative and quantitative information than any previous method of determining total protons. Method (6) permitted the precise and accurate determination of trace amounts of over 20 different metallic impurities. Method (3) represented a major analytical breakthrough in establishing the composition of liquid N_2O_4 systems. Because of this latter development, it became possible to establish the amount and nature of the protonated species in samples of liquid N_2O_4. Oxygenated N_2O_4 was found to contain only HNO_3; nonoxygenated N_2O_4 was found to contain variable amounts of HNO_3, HNO_2, and H_2O. In addition, techniques were developed for the quantitative adjustment of the minor constituent

composition of N_2O_4 systems, including a method for substantially reducing the level of protonated species.

By application of the above techniques and methods, it was possible to prepare and test a wide variety of N_2O_4 compositions. As a result, the SCC test behavior of 6Al 4V titanium alloy in the commonly encountered types of commercial N_2O_4 was established. Correlation of combined NO-protonated species concentrations with SCC test behavior was partially achieved in terms of critical concentrations. An interdependency between combined NO and protonated species concentrations was shown to relate to SCC test behavior. An attempt also was made to establish the effect of dissolved O_2 concentration.

The results of the above work indicated that an oxidative attack mechanism is the most likely source of the stress corrosion cracking. The specific nature of the attacking species was not established. The available evidence also indicated that the presence of HNO_2 and/or H_2O species in liquid N_2O_4 is the main critical indicator of a nonreactive system, providing extraneous organic and inorganic contaminants are absent. Again, the nature of the inhibitory process remained in doubt.

At the end of this program, fundamental aspects of the overall problem remained unresolved and some tentative conclusions arrived at during the course of the work required additional experimental verification. Consequently, a second contract was granted (NAS 8-30519) having the same overall goals as NAS 8-21207 but representing extensions and modifications of the original experimental program.

The specific objectives of the program under NAS 8-30519 were as follows:

(1) Define the roles of the impurities in N_2O_4 that are suspected of making positive contributions to stress corrosion cracking, e.g., O_2 and HNO_3.

(2) Define the roles of the impurities in N_2O_4 that are suspected of contributing inhibitory action to stress corrosion cracking, e.g., N_2O_3, HNO_2, H_2O.

(3) Establish the concentration levels of the above impurities that are critical to their respective actions.

The investigation was to be conducted in two phases involving a more extensive characterization of the N_2O_4 compositional system, and a more complete correlation of composition with stress corrosion cracking behavior.

The initial experimental efforts under Phase A were to be directed as follows:

(1) Design and construction of an improved apparatus for the production of substantial amounts of N_2O_4 containing the lowest possible level of protonated species, i.e., $<<50$ ppm.

(2) Design and construction of an improved system for the precise and accurate addition of known amounts of compounds to dehydrated N_2O_4 in amounts down to 25 ppm., and possibly lower.

(3) A study by near-infrared spectrophotometry of the distribution of protonated species in N_2O_4 as related to composition and temperature of the N_2O_4-NO-H_2O system.

(4) A study by gas chromatography of the $NO_2 \rightleftharpoons NO + 1/2\ O_2$ equilibrium in N_2O_4 systems in the temperature range of 60-75°C.

The Phase B experimental program had as its main overall objective the basic correlation of composition with stress corrosion cracking. Some aspects of the Phase B work were highly dependent on the extent of the capabilities developed in Phase A. Other aspects, such as certain additive and temperature dependence studies, could be carried out independently. Stress corrosion cracking tests were to be performed using the Teflon-glass test cells and 6Al 4V Ti alloy U-bend specimens employed in the test procedure developed under NAS 8-21207.

This final report describes the work and summarizes the results of the principal experimental investigations carried out during the contract period. It also presents the overall conclusions derivable from this work and from that performed under NAS 8-21207. A proposed mechanism of the stress corrosion cracking of 6Al 4V Ti alloy by liquid N_2O_4 is also presented.

DISCUSSION OF RESULTS

Phase A - Characterization of the N_2O_4 System

The great majority of the experimental data obtained under NAS 8-21207 and other previous investigations strongly supports the contention that the reactivity of liquid N_2O_4 with 6Al 4V Ti alloy is primarily related to the equilibrium concentrations of the normal minor constituents of the N_2O_4-NO-H_2O system at the temperature of reaction, i.e., NO_2, N_2O_3, HNO_3, HNO_2, H_2O, O_2. Although not entirely definitive, the available data do not indicate that the presence of some foreign metallic or non-metallic impurity in the N_2O_4 is critical to the stress corrosion cracking of Ti alloys in a manner analogous to the effect of halogens in aqueous or methanolic systems. This does not mean that the presence of alloying elements and impurities in the alloy itself is not related to reactivity and/or cracking susceptibility. This has been demonstrated in many metallic systems. However, for the purposes of this investigation, 6Al 4V Ti alloy was considered to be a fixed composition matrix whose susceptibility to stress corrosion cracking is related only to the composition of the contacting medium. Accordingly, the principal experimental effort in Phase A was directed toward the preparation of known compositions and the analysis of unknown compositions in the N_2O_4-NO-H_2O system under a variety of conditions. The preparation of known compositions mainly depended on the development of a procedure for reducing the level of protonated species in liquid N_2O_4 to a very low level. Adequate

adjustment of the composition of small and large samples for analysis and SCC tests was also essential.

The N_2O_4-NO-H_2O system basically consists of the molecular species N_2O_4, NO_2, N_2O_3, HNO_3, HNO_2, H_2O, and dissolved O_2 in a state of equilibrium. No pertinent equilibrium data were available for very low concentrations of N_2O_3 and the protonated compounds in liquid N_2O_4. In order to obtain this type of information as an aid to critical analysis of the system, the near-infrared spectrophotometric method developed under NAS 8-21207 had to be extensively studied in order to extend the range and sensitivity of the procedure. The complexity of the spectral analyses required computer analysis of the digitized spectra. A knowledge of the variation of the various equilibria with temperature was also essential to a characterization of the system and had to be determined experimentally.

Because of the potential importance of oxygen concentration suggested by previous work, a gas chromatographic study of the thermal dissociation of NO_2 into NO and O_2 at the SCC test temperature was also undertaken.

Many of the reactions of N_2O_4 with inorganic compounds involve an ionic mechanism. Measurements of some of the electrical properties of several N_2O_4 systems were made to evaluate the ionic character of these media.

Each of the above areas of investigation outlined above will be discussed in detail below.

A. Purification of N_2O_4

1. Fractional Distillation Using Desiccants

In previous work, the concentration of protonated compounds (HNO_3, HNO_2, H_2O) in liquid N_2O_4 was reduced by vaporization of the liquid N_2O_4, passage of the vapors through a column packed with Molecular Sieve Type 3A, and condensation at 0°C. (1). Red Reactive (RR) N_2O_4 containing about 6,000 ppm. HNO_3 was routinely reduced to below 500 ppm. and usually below 300 ppm. HNO_3. While this was adequate for preliminary work, a much more effective system was needed for the studies planned for this program.

Accordingly, a bench-scale, glass-Teflon apparatus for the purification of N_2O_4 was designed, constructed, and assembled. It was essentially a fractionation assembly fitted with a Dewar-type, low-temperature distilling head (see Figure 1). The column could be packed either with protruded packing, helices, or dehydrating adsorbents, and the reflux ratio could be controlled.

During the initial evaluation of the apparatus, a variety of column packing materials were tested. These included stainless steel protruded packing (Cannon-type), Molecular Sieve Types 3A, 4A, and 13X (1/16" pellets), and porous barium oxide. In the usual procedure, BaO was added to the distillation flask, the charge refluxed through the packed column for about 1 hour, and the distillation carried out at a reflux ratio of about 2/1. The distilled fractions were analyzed for combined NO and HNO_3 contents by visible and near-infrared spectrophotometry. Dry ice was used in the Dewar distilling head. The distillations proceeded smoothly

FIGURE 1

N_2O_4 PURIFICATION APPARATUS

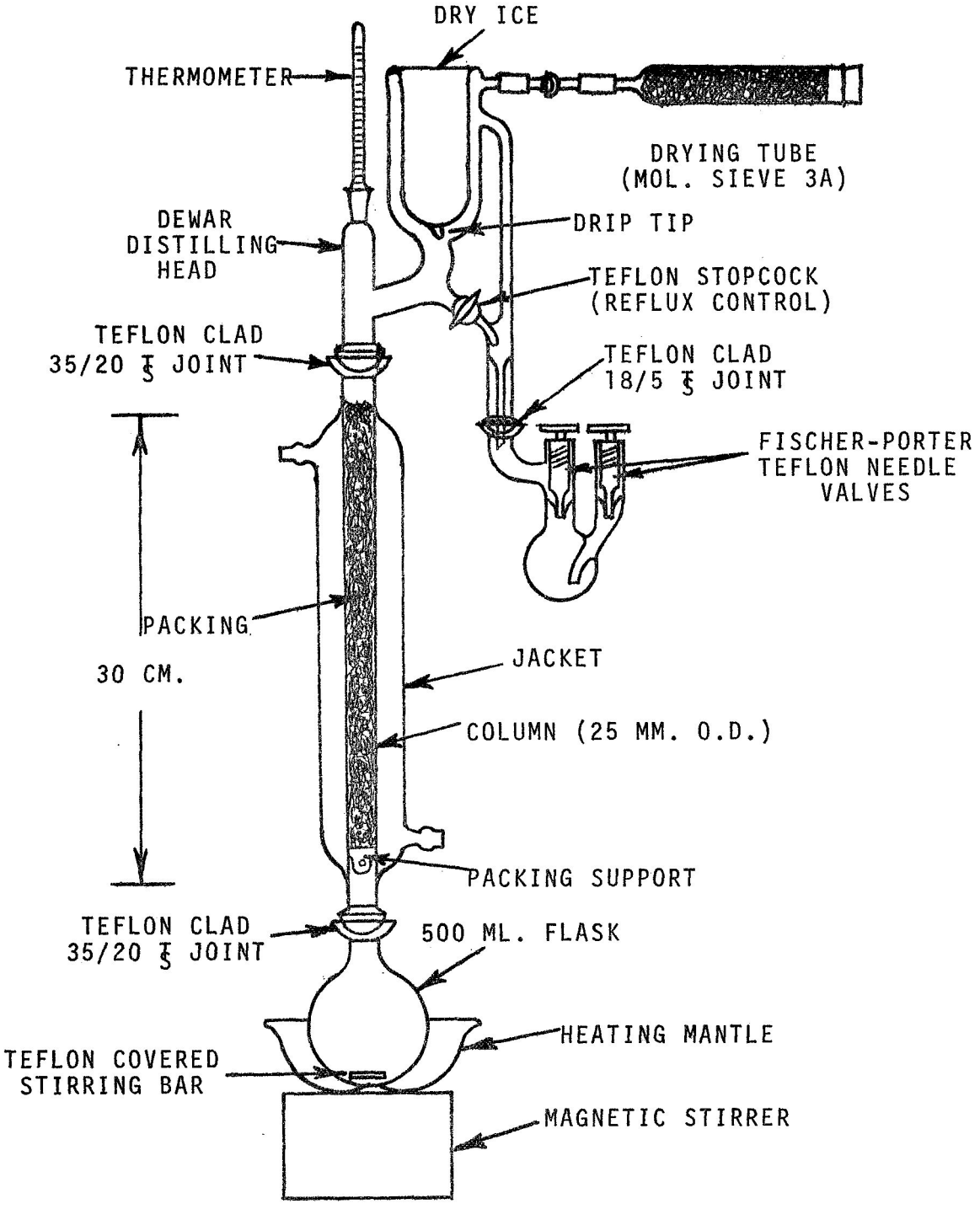

and were easily controlled. The following initial observations were made.

(1) Distillation through the protruded packing from BaO reduced the HNO_3 level by a factor of about 20, but this was not adequate.

(2) Distillation through Molecular Sieve Types 4A and 3A reduced the HNO_3 level the most and appeared to be equally efficient. Under the best conditions, the HNO_3 level was reduced below the limit of detection of the near-IR method, i.e., <10-20 ppm.

(3) Type 4A caused the generation of significantly greater amounts of NO than did Type 3A (ca. 100-200 ppm. versus 5-10 ppm.). The 4A became greener during distillation and retained its color after removal from the column. Type 3A turned pale green but returned to its neutral color upon removal.

(4) The use of activated 4A and 3A gave marginally lower HNO_3 levels than when the Molecular Sieves were used fresh from the cans.

(5) The use of BaO in the distilling flask appeared to aid in the removal of HNO_3.

It thus appeared that a purification system employing BaO treatment and distillation through activated Type 3A Molecular Sieve was close to optimum. Additional work was planned to establish the capacity of the Molecular Sieve and the maximum practical rate of distillation, and preliminary scale-up plans were made. However, from the outset of this work, serious moisture contamination problems arose that prevented the production of

suitably deprotonated N_2O_4 and thus made the capacity and rate studies impossible. The major contamination problems appeared to be due to atmospheric moisture adsorbed on the metal and glass surfaces of the distillate receivers, sample containers, and the spectrophotometer cell and connections. The weather during this work period was characterized by above-average rainfall and high humidity. The laboratories were air-conditioned for comfort but the humidity was not controlled. Despite extensive precautions in drying and desiccating the sample hardware, high and inconsistent values for combined NO (0-130 ppm.) and HNO_3 (50-600 ppm.) were obtained. Re-evaluation of the entire purification-sample handling-analysis system revealed several potential sources of contamination. Those related to the sampling and spectrophotometry will be discussed in the following section. Those related to the distillation step were investigated further. They included moisture strongly adsorbed on the sample cylinder walls and trapped within the valve passages, as well as trace water vapor leaks into the receivers during distillation. Modifications were made, both to the apparatus and operating procedures. These included the use of dry gas purges, replacement of valves, reworking of Teflon-clad joints, use of a heat gun, increased rinsing of distillate receivers, etc.

Subsequent testing of the improved distillation-analysis system showed that very low proton N_2O_4 could be produced periodically, but the system could not adequately be controlled for scale-up under normal environmental conditions. Results

obtained during several partially successful Molecular Sieve capacity tests indicated that approximately 5-6 g. of BaO-treated N_2O_4 could be deprotonated to a usable level (<50 ppm. HNO_3) per 1 g. of Type 3A Molecular Sieve. Consideration was given to translation of the BaO-3A system into an all-metal, heatable, closed loop apparatus.

2. Adsorbent Testing - Batch Contact

a. Carbon Tetrachloride System

Prior to the testing of an improved apparatus for the purification of N_2O_4, it was decided to briefly investigate several other adsorbent pretreatments that might result in higher efficiency and capacity. Principal candidates for testing were two Molecular Sieves from a new supplier (Davison Chemical Division, W. R. Grace & Co.). These materials were both reported to be Type 3A sieves, one of which was standard adsorbent and the other a special acid-resistant grade (AR 12-22). They were purchased in the form of 8-12 mesh spheres.

The initial experiments were carried out in 500 ml. flasks and consisted of mixing 100 g. of adsorbent with 400 ml. of CCl_4 containing about 7700 ppm. HNO_3. The flasks were shaken periodically and analyzed for HNO_3 content by near-IR spectrophotometry. The spectra were not digitized so an accurate water analysis was not made. However, since normal, undried CCl_4 was used in the reference beam, a negative absorbance at 1.40μ indicated the removal of water as well as HNO_3 from the CCl_4. Pertinent data are shown in Table 1. At the time of this work, the acid-resistant Type 3A, AR 12-22, had not been received.

Table 1

Removal of Nitric Acid from CCl_4 by Adsorbents

Time, Hrs.	HNO_3 Content, mg./liter					
	No. 1	No. 2	No. 3	No. 4	No. 5	No. 6
0	7780	7690	7690	∿7700	∿7700	∿7700
1	1950	953	24	8	930	55
2	828	230	9	14	226	45
3	511	72	6	---	---	---
4	325	28	20	0	31	35
5	196	8	20	---	---	---
6	---	---	---	0	0	26
22	27	4	8	---	---	---

Adsorbents

(1) Linde 3A Molecular Sieve

(2) Davison 3A Molecular Sieve

(3) Barium Oxide

(4) Woelm Alumina (Basic)

(5) Linde 4A Molecular Sieve

(6) Grace Silica Gel

Notes: (1) Limit of detection was about 10 ppm.

(2) All adsorbents except BaO indicated the removal of water after the first hour; BaO indicated H_2O removal only in 22 hr. sample.

The Linde 3A Molecular Sieve showed the slowest rate of removal of HNO_3, but an acceptably low acid level was achieved in 22 hrs. Davison 3A and Linde 4A showed faster HNO_3 removal and required only 5-6 hrs. to reach the limit of detection for HNO_3. The silica gel showed even faster acid removal but seemed to level out at a higher concentration level. Basic alumina and BaO showed very rapid acid removal but, as indicated in Table 1, BaO did not appear to adsorb water rapidly from the CCl_4. In previous work, it had been assumed that BaO would pick up H_2O almost simultaneously with the HNO_3. From these data, it was decided to test the Davison Molecular Sieves and basic alumina in an N_2O_4 system.

b. Red Reactive N_2O_4 System

Approximately 400 ml. of RR N_2O_4 was added to each of a series of 500 ml. flasks. Approximately 100 g. of the adsorbent to be tested was then added to each flask. The first series of tests included Davison Standard Type 3A Molecular Sieve, Davison Acid-Resistant Type 3A Molecular Sieve (AR 12-22), and Woelm Basic Alumina. The N_2O_4-adsorbent mixtures were shaken periodically and allowed to stand at room temperature for 3-4 days. Samples were then transferred to oven-dried and desiccated 90 ml. stainless steel sample cylinders for analysis. The results of the spectrophotometric analyses are shown in Table 2.

Table 2

Deprotonation of RR N_2O_4 by Adsorbents

Adsorbent	ppm., mg./1000 g. HNO_3	NO
Davison 3A	13, 4, 4 Av. 7	1821, 1817, 1798 Av. 1812
Davison AR 12-22	7, 9 Av. 8	1282, 1271, 1262 Av. 1272
Woelm Basic Alumina	828, 826, 826 Av. 827	833, 828, 826 Av. 829

The data showed that both Molecular Sieves achieved essentially complete removal of HNO_3 from RR N_2O_4. The NO levels obtained were much higher than previously observed but this could be eliminated by oxygen treatment. The alumina results showed that the HNO_3 level was only reduced to the 800 ppm. level and indicated that all of the results obtained in CCl_4 could not be extrapolated to N_2O_4 systems.

The deprotonation of RR N_2O_4 by batch contact with Davison acid-resistant Type 3A Molecular Sieve (AR 12-22) was confirmed by two experiments. In one case, the 300 ml. of deprotonated N_2O_4 taken from the flask containing the AR 12-22 adsorbent (see above) was replaced by ∿300 ml. of RR N_2O_4 and allowed to stand for additional 7 days. Analysis of the resulting N_2O_4 gave the following results:

ppm. by wt.			
NO	HNO_3	HNO_2	H_2O
1047	3	46	12

This showed that the Molecular Sieve still had sufficient capacity to reduce the level of the protonated species to an acceptably low value. No oxygen treatment was used in this work.

The second confirming experiment consisted of treating about 1300 ml. of RR N_2O_4 with 330 g. of AR 12-22 Molecular Sieve in a 1650 ml. stainless steel cylinder. The cylinder was pressurized with oxygen to 50 psig. several times during the contact period of 20 days. The spectrophotometric analysis results were as follows:

	ppm. by wt.			
Sample No.	NO	HNO_3	HNO_2	H_2O
1	0,0	11, 7	18, 19	4, 4
2	0,0	7, 5	30, 35	7, 8

This was the lowest proton level material that had ever been produced during this program. It should be pointed out that the numbers in the above table were generated in a computer analysis of the digitized spectra and are all below the estimated limits of detection of the spectrophotometric method.

c. Scale-Up

The previous experiments demonstrated that it was possible to reduce the total proton content of RR N_2O_4 to below the limit of detection of existing sensitive analytical methods by batch contact with Davison acid-resistant Type 3A Molecular Sieve (AR 12-22). The process is slow but effective at room temperature. At a ratio of 200 g. Molecular Sieve per liter, complete deprotonation of 1-2 liter batches usually required 2-3 weeks. The use of efficient agitation and temperature effects to speed up the process appears feasible but a definitive study was not made.

A 9-gallon stainless steel cylinder was fitted with a dip-tube assembly and drain. A Millipore filter holder was attached to the liquid line. The filters employed were Gelman Type A, glass fiber, 25 mm. diameter. The cylinder was originally solvent-rinsed and dried. Before loading, the cylinder was flushed with about 1 gallon of RR N_2O_4. The dip-tube assembly was removed and 10 lbs. of Davison acid-resistant Type 3A Molecular Sieve (8-12 mesh beads) were poured into the cylinder through a poly-propylene funnel. The cylinder + molecular sieve were placed on a scale and weighed. Approximately 7 gallons (85 lbs.) of RR N_2O_4 were then charged to the cylinder. The contents of the cylinder were agitated manually and allowed to stand overnight. The cylinde was then pressured with oxygen (50 psig.) and agitated again. This process was repeated twice more. The first stress corrosion cracking tests were performed 3 days after initial loading. It was planned that NO add-back experiments and SCC tests would be performed while the proton level of the N_2O_4 was decreasing (see Phase B). The HNO_3 levels decreased as follows:

Date	Days	HNO_3, ppm.
1-20	0	5146
1-23	3	2668
1-30	10	2076
2-6*	17	512
2-13	24	114
3-6	45	67

*An additional 5 lbs. of AR 12-22 was added on 2-4-70.

The question of the amount of metals that might be dissolved from the AR 12-22 was resolved by analysis of a sample of RR N_2O_4 and a sample of deprotonated N_2O_4 that had been in contact with AR 12-22 for more than 30 days. Type 3A Molecular Sieves are crystalline metal aluminosilicates in which a large proportion of the usual sodium cations have been replaced by potassium. The nature of the treatment to make this material acid-resistant is not known. The samples were evaporated in platinum dishes under controlled conditions and the residue was analyzed by atomic absorption. The results are shown in Table 3.

Table 3

Metal Content of Deprotonated N_2O_4*

	ppm.	
	RR N_2O_4	Deprotonated N_2O_4
K	<0.04	0.06
Na	<0.02	0.05
Fe	0.26	0.18
Cr	<0.07	0.08
Ni	<0.04	0.05
Si	<0.7	<0.4
Al	<0.7	<0.4

*After 30^+ days contact with Davison AR 12-22 Molecular Sieve in a 1.7 liter stainless steel cylinder.

The data show a very slight increase in the Na, K, Cr, and Ni levels and a possible slight decrease in the Fe level. Changes in the Si and Al levels could not be ascertained with certainty.

B. Spectrophotometric Analysis

At the start of this contract, an established spectrophotometric method for the determination of combined NO in liquid N_2O_4 (1,2), and a partially developed near-infrared spectrophotometric method for the determination of HNO_3, HNO_2, and H_2O (1) were available. In order to achieve the objectives of this program, it was necessary to modify and improve both procedures by means of an extensive development effort. These improved methods provide the essential base for the entire N_2O_4 characterization program. Because of the spectral complexity of the N_2O_4 system, digitization and computer processing of the data was a necessity. Using these procedures, it was possible to define the nature and quantitative distribution of the minor constituents of N_2O_4 to a previously unattainable degree. The important development work and the application of the methods to composition and equilibrium studies will be described in the following sections.

A brief review of the principles of the two methods is indicated at this point. Nitric oxide dissolves in liquid N_2O_4 and reacts with the NO_2 present to form N_2O_3, which imparts a green color to the liquid. The intensity of the green color is proportional to the N_2O_3 concentration and can conveniently be measured at 700 nm. Absorbance measurements are normally made at subambient temperature (-10°C.) and Beer's Law is obeyed. The protonated species that can exist in liquid N_2O_4 are HNO_3, HNO_2, and H_2O. These compounds exhibit characteristic absorption bands

in the 1.4-1.5μ region of the infrared spectrum that can be used for qualitative and quantitative analysis. The specific band assignments are 1.470μ (HNO_3), 1.448μ (HNO_2), and 1.404μ (H_2O). The 1.404μ H_2O band is well resolved but is in a region where the instrumental background under high sensitivity distorts the spectrum. The 1.448μ HNO_2 and 1.470μ HNO_3 bands overlap sufficiently so that it is difficult to detect and determine small amounts of HNO_2 in the presence of larger amounts of HNO_3. Background interferences and band overlapping can often be corrected for by computer processing of the digitized spectra. The detailed spectrophotometric procedures used in this work are given in Appendix I.

1. Apparatus Development

a. Spectrophotometric Cell

The cell used for measurements in both the visible and near-IR region was a Research & Industrial Instruments Co., Model F-07, high pressure UV cell with a path length of 5.85 cm. The UV silica windows were replaced by NIR silica windows of identical dimensions. Three stainless steel valves and Swagelok fittings were added to permit attachment of stainless steel sample cylinders, gas lines, or a septum injection system. Two of these valves (fill and gas inlet) connect through appropriate fittings to openings in the top of the cell's cylindrical sample space; the third valve (outlet) connects to an opening in the bottom of the sample space to facilitate complete emptying of the cell. The gas inlet valve and fittings are removable permitting attachment

of the septum injection system for the addition of liquids. An 1/8" SS Swagelok union on the gas inlet valve permits attachment of a 1/8" SS gas line (coiled for flexibility) for introduction of gases such as nitric oxide and oxygen into the cell.

The cell was fitted with a removable jacket through which a heat-exchanging liquid could be circulated for temperature control. The jacket was insulated with an exterior 1/4" layer of polyurethane foam. The cell is shown in the assembled and disassembled states in Figures 2 and 3.

b. Dry Box

Serious moisture contamination problems were encountered during the early phases of this program. To prevent these problems, and other effects such as fogging of cell windows at subambient temperatures, a dry box was built to cover the entire sample, reference, and phototube compartment of the Cary 14 spectrophotometer. See Figures 4 and 5.

The box was constructed of wood and Plexiglas and was fitted with two rubber gloves for manipulation of the cell and sample cylinders. The dry box also contained refrigerant lines, a dry air purge line, a nitrogen line for cell purging, and an exit port leading to a small hood mounted on the back of the box. A waste receptacle was placed in the exit port when it was necessary to dispose of liquid samples between runs.

c. Temperature Control

A Forma Temp Jr. refrigeration-circulating unit was used to pump 50/50 glycol/water coolant to the cell for subambient

FIGURE 2

THERMOSTATTED SPECTROPHOTOMETRIC CELL - ASSEMBLED

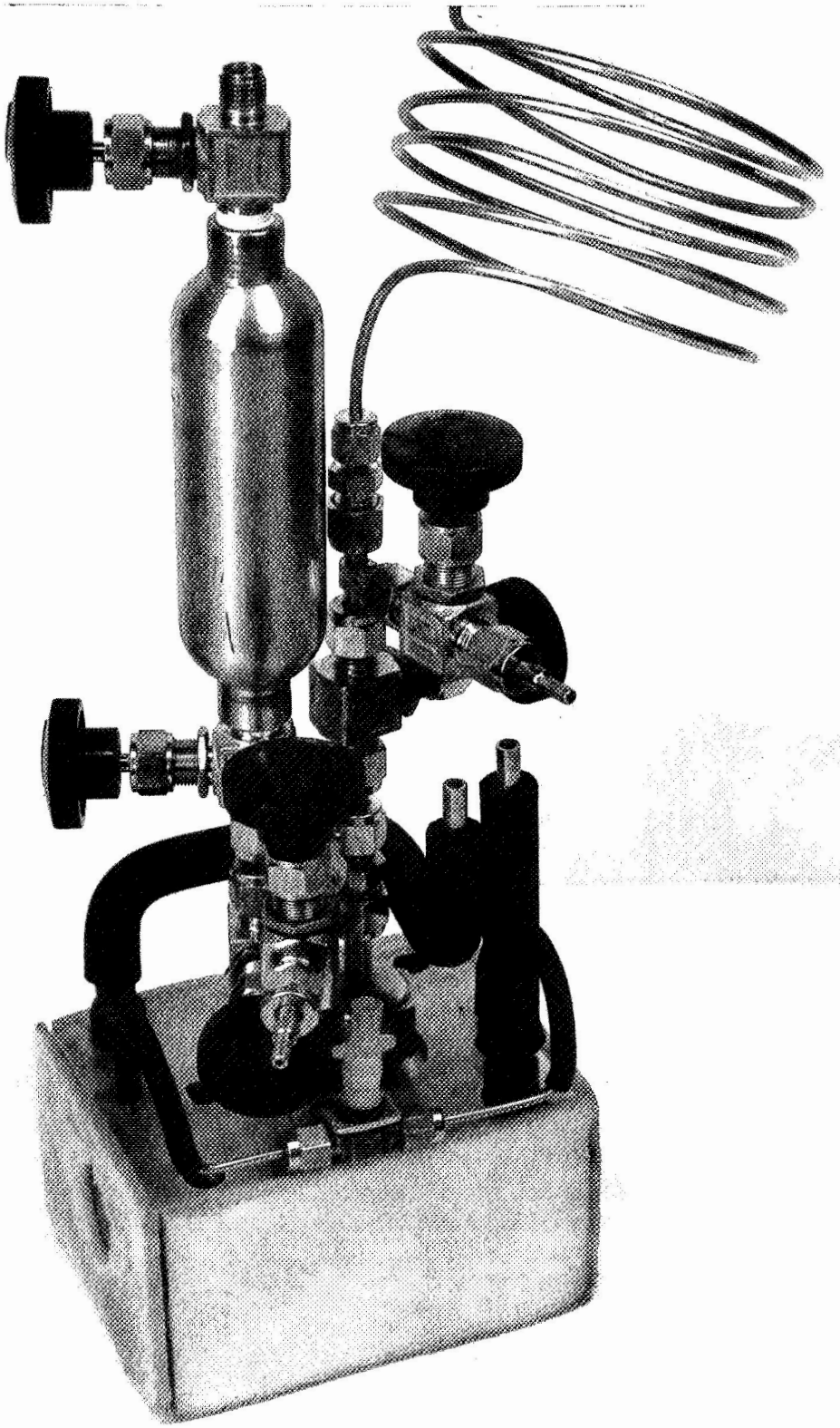

FIGURE 3

THERMOSTATTED SPECTROPHOTOMETRIC CELL - DISASSEMBLED

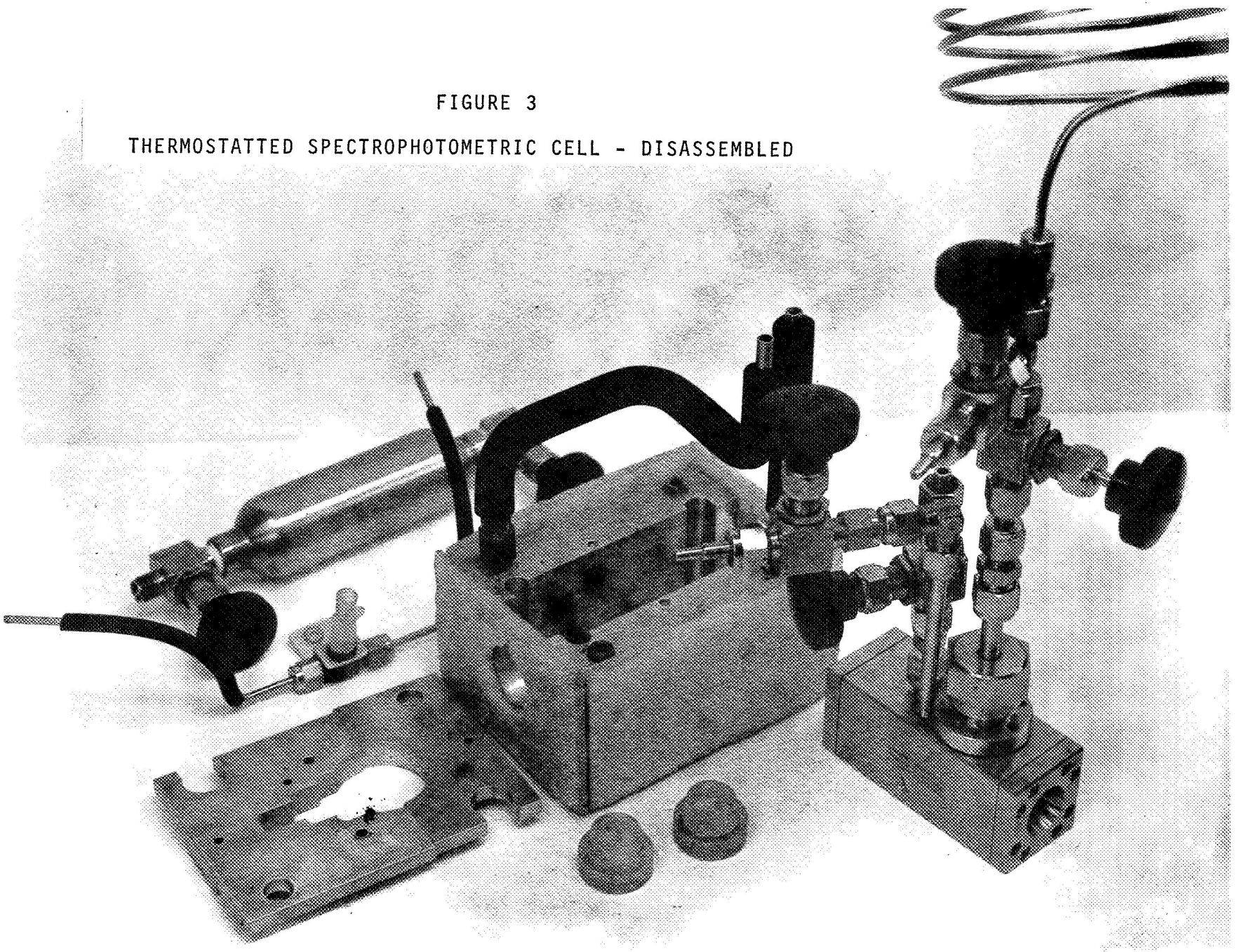

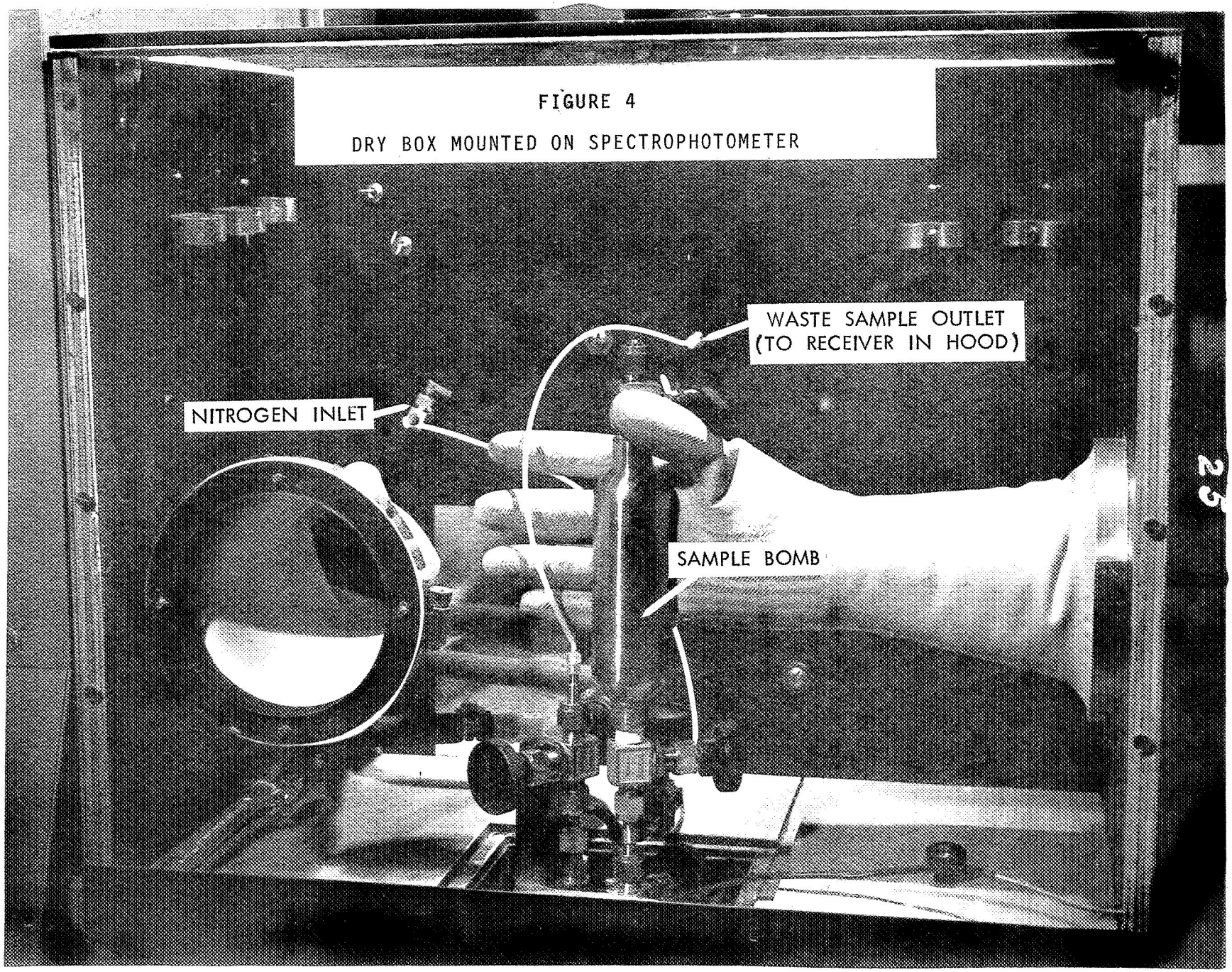

FIGURE 4

DRY BOX MOUNTED ON SPECTROPHOTOMETER

FIGURE 5

SPECTROPHOTOMETER AND ACCESSORIES

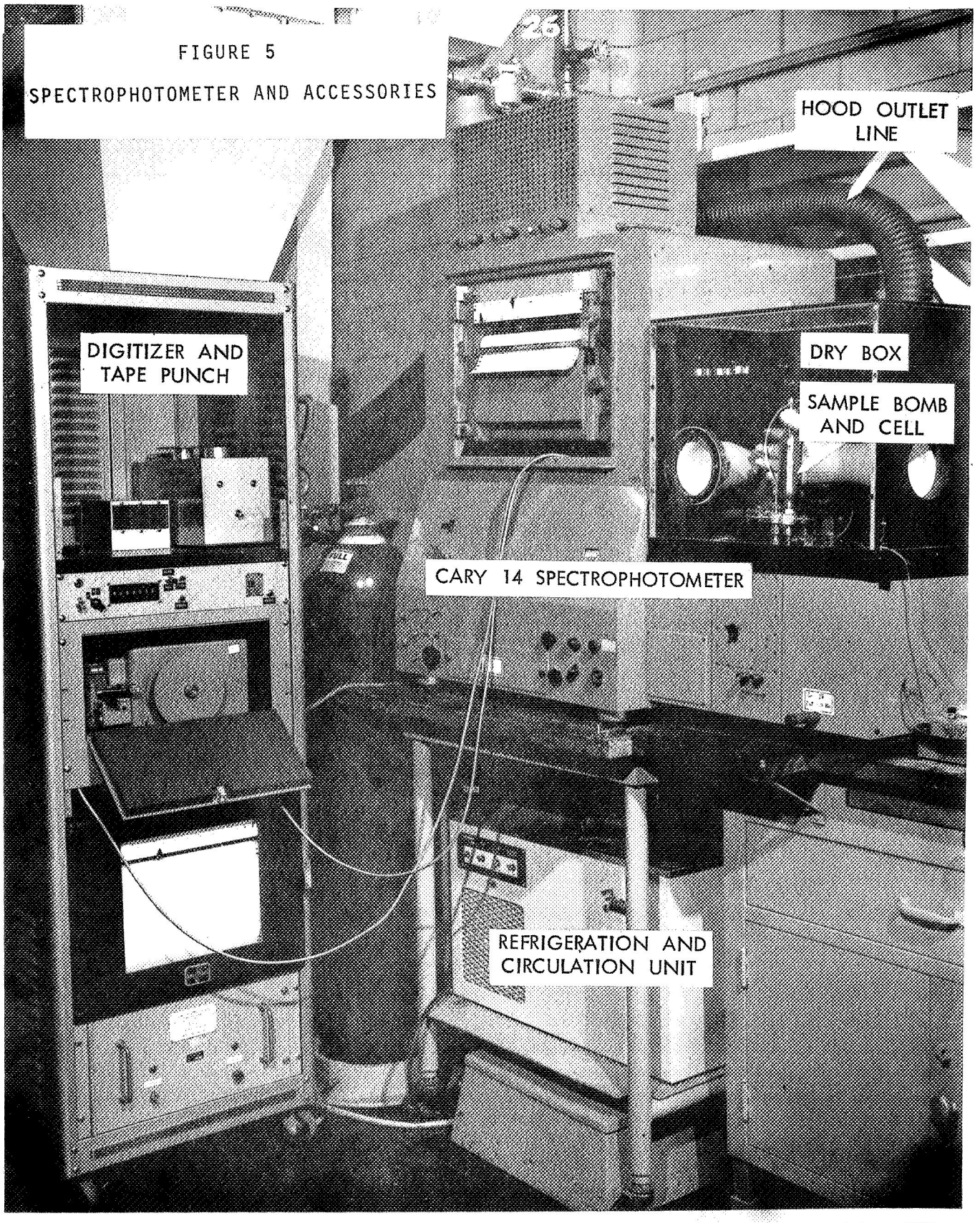

temperature work. (See Fig. 5.) A copper-constantan thermocouple located in a well in the cell block was used with a Leeds & Northrup potentiometer to measure cell temperature. With the refrigeration unit set to minimum bath temperature (-15°C.), the cell attained a steady state temperature between -10 and -11°C.

For experiments where temperatures above -10° were desired, an auxiliary, small capacity, heater-circulator bath was used. (Haake Series F, 1.7 liter capacity.) The circulating lines from the Forma Temp were connected to the cooling coil of the Haake unit. 50/50 glycol/water was then circulated from the Haake to the cell. Using the Haake heater and temperature controller, temperatures from 5 to 70°C. could be maintained in the cell to within 0.5°. For temperature between -10° and +5°, the cooling coil had to be assisted by the addition of dry ice to the Haake reservoir.

d. Digitized Spectra

A Cary Model 14 spectrophotometer with a 2-pen slidewire system was used to obtain all of the spectra used in this work. The spectrophotometer was modified to produce digitized spectra by gearing a 10-turn potentiometer to one of the pen-drive systems. The potentiometer-attenuated output from a mercury cell is fed to an auxiliary recorder capable of driving a shaft encoder which converts the analog signal to a digital signal which in turn is fed to a paper tape punch. The punch is actuated on signal from a photo diode-lamp system which scans a radially striped disk mounted on one of the scan drive gears in the

spectrophotometer. The stripes on the disk are spaced to give a punch signal optionally at one punch per 1, 2, 5, or 10 nm.

2. Computer-Processing of Spectral Data

The analog spectra produced by the Cary Model 14 spectrophotometer were converted to digital form and recorded on punched paper tape as described above. The data tape formats are detailed in Appendix V. The tapes were processed by an EMR 6130 computer (Computer Division of Electro-Mechanical Research, Inc., Minneapolis, Minn.) with 24K of 16-bit core memory. Additional auxiliary bulk memory is provided by a rapid access disc memory unit. Input-output devices used in processing the tapes include a 600 card/min. reader, a 600 line/min. printer, a Model 33 Teletype, a 300 character/sec. paper tape reader, and a Calcomp digital plotter.

a. General Computer Operations

A raw spectrum is corrected for the contributions of instrumental and cell background, and the contributions of N_2O_3 and N_2O_4. During this process, the concentration of N_2O_3 is computed. The net result is a spectrum representing the HNO_3 HNO_2, and H_2O present. This spectrum is smoothed by a least squares procedure to minimize noise, and is then used to calculate the concentration of the three protonated species. All calculated values are output with complete documentation on the line printer along with a tabular listing of the digital spectrum. In addition, the contributions of any combination of the protonated species may be subtracted as a performance check or to aid in

spectral interpretation. Optionally, any of the computed spectra may be drawn on the digital plotter.

b. Reference Spectrum Storage

Reference spectra in digital form of pure N_2O_4, N_2O_3, HNO_3, HNO_2, and H_2O are stored on cards along with the program deck. The first card of each reference compound file contains, in order: the number of data, the last wavelength (nanometers) in the range, an identification number, Cary 14 recorder slidewire range, cell pathlength, temperature, and concentration in ppm. The remaining data are absorbance values at 1 nanometer intervals. They are recorded in I4 format, 20 per card. The integer format for absorbance values originates with the tape punch format (e.g., an absorbance of 0.253 is recorded as 253), but it is retained as long as possible throughout subsequent processing in the interests of time and space economy both internal and external to the computer.

c. The Computer Program - A Functional Description

A complete list of the Fortran IV program with basic documentation is contained in Appendix II. The Fortran is standard, but several special subroutines are used which are not included in the listing. All but one of these subroutines are part of the plotter package supplied by the computer manufacturer. Because such routines vary in detail from one manufacturer to another, a complete functional description is not included. The remaining subroutine, called IRD, was written by Hercules personnel. It

permits the computer to read the special binary coded decimal punching format produced by the spectrum digitizer. It is written in assembly language (called ASSIST by the computer manufacturer) and has the form: CALL IRD (ARRAY, M, N, MAX).

ARRAY is the name of an integer array where the values read are to be stored. A single subscript tells which array element is to receive the initial value.

M is an integer which sets the length (in decimal digits) of the data word.

N counts the number of data words read.

MAX sets a limit on N.

When IRD is called, the subroutine ignores leading blank tape (i.e., sprocket holes only), reads and stores N decimal numbers of length M and stops when N = MAX or when a blank character (a single sprocket hole) is received.

A function subprogram called KSS(N) appears in the program. It was also written by Hercules personnel and it serves to test the sense switches on the computer console. The more familiar IF (SENSE SWITCH) is not part of the Fortran package.

Note that sixteen bit integer numbers have a decimal equivalent maximum of 32,767. This limitation, along with certain idiosyncracies of the tape punching equipment, leads to some arithmetic stunts in the program when numbers larger than this are punched in the tape.

The following is a description of the spectroscopic and analytical functions which are required along with a description of how the computer program performs them. The square brackets contain references to locations in the program list (see Appendix II). Some conventions in naming Fortran variables have been adopted when referring to the five components in the N_2O_4 analysis. In general, variable names beginning with K refer to spectra. The suffices 3, 4, 3H, 2H, and 1H refer to N_2O_3, N_2O_4, HNO_3, HNO_2, and H_2O, respectively. Occasionally, an additional suffix, R, is added to distinguish, when necessary, the reference spectra and their associated parameters. Variable names in the text which follows will be capitalized.

Certain basic, "relatively permanent", spectroscopic data are stored on cards or in DATA statements and read at the beginning of the program run. Calibration data for the measurement of N_2O_3 in any one of six wavelength ranges are stored in DATA statements. Six ranges are required in order to keep all of the very wide range of N_2O_3 concentrations which must be measured on scale. The six values stored as SCALE are scaling factors for the temperature dependent contribution of NO_2 to the measured absorption. The six values of ABNO are the ppm absorptivities of N_2O_3 in the six ranges, and the twelve values in NM are the six pairs of nanometer values which define each range of measurement. Other data stored on cards are KAB, the absorbance scale values output by the A/D converter corresponding to known

recorder pen positions which are assumed to be linear. AINV is the inverse matrix of absorptivities of HNO_3, HNO_2, and H_2O at the three analytical wavelengths. The five READ statements following [11] are for the reference spectra described in a following section.

All spectra are corrected for instrument and cell background. The tape containing these data is preceded by some basic spectral information including the beginning and ending wavelengths, the absorbance scale zero offset and, when necessary, the data recording interval. These data are read with the IRD subroutine. The header data are first read and processed. The zero offset is incorporated into the calculation [loop 10] which interpolates linearly between the 20 absorbance scale correction values (KAB), assigning a corrected absorbance for each unit (= 0.001 of true absorbance) of measured absorbance between 0 and 1000. These corrected values are stored in array KORR. The background spectrum is read in and stored in array KBG. It is checked for internal agreement with the header information, and the absorbance scale corrections are applied by substituting for each value of KBG the absorbance value stored in that element of KORR whose index is the measured value of KBG.

The header data of the sample spectrum is next read and processed [27, et.seq.]. There are several options in the format of this data which are described in Appendix V, but the complete set includes the date, an identification number, recorder slidewire, cell pathlength and cell temperature. It may also include the

slidewire, pathlength, and wavelength interval used, and the absorbances found in the measurement of N_2O_3. The specific absorbance of NO_2 (AREL) is calculated from its temperature relationship and scaled to a magnitude appropriate to the wavelength interval (coded as a number 1 to 6 and stored in LINT) over which N_2O_3 has been measured. This value, ANO2, is subtracted from the measured specific absorbance ($cm.^{-1}$) and the ppm. of N_2O_3 is calculated from the appropriate absorptivity, ABNO(LINT).

The sample spectrum (up to 400 data points) is read from the data tape and stored in array K. This array is dimensioned at 1200 words, i.e., large enough for three spectra. Thus, various versions of the spectrum may be stored and output merely by changing the array indices in the transmission statements. For example, the original sample spectrum is stored in locations beginning at index 801 [35]. The spectrum corrected for instrumental background, N_2O_3, and N_2O_4 is stored beginning at 401. Corrections are applied to the original spectrum in the loop which begins at [39]. The individual data points of the sample spectrum are tested for an off-scale (>0.990 absorbance) condition, and those of the N_2O_3 and N_2O_4 reference spectra are tested similarly. (In the case of the reference spectra, off-scale or otherwise invalid data are indicated as negative values.) If any of the input data for a wavelength is invalid, the output is marked by assigning it a very large value. Valid data points are corrected for absorbance scale errors, and the spectral contributions of background, N_2O_3,

and N_2O_4. Each of these spectra is adjusted by its scaling factor, BGSW, CORR3, or CORR4 as it is subtracted from the sample. The corrected spectrum is stored in the upper third of K.

Loops [38] and [42] find the minimum value in the corrected spectrum and translate the entire spectrum to make the minimum equal to zero. Invalid data points previously marked with very large values are set to -1.

The corrected spectrum is further refined by a smoothing procedure which uses a seven point least squares fit to a quadratic function after the method of Savitzky and Golay (3). The resulting spectrum is stored in the middle third of K.

The smoothed version which is the best measure of the absorption of the three protonated species is used to calculate their concentrations in the sample. The peak wavelengths for H_2O, HNO_2, and HNO_3 are, respectively, 1404, 1448, and 1470 nanometers which in turn correspond to data in the K array at 547, 503, and 481. The "integer absorbances" are converted to true absorbance and then in loop [51] to ppm by multiplying by the inverse matrix of absorptivities. The two calculations following [51] compute the ppm of H_2O and HNO_2 from those of HNO_3 and N_2O_3 using relationships derived from the study of equilibria and equilibrium constants.

The program provides for a large number of options in output. Control of these options is performed mainly by the programming between [7] and [80]. Also included in this section [loop 60] are the calculation of scaling factors and the subtraction of the

spectra of the protonated species in any combination. The control parameters for this operation are set in loop [56]. Almost all of the control of program flow is through the READ at [52] which may reference either the console Teletype or the card reader. Details on the exercise of this control are included in the program documentation [preceding 54].

Output of spectra and the results of analyses performed on these spectra can be in the form of punched paper tape, tabular listings, and plots on the digital plotter. Many examples of plotted output are included in this report. Figure 6 illustrates the tabular version of a typical sample.

3. Calibration for the Determination of Protonated Species

The calibration procedure employed for the three protonated species, i.e., HNO_3, HNO_2, and H_2O, based on their near-infrared absorption bands was divided into two distinct parts. First, the spectrum of each component had to be defined, and second, absorptivities had to be determined for all three components at the wavelengths chosen for analysis.

a. Individual Reference Spectra (Fig. 7)

(1) Dinitrogen Tetroxide, Proton-Free

A sample of N_2O_4 was treated with barium oxide and then distilled from BaO through 3A Molecular Sieve to give a proton-free sample. The fact that the 1.477μ and 1.408μ bands of N_2O_4, close to those of HNO_3 and water, did not change on addition of NO in the preparation of the NO standard described below, was evidence that the sample was indeed proton-free below the limit of detection,

FIGURE 6

TABULAR SPECTRUM OF TYPICAL N_2O_4 SAMPLE

3/17/70 3

SAMPLE NO. -119 -2

INST. BKGD.	317	N2O3 ANALYSIS S/W	1.0
SCAN RANGE	1350-1550	CELL	5.85
SAMPLE S/W	1.0	A(900)	.2040
SAMPLE CELL	5.85	A(700)	.6260
SAMPLE TEMP.	-10.0	PPM	224.

3512. PPM HNO3
58. PPM HNO2
50. PPM H2O
52. PPM HNO2 FROM EQUIL. CONST.
68. PPM H2O FROM EQUIL. CONST.

-1	-1	-1	-1	-1	-1	-1	-1	-1	-1
-1	-1	-1	-1	16	16	16	16	17	17
18	19	20	21	23	23	25	26	28	31
33	34	36	38	40	41	43	45	48	51
54	58	61	65	69	73	77	82	87	92
98	104	111	117	124	130	138	145	152	159
167	175	183	192	201	210	220	230	239	249
259	268	278	287	297	305	313	320	325	330
333	334	332	328	320	310	296	281	263	245
225	204	183	163	144	126	109	94	81	69
59	51	43	37	31	27	24	22	19	16
14	12	11	9	8	7	7	6	5	4
4	3	3	4	4	4	4	4	3	3
2	3	4	5	5	6	7	8	9	11
12	13	14	15	16	18	19	21	22	23
24	23	22	20	17	15	14	13	12	12
11	10	10	10	10	9	10	9	9	10
11	11	12	12	12	11	11	10	10	9
8	7	7	6	6	5	4	3	3	3
3	3	3	2	2	1	1	-1	-1	-1

FIGURE 7 - NEAR-INFRARED REFERENCE SPECTRA

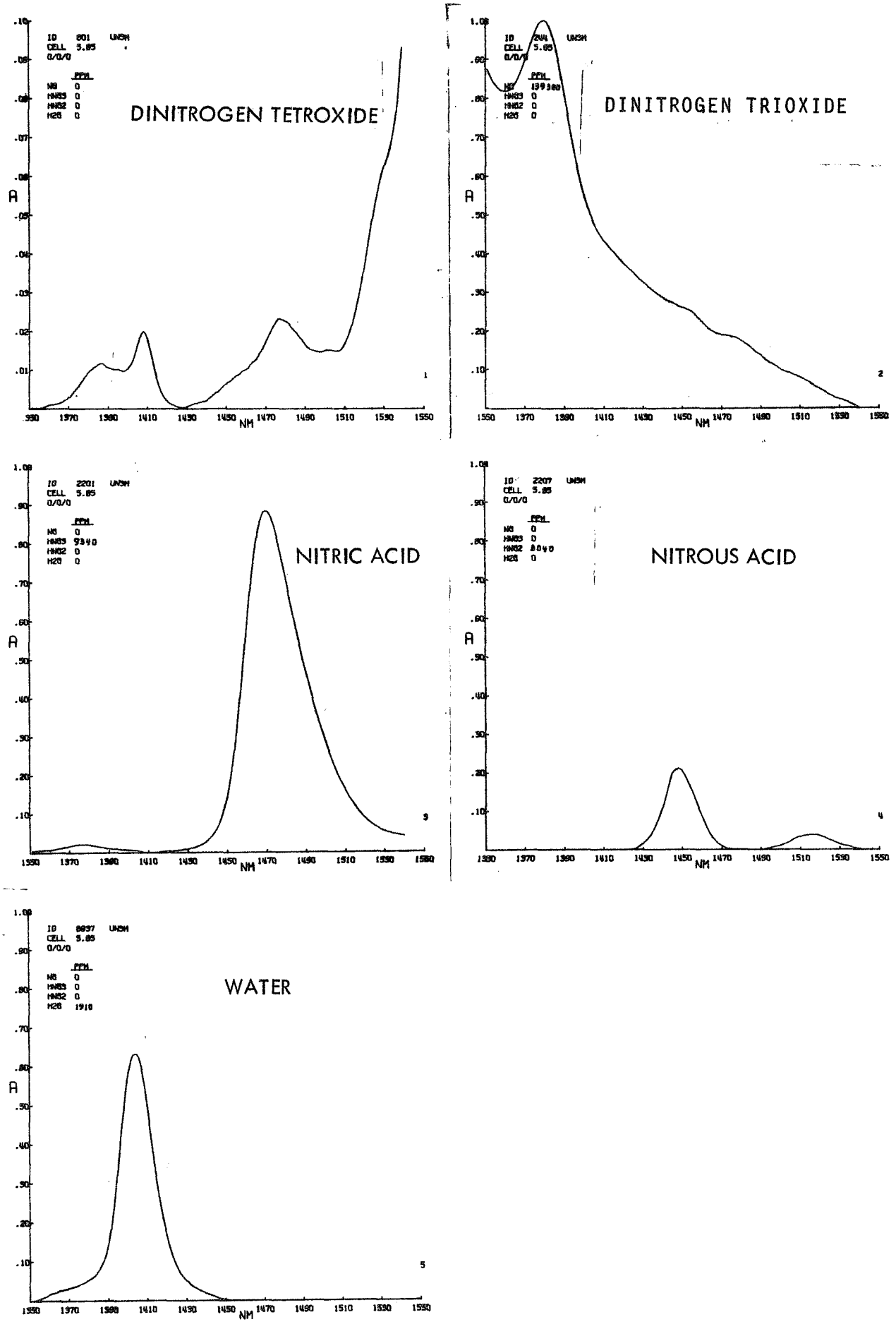

i.e., <10 ppm. HNO_3. The digital spectrum of the instrument/cell background was computer-subtracted from the spectrum of this sample scanned at -10°C., to give the N_2O_4 reference spectrum.

(2) Combined Nitric Oxide (N_2O_3)

This constituent is measured as N_2O_3, but calculated as NO. The basis of measurement of combined NO is its broad electronic band peaking at 700 nm. At high NO concentrations, the trailing of this absorption band extends into the 1550 to 1350 nm. near-IR region where the protonated species are measured and corrections, therefore, must be made. Additionally, at high NO concentrations, the 700-900 nm. absorbance difference is too high to be read within the 0 to 1.0 absorbance range available. Consequently, a standard series was prepared as follows. First, the spectrum of proton-free, oxygenated N_2O_4 was obtained from 1550 to 700 nm. as a baseline, then dry NO was added through the gas handling system until a large on-scale 700-900 nm. absorbance difference was obtained. After equilibrium was established, the absorbance difference was read for the 700-900 nm. pair, and also for the 850-900 nm. and 920-950 nm. pairs. Since NO concentration could be calculated from the 700-900 nm. difference, the Δa for the other pairs could be calculated. Additional NO was added in several increments in amount such that a new wavelength pair and a previously calibrated pair could be obtained on-scale in the same spectrum. This procedure was continued until six wavelength pairs were obtained so that at least one pair could be used to calculate NO concentration in the range from 1 ppm. to 15 percent. At the highest NO level (about 15%

the spectrum from 1550 to 1350 nm. was recorded, corrected for instrument/cell background and N_2O_4, and was retained as the reference spectrum shown in Fig. 7.

(3) Nitric Acid

Microsyringe addition of increments of 100% HNO_3 to weighed samples of oxygenated, proton-free N_2O_4 through a septum in the spectrophotometric cell yielded both quantitative calibration data (Table 4) and, after subtraction of instrument/cell background and N_2O_4 spectra, a reference spectrum of HNO_3. The large absorption band at 1.470μ is attributed to the first overtone of the fundamental hydroxyl stretching vibration.

(4) Water

Since both nitrous acid and water can exist in N_2O_4 only in equilibrium with HNO_3 and N_2O_3, the individual reference spectra of these two compounds were much more difficult to obtain. Addition of water by syringe to a sample of RR N_2O_4 produced a spectrum with a strong 1.470μ HNO_3 band, a strong 1.404μ H_2O band and a weak 1.448μ HNO_2 band (Fig. 8). The approximate shape and location of the water band were estimated from the spectrum of water-saturated CCl_4 which shows a water band at 1.395μ (Fig. 9). Two bands, at 1.446 and 1.514μ, were observed when HNO_2 was generated in water-saturated CCl_4 by the addition of liquid N_2O_3 (Fig. 10). (The bands at wavelengths lower than 1.43μ in the HNO_2 in CCl_4 spectrum can be accounted for by excess N_2O_3, water, and water vapor in the cell compartment.)

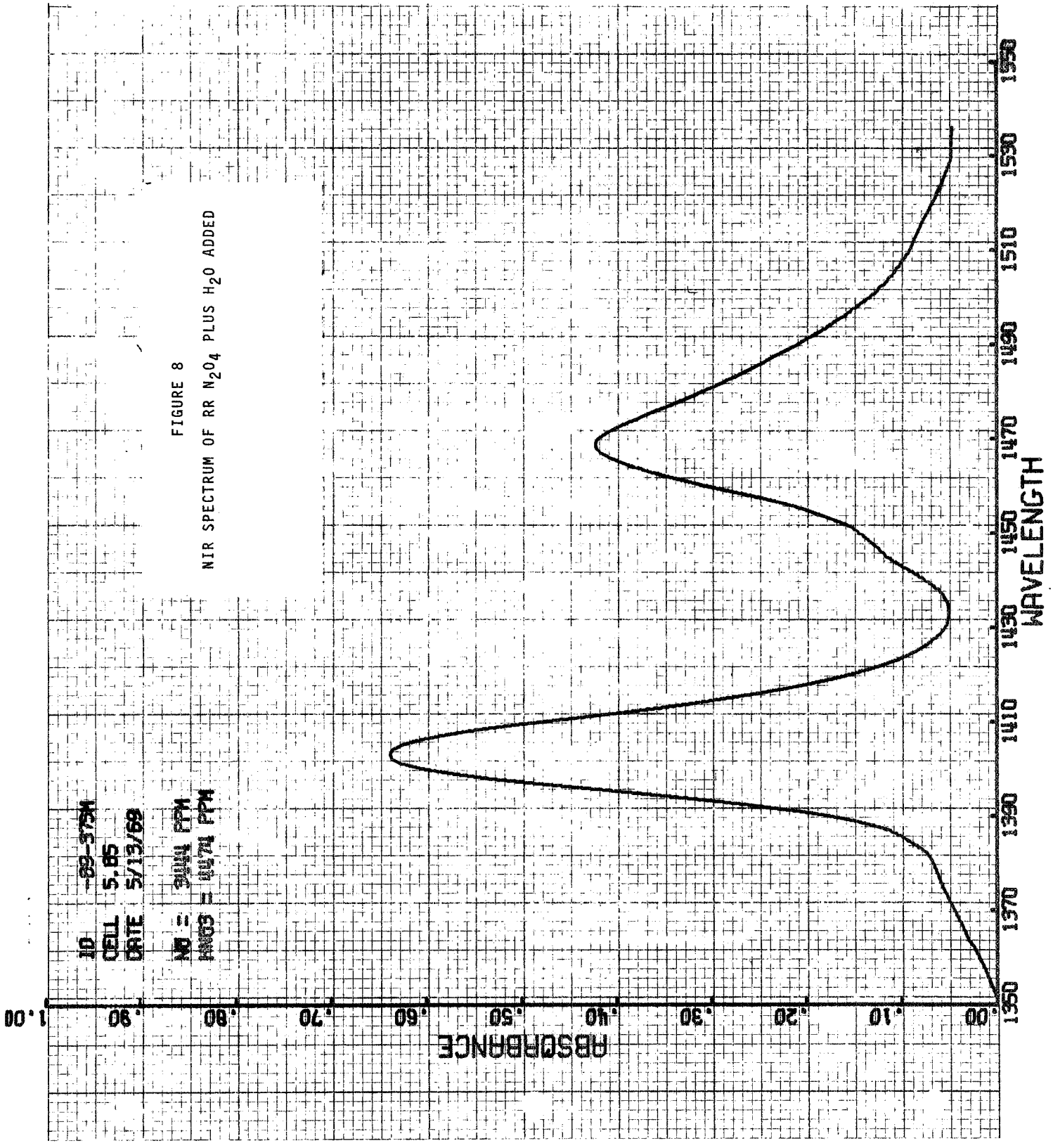

FIGURE 8

NIR SPECTRUM OF RR N_2O_4 PLUS H_2O ADDED

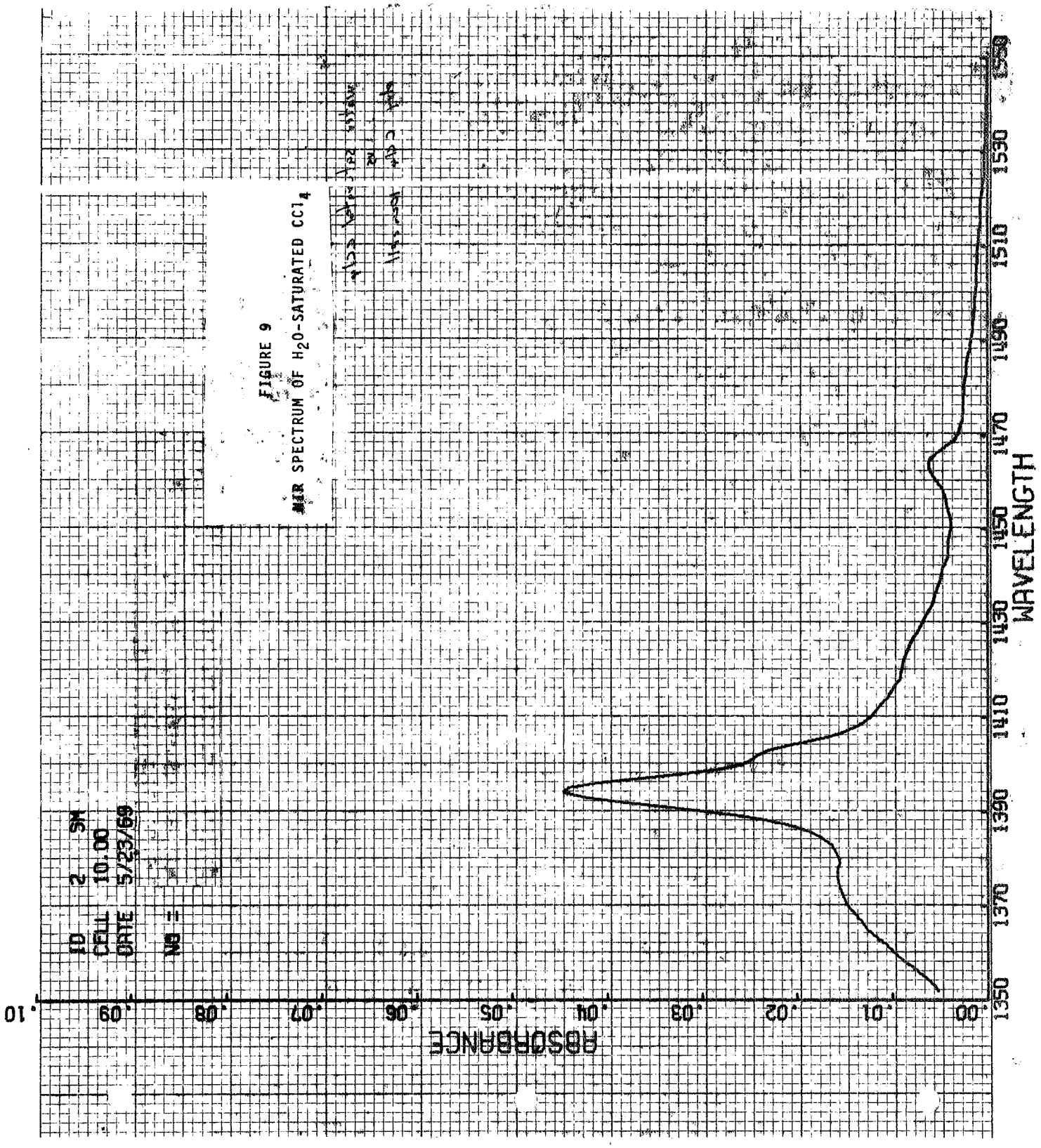

FIGURE 9

IR SPECTRUM OF H_2O-SATURATED CCl_4

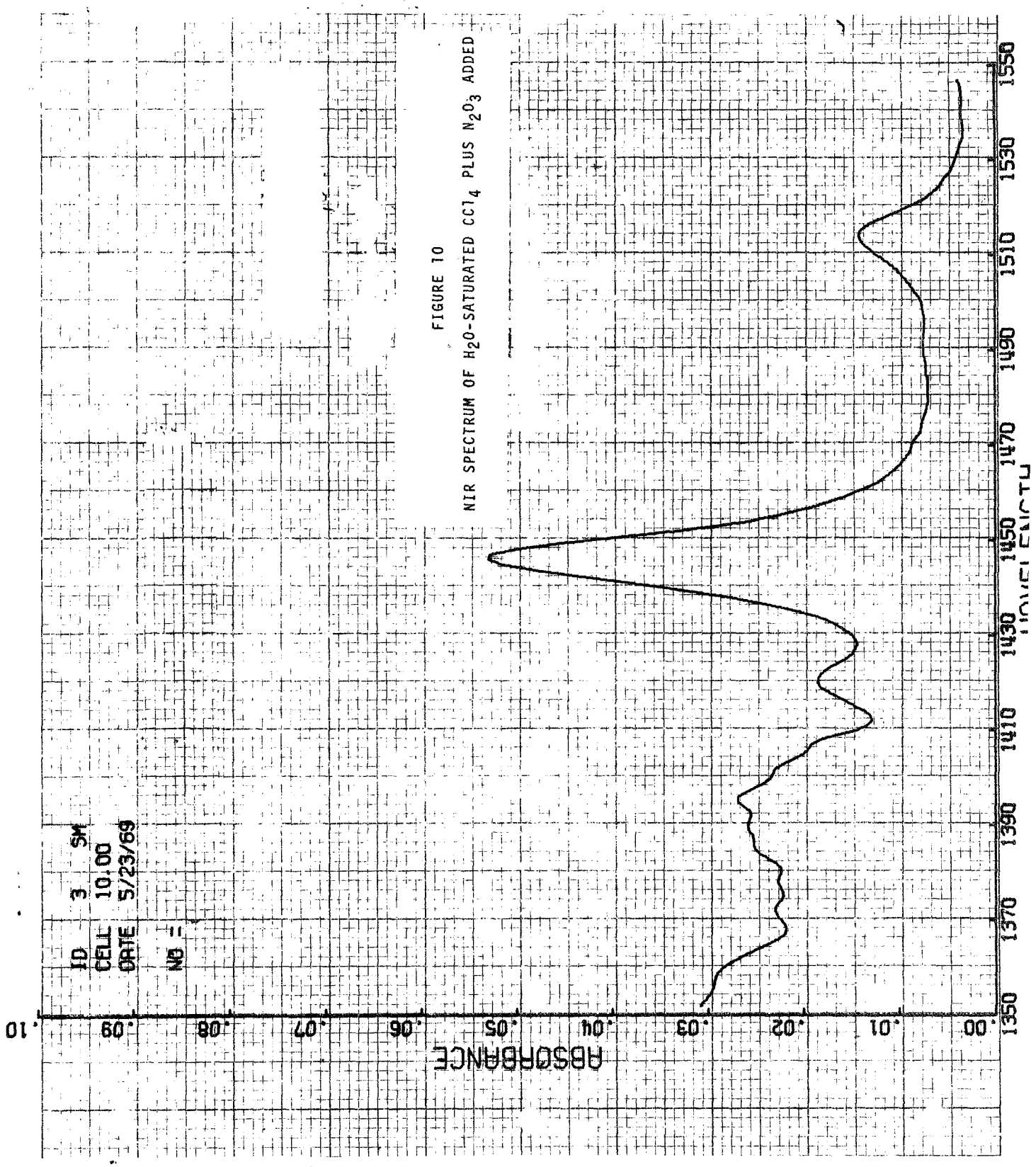

FIGURE 10

NIR SPECTRUM OF H_2O-SATURATED CCl_4 PLUS N_2O_3 ADDED

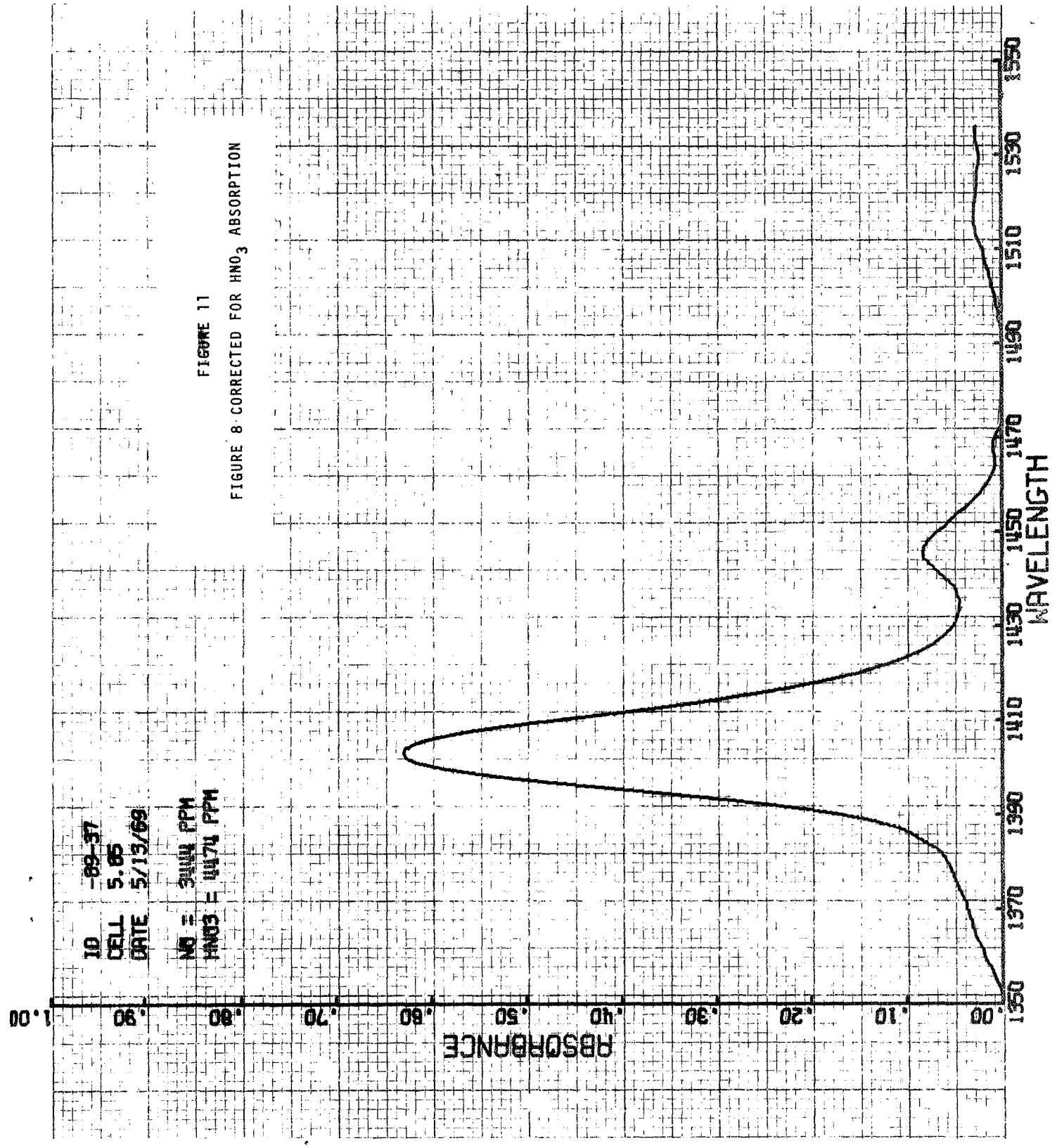

FIGURE 11

FIGURE 8 CORRECTED FOR HNO_3 ABSORPTION

Computer-subtraction of the scaled HNO_3 spectrum was readily accomplished (Fig. 11). The small contribution of HNO_2 was then empirically subtracted from the residual spectrum on the basis of the band locations and relative intensities as observed in the CCl_4 spectrum. The residual from this correction was then stored as the H_2O reference (Fig. 7). The major band at 1.404μ has been assigned to a combination tone of the symmetric and asymmetric stretching fundamental vibrations, after work compiled by Herzberg (4) in which H_2O vapor was found to absorb at 7252 $cm.^{-1}$. The same reference also includes a weak band in water vapor at 6874 $cm.^{-1}$ which is due to another combination tone. The spectrum of H_2O in CCl_4 has corresponding bands at 7172 $cm.^{-1}$ (1.394μ) and 6830 $cm.^{-1}$ (1.464μ), in good agreement when the change of phase is considered. Water in N_2O_4 absorbs at 7124 $cm.^{-1}$ (1.404μ) which leads to the suspicion that it also absorbs weakly near 6800 $cm.^{-1}$ (1.470μ), the same wavelength as HNO_3. This suspicion could not be confirmed because HNO_3 is always present with H_2O, but the presence of such a band due to H_2O would cause errors in the quantitative analysis and may be responsible for some of the difficulty encountered in obtaining good residual spectra.

(5) Nitrous Acid

The spectrum of HNO_2 was the most difficult to isolate for several reasons. First of all, HNO_2 is usually present in relatively low proportion to the other protonated species unless the equilibrium is forced by the addition of large amounts of NO. Second, the spectrum could only be obtained as the residual remaining after

Table 4

Calibration Data - HNO_3

Path Length: 5.85 cm. Wave Length: 1.470μ
Cary Model 14

	HNO_3 Added			
	μl.	mg.	ppm.	Absorbance
Series 1	50	75.65	3340	0.350
	60	90.78	4010	0.430
	70	105.91	4680	0.505
	80	121.04	5340	0.570
	90	136.17	6010	0.635
	100	151.30	6690	0.700
	150	226.95	10030	1.005
	200	302.60	13370	1.270
	250	378.25	16720	1.540
Series 2	10	15.13	730	0.062
	20	30.26	1460	0.138
	30	45.39	2190	0.194
	40	60.52	2930	0.270
	50	75.65	3660	0.349
	60	90.78	4390	0.413
	70	105.91	5120	0.485
	80	121.04	5850	0.554
	90	136.17	6580	0.621
	100	151.30	7320	0.686
	110	166.43	8050	0.750
	120	181.56	8780	0.797

Note: N_2O_4 Sample Wt. - Series 1 = 22.625 g.
Series 2 = 20.682 g.

subtraction of instrument/cell background, N_2O_4, N_2O_3, HNO_3, and H_2O scaled reference spectra. This residual spectrum is thus subject to the cumulative errors of all of these individual spectra. The HNO_2 spectrum was obtained from a sample prepared by adding about 7% NO to RR N_2O_4. The residual was empirically smoothed and adjusted on the basis of relative band intensities and positions as observed for HNO_2 in CCl_4 (Fig. 10). Two bands were observed for HNO_2 at 1.448 and 1.516μ. The stronger of the two at 1.448μ is slightly skewed toward the short wavelength side. It probably represents the first overtone of the OH stretching fundamental vibration in the trans configuration. The weaker band at 1.516 has not been assigned to the cis configuration. Although spectrum quality is not good enough to be certain, this band does not appear to be skewed, possibly because the hydroxyl forms a weak intra-molecular hydrogen bond and is less available to bond strongly with the solvent.

b. Determination of Absorptivities

Nitric acid was the only compound for which calibration could be obtained directly, since it is the only protonated species that can exist alone in liquid N_2O_4. An absorptivity value was obtained from a plot of the absorbance versus concentration data shown in Table 4.

Because HNO_2 and H_2O exist in equilibrium with HNO_3 and N_2O_3 in liquid N_2O_4, an experiment was devised for the simultaneous calibration of the HNO_2 and H_2O near-IR bands. In this experiment, 100% HNO_3 was added to RR N_2O_4 until the 1.470μ HNO_3 band was just

short of full scale (∿9300 ppm.). A sample was then transferred to the spectrophotometric cell, pressurized with oxygen to assure that all protons were present as HNO_3, and scanned at -10°C. From the resulting spectrum (Figure 12, 22-1), the exact concentration of HNO_3 could be calculated based on the previously determined absorptivity value. Six incremental additions of NO to the cell through the gas handling system produced the spectra shown in Fig. 12, 22-2 to 22-7. These spectra showed that the equilibrium was shifted away from HNO_3 toward H_2O and HNO_2 while the total protons remained constant. The sample was then oxygenated to produce the final spectrum, -22-8, in which HNO_3 was again measured to determine total dilution of the protonated species by the NO added. The above spectra were used to calculate the absorptivities of all three components by a mathematical procedure. The analytical wavelengths chosen for the quantitative analyses were:

H_2O, 1.404μ

HNO_2, 1.448μ

HNO_3, 1.470μ

(1) Mathematical Expression of the Problem - The Beer's Law expressions for the three wavelengths are:

$$A_{1404}/b = a_{1,1404}*c_1 + a_{2,1404}*c_2 + a_{3,1404}*c_3$$

$$A_{1448}/b = a_{1,1448}*c_1 + a_{2,1448}*c_2 + a_{3,1448}*c_3$$

$$A_{1470}/b = a_{1,1470}*c_1 + a_{2,1470}*c_2 + a_{3,1470}*c_3$$

where A, a, b, and c are absorbance, absorptivity, cell path, and concentration, respectively, and the subscripts are wavelength in

FIGURE 12 - NIR SPECTRA - CALIBRATION SERIES X16054-22

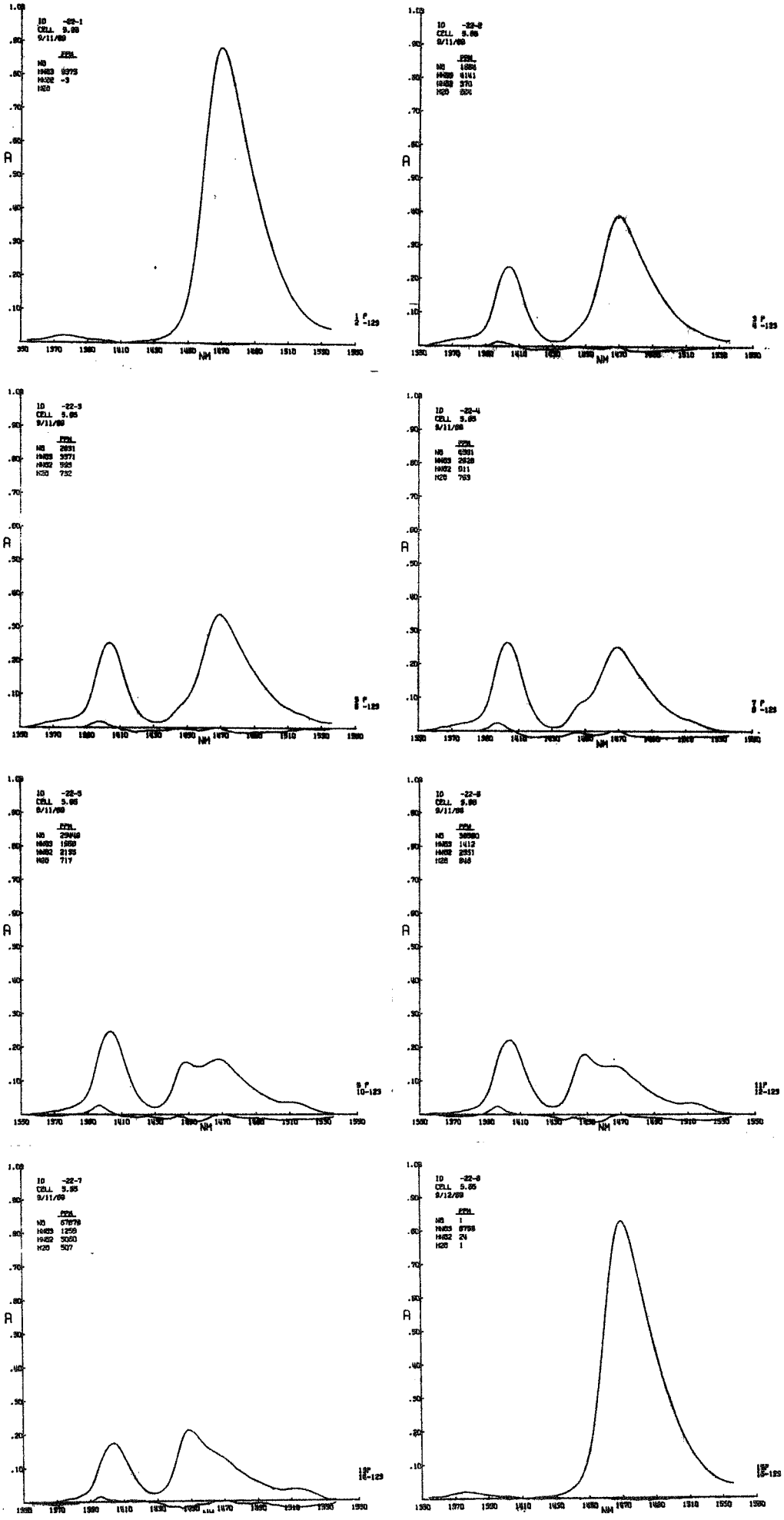

nanometers or 1, 2, and 3 to represent H_2O, HNO_2, and HNO_3, respectively. Note that the subscript is the same as the number of oxygen atoms in the molecule. The asterisk denotes multiplication.

(2) The Use of the Reference Spectra - The absorptivities at each wavelength for each of the three components are, of course, related to one another in fixed ratios which are determined by the shape of the reference spectrum. By normalizing these ratios (relative absorptivities) to the absorbance of the analytical band in each case, the equations become:

$$A_{1404}/b = 1.0*a_1*c_1 + 0.0*a_2*c_2 + 0.006*a_3*c_3$$

$$A_{1448}/b = 0.006*a_1*c_1 + 1.0*a_2*c_2 + 0.118*a_3*c_3$$

$$A_{1470}/b = 0.0*a_1*c_1 + 0.043*a_2*c_2 + 1.0*a_3*c_3$$

(3) Reference Spectra Applied to Calibration Mixtures - Using the absorbances at the three wavelengths as measured in a series of seven calibration spectra, these equations can be solved for the three products, (a_1*c_1), (a_2*c_2), and (a_3*c_3) by inversion of the matrix of relative absorptivities. These results are seven sets of three values. For example, the first two of these seven sets can be expressed as:

$$a_1*c_1 = K_1 \qquad a_1*c_1' = K_1'$$

$$a_2*c_2 = K_2 \qquad a_2*c_2' = K_2'$$

$$a_3*c_3 = K_3 \qquad a_3*c_3' = K'$$

where the K values are the solutions of the simultaneous equations above. Note that the absorptivities, a, are assumed to be the same in all seven sets.

The total proton content represented by each set of data is the same. It has been determined by measuring the 1.470μ band after treatment with O_2 and found to be 9340 ppm. as HNO_3. The dilution factor due to NO added to shift the equilibria can be calculated by:

$$D.F. = 1 - (\text{ppm. NO}/10^6).$$

Thus, the three equations which represent the proton material balance for the first three of the seven sets of data are:

$$2*c_1 + c_2 + c_3 = 9340*(D.F.)/63$$

$$2*c_1' + c_2' + c_3' = 9340*(D.F.)'/63$$

$$2*c_1'' + c_2'' + c_3'' = 9340*(D.F.)''/63$$

The constant factor of 2 is necessary because of the two protons in H_2O, and that of 63 serves to convert ppm. of HNO_3 into ppm. of protons. When the c's above are replaced by their equivalents in terms of K/a, the three equations can be solved for the a's.

A computer program to perform these calculations is described in Appendix III.

Any combination of three of the seven sets of data would yield a solution. Ideally all combinations would produce the same solution, but several factors made the use of all combinations impractical. Primary among these is the fact that the concentrations of the components were not sufficiently different in all of the samples to provide reliable results after matrix inversion. Therefore, nine combinations were chosen based on the relative concentrations as indicated by inspection of the calibration spectra, Fig. 12. Spectrum -22-1 was used in all nine because it represents

pure HNO_3. Combined with it successively were -22-2, -22-3, and -22-4, all relatively high in H_2O and low in HNO_2. Then -22-5, -22-6, and -22-7, all relatively high in HNO_2, were combined successively with each of the binary combinations. The nine absorptivities calculated for each component were averaged and the means used as the working absorptivities for initial quantitative analyses. These results are summarized in Table 5.

Table 5

Calculated Absorptivities
(Concentrations expressed as ppm of Protons)

Combination	H_2O	HNO_2	HNO_3
1, 2, 5	1.056×10^{-3}	5.448×10^{-4}	1.017×10^{-3}
1, 2, 6	1.064	5.084	1.017
1, 2, 7	1.076	4.573	1.017
1, 3, 5	1.070	5.326	1.017
1, 3, 6	1.081	4.982	1.017
1, 3, 7	1.100	4.500	1.017
1, 4, 5	0.973	6.485	1.017
1, 4, 6	1.001	5.532	1.017
1, 4, 7	1.037	4.704	1.017
Mean	1.051×10^{-3}	5.182×10^{-4}	1.017×10^{-3}
Rel. Std. Deviation	3.86%	11.87%	0%
Working Absorptivity(1)	5.84×10^{-5}	1.10×10^{-5}	1.61×10^{-5}(2)

(1) Concentrations expressed as ppm of the molecular equivalents.

Note (2): This value compares to 1.616×10^{-5} used originally to calculate HNO_3.

The data clearly showed that HNO_2 was the most troublesome component. It also showed that, with these reference spectra, there were distinct trends in the calculated absorptivities of H_2O and HNO_2 as spectra -22-5, -22-6, and -22-7 were used in the analysis.

(4) Use of the Absorptivities in Quantitative Analysis

The working absorptivities which are listed at the bottom of Table 5 are provided to the computer program in the form of the inverse matrix from which the concentrations of each component can be calculated as the digital spectra are processed.

Use of the inverse matrix to calculate the concentration of each of the protonated species in the calibration series gave the results shown in Table 6.

Table 6

Computer Analyses of Calibration Mixtures

Sample Designation	Concentration, ppm. by wt.			
	NO	HNO_3	HNO_2	H_2O
X16054-22-1	0	9375	-	-
-2	1664	4141	370	684
-3	2831	3571	593	732
-4	4591	2628	911	763
-5	25448	1658	2135	718
-6	38580	1412	2551	648
-7	67878	1259	3060	507
-8	1	8769	24	1

The concentration of HNO_3 in the oxygenated starting material (-22-1) was 9375 ppm. but in the final oxygenated sample (-22-8) it had dropped about 6.5% to 8769 ppm. This was accounted for by dilution due to addition of NO and was in reasonable agreement with the calculated amount of NO added, 67878 ppm. or 6.8%. Because of this agreement, the calculated ppm. of NO in each sample of the series was used as the dilution factor to calculate the total concentration of protons (as HNO_3). Converting the computer-calculated concentrations of HNO_2 and H_2O to ppm. HNO_3 by multiplying by 63/47 and 63/9 respectively, and adding these to HNO_3 provided data for the proton balance shown in Table 7.

Table 7 - Proton Balance (X16054-22)

	Experimental Protons as ppm. HNO_3 converted from:				Known Total Proton conc. as ppm. HNO_3 corrected for dilution by NO	Balance Exper. x 100/ Known
	HNO_3	HNO_2	H_2O	Total		
-1	9375	-	-	9375	9375	100
-2	4141	496	4788	9425	9355	100.5
-3	3571	795	5125	9491	9335	101.5
-4	2628	1222	5340	9190	9315	98.8
-5	1658	2860	5025	9543	9130	104.2
-6	1412	3420	4535	9367	9000	104.0
-7	1259	4103	3550	8909	8730	102.0
-8	8769	32	7	8808	8730	100.7

The calibration procedure described above was repeated because its complexity provided many possibilities for errors and because it was important to establish the significance of the apparent trends in the absorptivities of the protonated species at high NO levels.

An experiment was performed using about the same total proton concentration (9161 ppm. vs. 9375 ppm.) but proceeding to higher NO concentrations (Tables 8 & 9). The overall experiment was found to be satisfactorily repeatable (Fig. 13), but it also appeared to show that at NO concentrations greater than about 7.5%, protons were apparently lost from the solution phase. The apparent loss of protons was illustrated by the following trends and data. HNO_3 decreased very rapidly initially, then more slowly. H_2O reached its maximum concentration at a NO level of less than 1.0% and decreased at a nearly constant rate thereafter HNO_2 increased at a rate which kept the total proton count nearly constant up to about 7.5%, after which it leveled off. The net result of these trends is shown by the material balance which accounted for only about 92% of the protons as soluble species at 10% NO. This phenomenon might be explained in several ways:

(a) The nature of the O-H bonds which give rise to the absorption bands used in the analysis have changed so as to change the absorptivities.

(b) Protonated species have precipitated or entered the gas phase.

Table 8

Computer Analysis of Calibration Mixtures

Sample Designation	Concentration, ppm. by Weight NO	HNO_3	HNO_3	H_2O
X16054-23-1	7	9161	65	1
-2	748	5142	244	525
-3	1524	4290	360	617
-4	2805	2831	860	724
-5	19838	1897	1939	711
-6	35071	1512	2410	624
-7	55081	1360	2871	545
-8	76062	1290	3086	455
-9	100964	1250	3000	332
-10	51	8016	14	5

Table 9

Proton Balance (X16054-23)

	Experimental Protons as ppm. HNO_3 converted from HNO_3	HNO_2	H_2O	Total	Known Total Proton conc. as ppm. HNO_3 corrected for dilution by NO	Balance Exper. x 100/ Known
-1	9161	-	-	9161	9161	100.0%
-2	5142	327	3675	9144	9155	99.9
-3	4290	482	4319	9091	9147	99.4
-4	2831	1152	5068	9051	9135	99.1
-5	1897	2594	4977	9468	8980	105.4
-6	1512	3230	4368	9110	8839	103.1
-7	1360	3848	3815	9023	8656	104.2
-8	1290	4136	3185	8611	8464	101.7
-9	1250	4021	2324	7595	8236	92.2
-10	8016	-	-	8016	8236	97.3

X16054- 22 -23

FIGURE 13

CONCENTRATION OF HNO_3, HNO_2, AND H_2O VERSUS NO ADDED

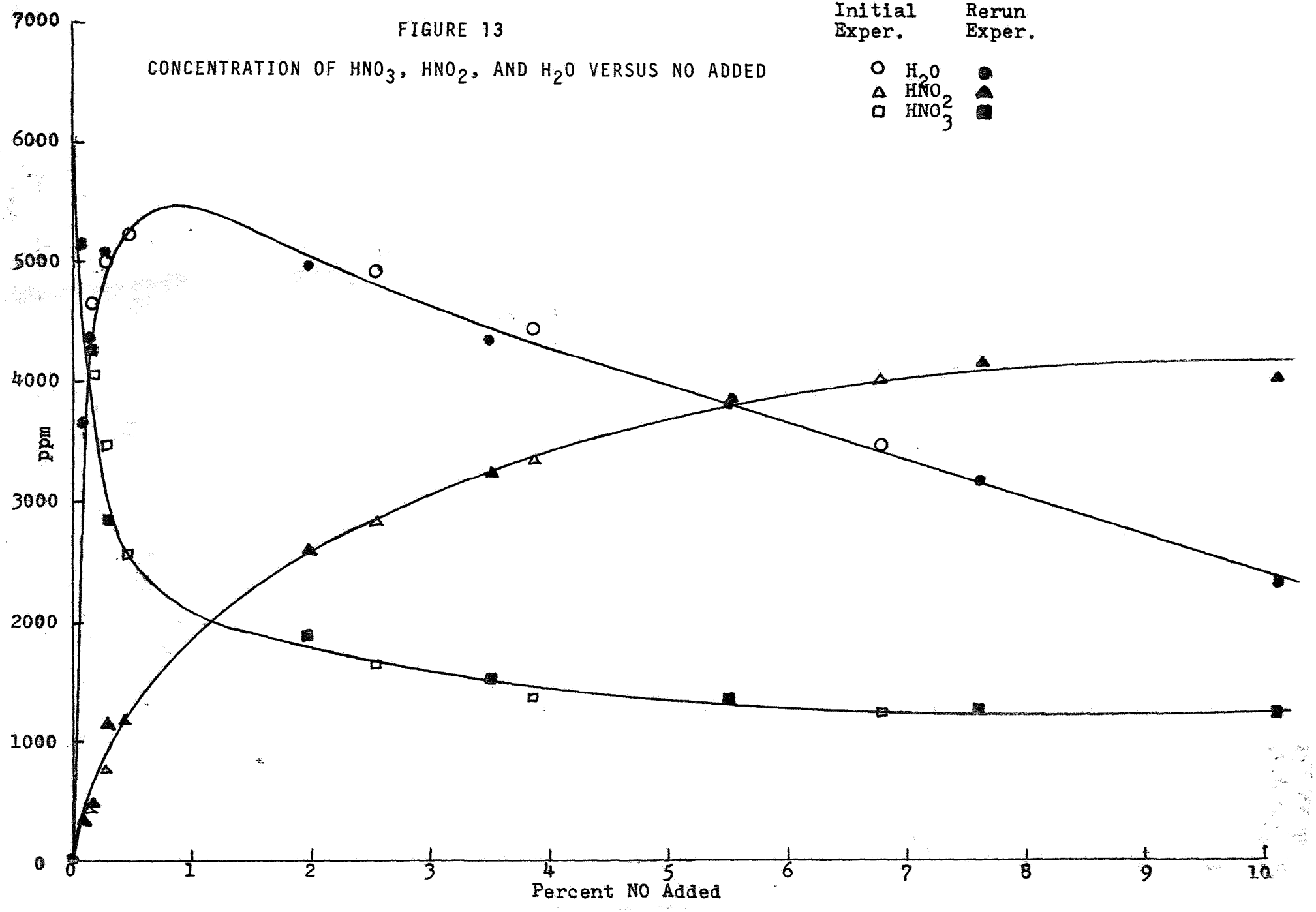

The first explanation is less likely for the following reasons. The shapes of the bands did not change significantly, thus changes in hydrogen bonding would not seem to be important. No new bands were observed in the range 1350-1550 nm. where any new O-H species is expected to absorb. The broad, greatly shifted absorption bands due to polymeric hydrogen bonds would probably fall outside this range, but it is difficult to imagine how continued addition of NO would produce such results. Protons directly bonded to nitrogen might also fall outside the range. This again seems to be an unlikely possibility, although the existence of two tautomeric forms, HONO and HNO_2, have been postulated for nitrous acid.

At high NO levels, the solution is opaque to visible light so that no visual observation of an insoluble phase is possible. However, the effects of Rayleigh scattering from small particles of a second phase would be readily observed in this wavelength region. No such effect was observed. An insoluble phase adhering preferentially to the side walls of the cell is still a possibility, however. The remaining explanation in which a protonated species is concentrated in the gas phase is supported by two bits of information. The concentration of HNO_2 levels off near 3000 ppm. at NO concentrations greater than 7.5% even though HNO_3 and H_2O continue to decrease. This apparent saturation of HNO_2 in N_2O_4 was unexpected but is not unreasonable because HNO_2 is sufficiently different chemically from both HNO_3 and H_2O. The second piece of evidence to support this theory was obtained when

some of the gas phase in the sample cell was vented after the final addition of NO. The venting was done to facilitate the addition of oxygen which converts all of the protonated material back to HNO_3 as a check on the material balance. This time the final proton count was low by 2.5% although in the similar calibration experiment performed earlier and at lower NO concentration the check was much better. Such a result permits one to speculate that a disproportionate amount of HNO_2 was removed along with the vented NO.

(5) Comparison of Absorptivities - Only those spectra with NO levels near 5% or less were used to calculate a new set of absorptivities for HNO_3, HNO_2, and H_2O. The absorptivities and their 95% confidence intervals are summarized in Table 10.

Table 10

Absorptivities of Protonated Species

	Absorptivity x 10^5 (concentration in ppm. by wt.)		
	H_2O	HNO_2	HNO_3
Calibration 1	5.84 ± 0.52	1.10 ± 0.30	1.61 ± 0.0
Calibration 2	5.70 ± 0.10	1.10 ± 0.06	1.63 ± 0.02
Average	5.77	1.10	1.62

The agreement between the two calibrations is excellent. The average values were incorporated in the computer program as the new absorptivities for the analysis of mixtures. The greatly improved precision of the data in the second experiment reflected increased skill in the experimental manipulation of this difficult system.

(6) Water Addition to Deprotonated, NO-Free N_2O_4 - The 5.85 cm. spectrophotometric cell was fitted with a septum through which water could be introduced from a microliter syringe. After drying thoroughly in a 110°C. oven, the tared cell was filled with deprotonated, NO-free N_2O_4, and reweighed. After chilling to -10°C. in the spectrophotometer, the sample was scanned. Five 5.0 µl. and four 10.0 µl. increments of water were injected into the sample followed by a thorough mixing and a scan after each addition. The analytically determined concentrations of HNO_3 and HNO_2 expressed as ppm. H_2O (Table 11) were added to the determined concentration of H_2O. The total was plotted against known ppm. H_2O added as calculated from the volume of water added and the weight of the N_2O_4 sample. This plot is shown in Figure 14. The incongruous offset observed between the fifth and sixth additions in the otherwise linear plot can most reasonably be explained by a bubble in the syringe causing the actual addition of less water than was intended. Assuming that this explanation is correct, the unit slope of the plot confirms the accuracy of the computer analysis of the digitized spectra. Figure 15 shows the three species (calculated as ppm. H_2O from the computer analysis plotted) versus ppm. H_2O added. In this plot, the "ppm. H_2O added" has been corrected for the offset in Figure 14 to reflect water actually added. For comparison to Figure 15, which shows the proton distribution at a relatively low NO to proton ratio, Figure 13 shows the proton distribution at a relatively high NO to proton ratio. It is a plot of the concentration of each of the protonated species, versus % NO added.

FIGURE 14

TOTAL PROTONS (AS H_2O) FOUND VERSUS H_2O ADDED TO DEPROTONATED NO-FREE N_2O_4

X16054-26

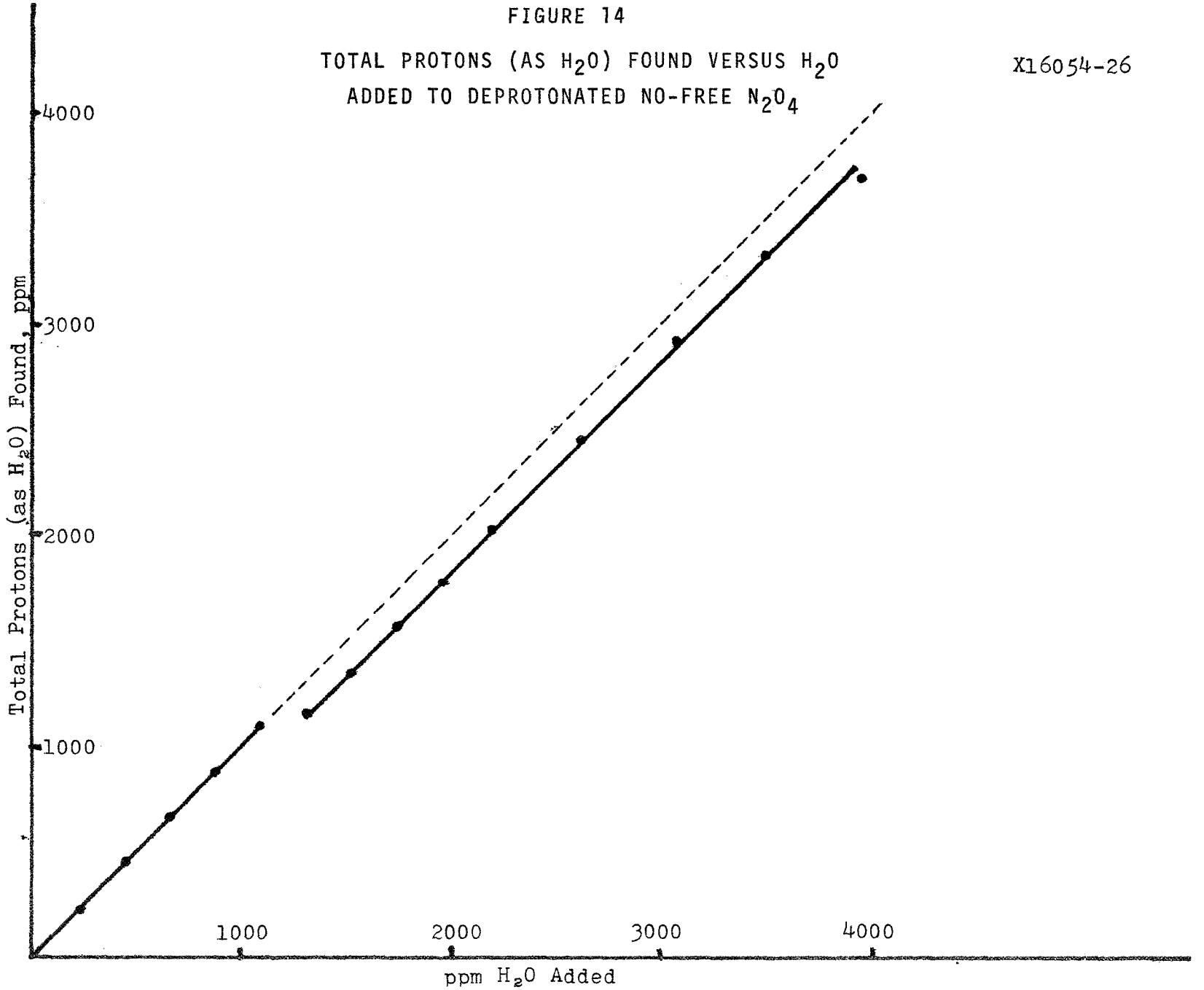

FIGURE 15

CONCENTRATION OF HNO_3, HNO_2, H_2O AND NO VERSUS H_2O ADDED

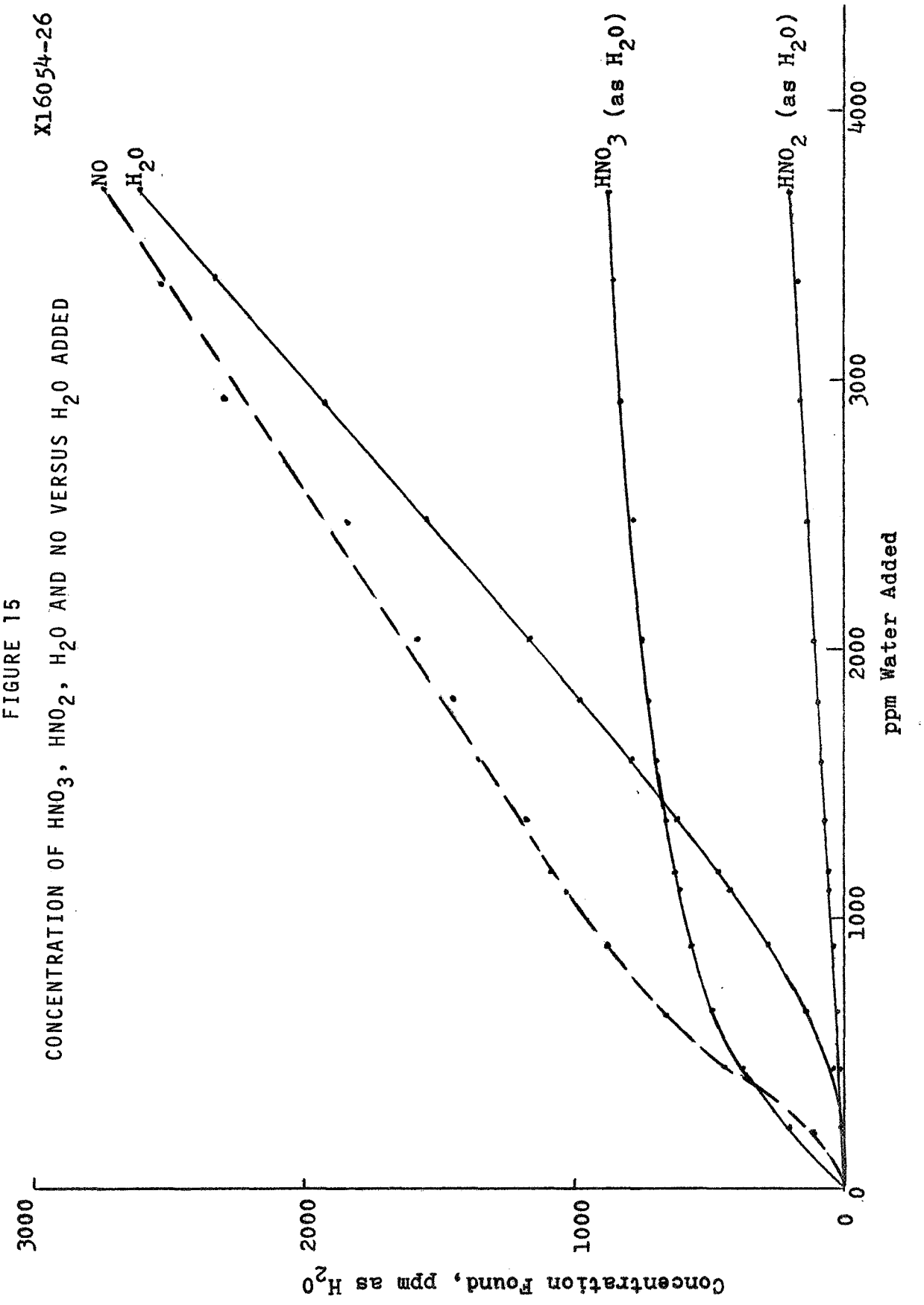

Table 11

Addition of Water to Proton-free N_2O_4
Cell Length - 5.85 cm. N_2O_4 wt. - 22.9 g.

				Computer Analysis, ppm.					
		H_2O Added		Protonated Species			Protonated Species, calc. as H_2O		
	NO, ppm.	µl. (mg.)	ppm.	HNO_3	HNO_2	H_2O	HNO_3	HNO_2	Total
1	5	-	-	20	21	4	3	4	11
2	104	5	218	1380	71	12	197	14	223
3	441	10	437	2657	83	43	380	16	439
4	676	15	655	3426	104	145	489	20	654
5	867	20	873	3941	185	289	562	35	886
6	1036	25	1092	4297	294	428	614	56	1098
7	1084	30	1310	4434	301	478	633	58	1169
8	1180	35	1528	4631	391	623	662	75	1360
9	1353	40	1747	4904	452	794	700	87	1581
10	1456	45	1965	5071	515	981	724	99	1804
11	1589	50	2183	5259	575	1167	751	110	2028
12	1842	60	2620	5508	718	1546	787	137	2470
13	2289	70	3056	5758	844	1936	823	162	2921
14	2535	80	3493	5988	928	2327	855	178	3360
15	2738	90	3930	6152	1069	2614	879	205	3698

The data for this plot was taken from the proton calibration experiments in which NO was added incrementally to N_2O_4 containing about 9000 ppm. HNO_3. Reasonably good agreement is apparent between the duplicate calibration experiments.

4. Elevated Temperature Studies

Prior to making elevated temperature composition studies of the protonated species in N_2O_4, it was necessary to determine the absorbance contribution versus temperature of NO_2 in the spectral region where NO is measured. An experiment was run in which deprotonated RR N_2O_4 was repetitively scanned from 1550 to 700 nm. as the temperature was raised in approximately 5° intervals, from -10° to +50°C. The first scan (-10°C.) was used as reference and subtracted from the remaining spectra. Figure 16 shows the net spectra of the scans at -2, 5, 10, 15, 20, 25, and 30°C. using the 0 to 0.1 absorbance slidewire. Figure 17 shows the net spectra of the scans at 35, 40, 45, and 50°C. using the 0 to 1.0 absorbance slidewire. The absorbance difference between 752 nm. (the shortest wavelength at which an absorbance measurement could be made on all of the curves) and 940 nm. (the shortest wavelength at which the absorbance appeared essentially independent of temperature) was measured and plotted against temperature, (Figure 18). The actual concentration of NO_2 was not known at any temperature in the range, but the plot is an accurate representation of the relative concentration at all temperatures in the range.

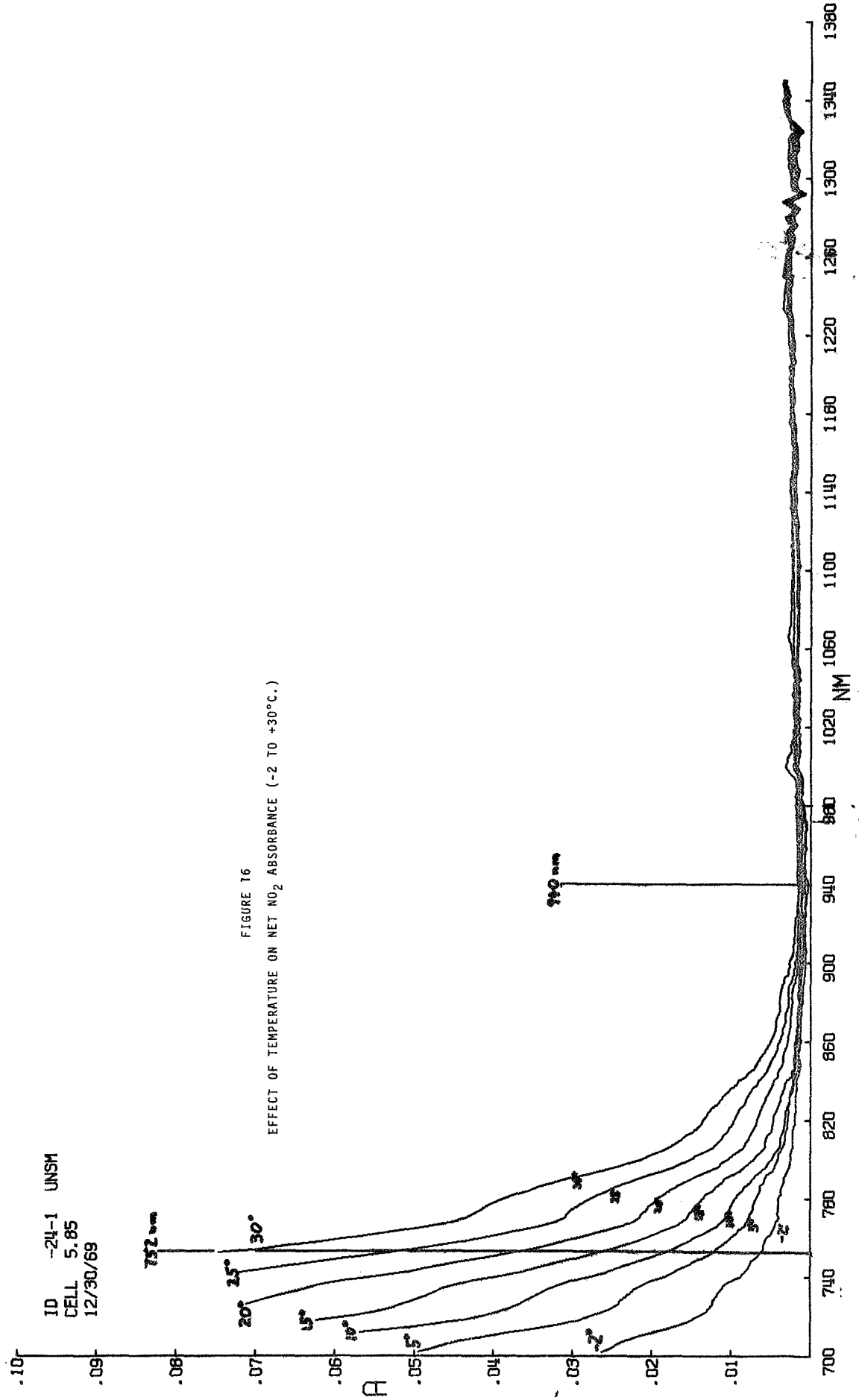

FIGURE 16

EFFECT OF TEMPERATURE ON NET NO_2 ABSORBANCE (-2 TO +30°C.)

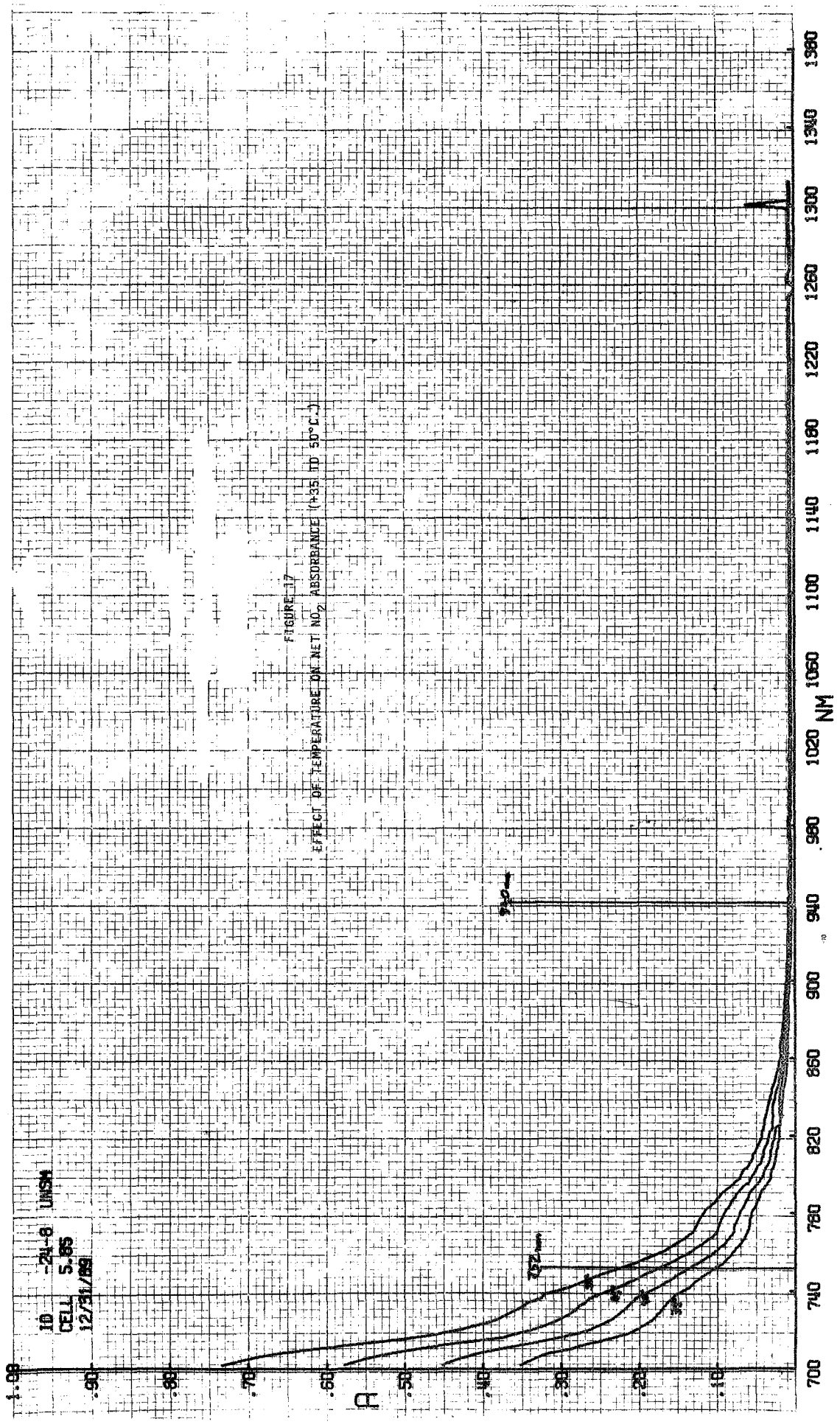
FIGURE 17
EFFECT OF TEMPERATURE ON NET NO_2 ABSORBANCE (+35 TO 50°C.)
ID -24-8
CELL 5.0S
12/31/69
UNSM
1.00
.90
.80
.70
.60
.50
.40
.30
.20
.10
700
740
780
820
860
900
940
980
1020
1060
1100
1140
1180
1220
1260
1300
1340
1380
NM
A
+50
+45
+40
+35
472 nm

FIGURE 18

NET NO_2 ABSORBANCE VERSUS TEMPERATURE

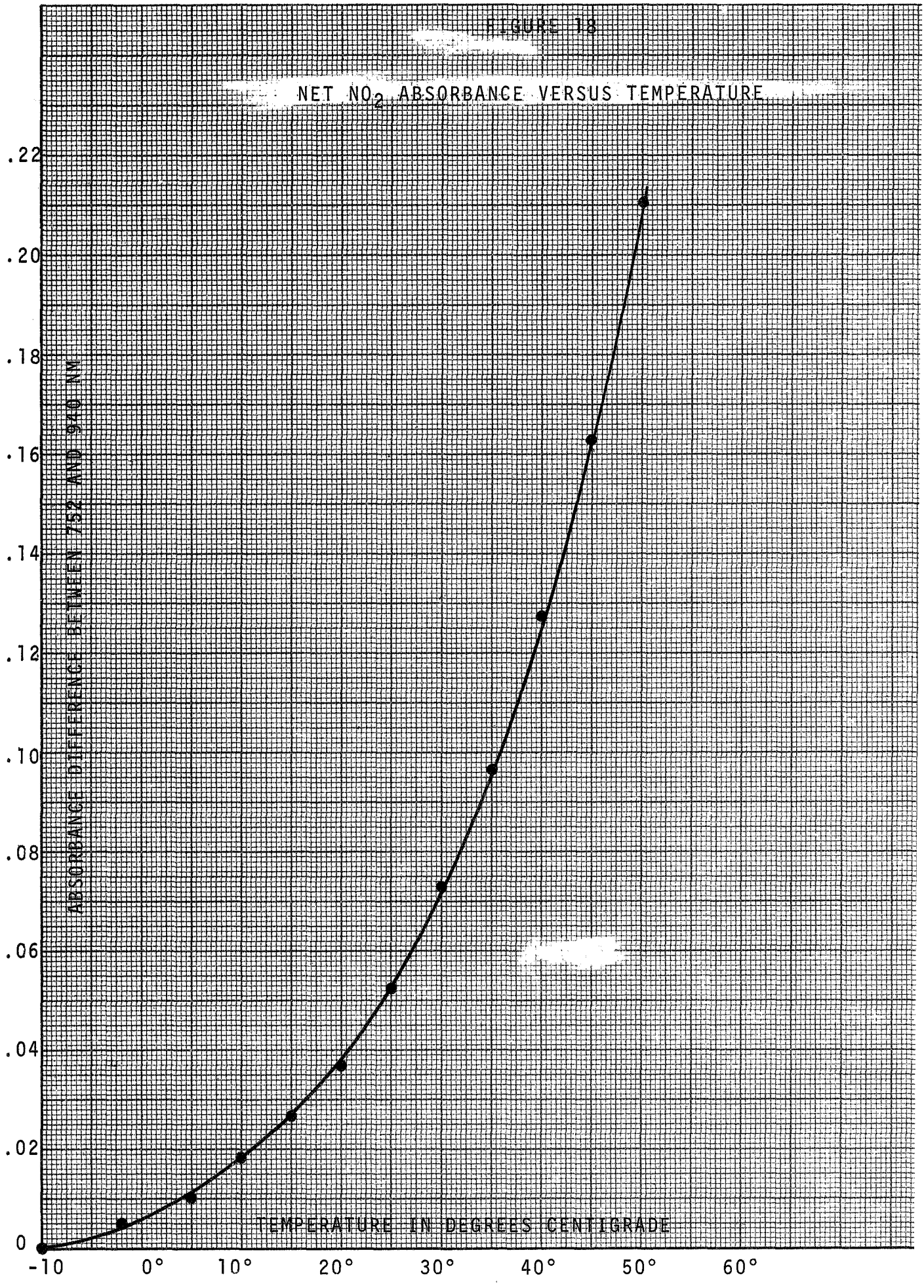

For the purposes of this work, only the relationship between absorption due to NO_2 and temperature was required so that corrections could be made for the absorption due to NO_2 when measuring the absorption of NO at temperatures above -10°. Because these calculations are performed by a computer, it was necessary to obtain a mathematical model to represent the curve. The absorbance vs. temperature data were fitted to a polynomial using least squares as a criterion for goodness of fit. A second order polynomial gave a poor fit at the low end, but a third order polynomial produced a good fit with a standard error of estimate of 0.0011 for absorbance in the range 0 to 0.211. Because the relationship is expected to be smooth and continuous, most of this deviation represents experimental error. Nevertheless, absorbance errors of this magnitude reflect excellent control over the experiment. The equation is $\Delta A = 7.069 \times 10^{-3} + 8.037 \times 10^{-4} \cdot t + 1.643 \times 10^{-5} \cdot t^2 + 9.720 \times 10^{-7} \cdot t^3$, where ΔA is the absorbance difference between 752 and 940 nm. and t is temperature, °C. The computer program was modified to calculate the relative absorbance, to scale it according to the various wavelength intervals, cells, and slidewires used, measure NO, and to subtract it from the total absorbance to yield absorbance due to NO.

An experiment was run to investigate the suspected change of band shape, peak intensity, and wavelength shift of the HNO_3 band with temperature. RR N_2O_4 in the 5.85 cm. cell was scanned as the temperature was raised in 5 to 10° intervals from -10 to +70°C. (X16054-27). Above 40°C. the spectra became somewhat

noisy suggesting localized bubble formation or boiling. Sharp edges around the outlet orifice could be conducive to localized boiling, therefore a smooth stainless steel sleeve was made and inserted in the cell prior to a second run (X16054-30). Some spectral improvement was noted but the problem was not entirely eliminated. Data from these two runs, shown in Table 12, confirmed the shift to lower wavelength and increase of peak intensity with increasing temperature. Also observed was a reasonably constant band area over the temperature range -10 to +30°C. where the good quality spectra were obtained. Two experiments were run using G8 N_2O_4, identical to the previous RR runs. Handling of the data obtained from these experiments is discussed in the section on Equilibrium Studies.

5. Accuracy & Precision in the Determination of Combined NO, HNO_3, HNO_2, and H_2O

No comprehensive analysis of accuracy and precision was performed during the contract work period. However, data which bear on some of the more critical parameters has been assembled.

The accuracy of the analyses for NO and HNO_3 can be estimated because they were both calibrated directly by incremental addition of samples of known purity to known amounts of N_2O_4. The basic calibration for NO has previously been reported (1). The calibration for HNO_3 is described in Section I.B.3. In each case the assumption is made that no systematic error is present in the experimental procedures and that accuracy attained in the analysis of the pure components is retained during the analysis of mixtures.

Twenty-nine additions of NO to N_2O_4 yielded a calculated absorptivity which exhibited a relative error of 1.47% at the 95% confidence level. The data for the addition of HNO_3 to N_2O_4 was obtained from two experiments in which the total HNO_3 added was compared to the total absorbance measured (Table 4). These data were treated by least squares fits to straight lines. The standard errors of estimate for these two sets were pooled and compared to the mean. The relative error at the 95% confidence level is 2.0%.

The accuracy of the analyses for HNO_2 and H_2O depend on the accuracy of those for HNO_3 and NO since they are based on measurement of the latter two. However, because of the complexity of the analysis procedure for HNO_2 and H_2O and the increased possibilities for systematic errors, one must assume that the accuracy of these analyses may be poorer.

In evaluating precision, the analysis for HNO_3 and NO must again be considered separately from that for HNO_2 and H_2O. The standard deviations found for the entire analysis, from sampling through computer processing, for randomly selected samples (34 degrees of freedom), is 28 ppm. for HNO_3 and 18 ppm. for NO. The standard deviations found for HNO_2 and H_2O are about the same, but because they are normally the minor components, the relative errors are high. This problem is accentuated by the presently poorly understood variations in "spectroscopic background" (e.g., see Figure 12). They are often severe enough to cause directly determined concentrations of HNO_2 and H_2O to be

unacceptable. For this reason, the concentrations of HNO_2 and H_2O are calculated from their equilibrium relationships to HNO_3 and NO as described in Appendix IV. The effect of this procedure is to impose the relative precision in the determination of HNO_3 and NO on that for HNO_2 and H_2O.

C. Equilibrium Studies

The primary equilibria which represent this system are:

$$N_2O_4 + H_2O \rightleftharpoons HNO_3 + HNO_2 \quad (1)$$

$$3HNO_2 \rightleftharpoons HNO_3 + 2NO + H_2O \quad (2)$$

The commonality of reactants and products in both equilibria makes them strongly interactive. The equilibrium constants associated with these equilibria are expressed as:

$$K_1 = \frac{[HNO_3][HNO_2]}{[N_2O_4][H_2O]} \quad (3)$$

$$K_2 = \frac{[HNO_3][NO]^2[H_2O]}{[HNO_2]^3} \quad (4)$$

where the component concentrations are expressed as moles/liter. Note that this system in the condensed phase, as in this work, has N_2O_4 both as solvent and reactant.

The analytical system previously described is capable of measuring the concentrations of all five components (N_2O_4 by difference). Thus, it was a simple matter to calculate the equilibrium constants by converting from ppm. to moles/liter and substituting in the above equations. Unfortunately, this elaborate analytical procedure was geared to produce accurate analyses only at -10°, and one of the great advantages to be gained by a knowledge of the equilibrium relationships is the ability to

predict the composition of a system at different temperatures. In the present case, it was necessary to predict the composition of the system at 70°, the stress corrosion test temperature, from analyses performed at -10° because the experimental problems involved in direct analyses near 70° were too formidable.

The protons in RR and G8 N_2O_4 are all attached to oxygen. These NOH groups are hydrogen-bonded to the solvent N_2O_4 and exhibit the expected changes in shape and position of the near-IR absorption bands when the temperature is increased. The modified analytical procedure which was devised to accommodate these changes is based on the assumption that the integrated intensity of the bands is constant over the temperature range of interest. Several observations serve to verify this assumption within acceptable limits. They are especially important because in more ordinary cases of hydrogen-bonding (e.g., alcohols), the intensities of these absorptions may suffer order of magnitude decreases as the temperature increases through this range. In the case of RR N_2O_4, however, the integrated intensity of the OH band of HNO_3 does not decrease as the solution is heated from -10° to 30°. In fact, whereas the measured area remains constant, the density decreases by about 6%. This corresponds to a 6% increase in integrated intensity. Further evidence that the hydrogen bonds in this system are different in their response to temperature change is the rate of change of peak position. The HNO_3 peak moves at a rate of about 0.5 $cm.^{-1}$/degree. By comparison, the rate is about 3 $cm.^{-1}$/degree for alcohols. The band widths are

about half those of alcohols. The assumption thus validated for HNO_3 is extended to HNO_3 and H_2O.

Band areas were measured in arbitrary units using a planimeter. The slight distortion which results from measuring band areas on a scale linear in wavelength is self-compensating. The baseline for the H_2O band is drawn between 1380 nm. and 1430 nm. That for the merged HNO_2 and HNO_3 bands is drawn between 1430 nm. and 1530 nm. These data for RR and G8 N_2O_4 are summarized in Tables 12 and 13. All measurements were made on computer drawn spectral plots which were corrected for instrument, N_2O_3, and N_2O_4 background. The computer was not used directly for making these measurements because the programming effort would have been greater than that required to obtain this limited data manually.

At temperatures above 30° a bubble problem developed in the absorption cell which appeared to be the prime contributor to uncertainty in the spectrophotometric data. Thus, only the data in the range -10° to 30° were used to establish the equilibrium constant-temperature relationships (Figure 19) and these results were then extrapolated to 70°. Because there is no evidence for discontinuous changes in chemical or physical properties in the total range, the extrapolation appears to be a reasonable procedure.

The scheme for calculating concentrations from spectra obtained at temperatures above -10° is the following. The relationship between the absorptivity of HNO_3 at 1470 nm. and temperature is summarized at the end of Table 12. The small

FIGURE 19 - EFFECT OF TEMPERATURE ON PROTON DISTRIBUTION

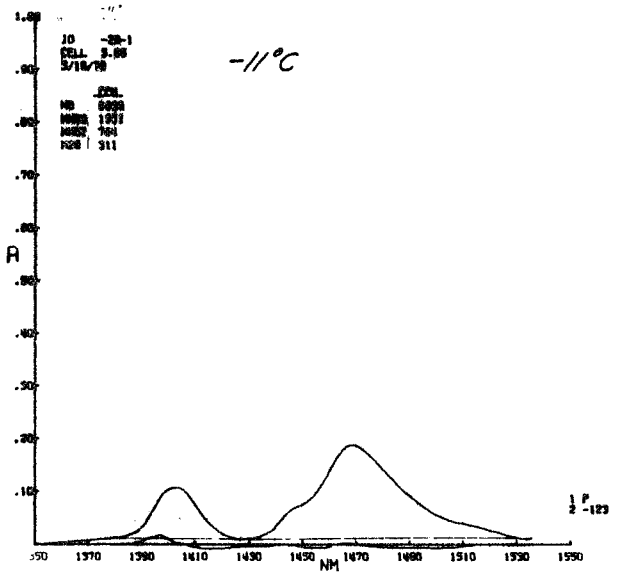

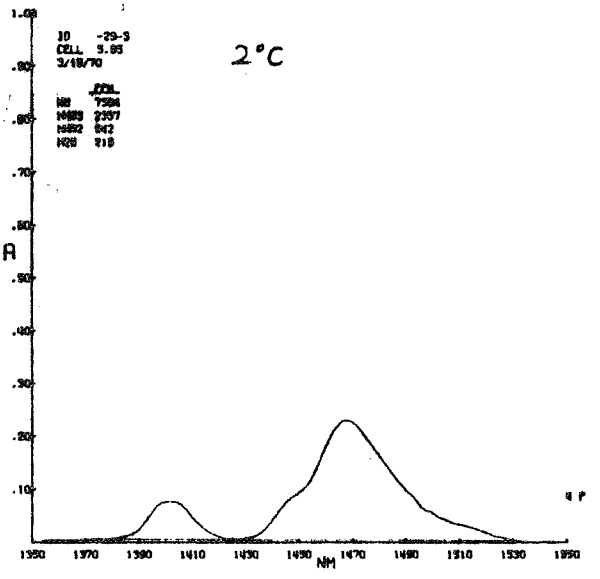

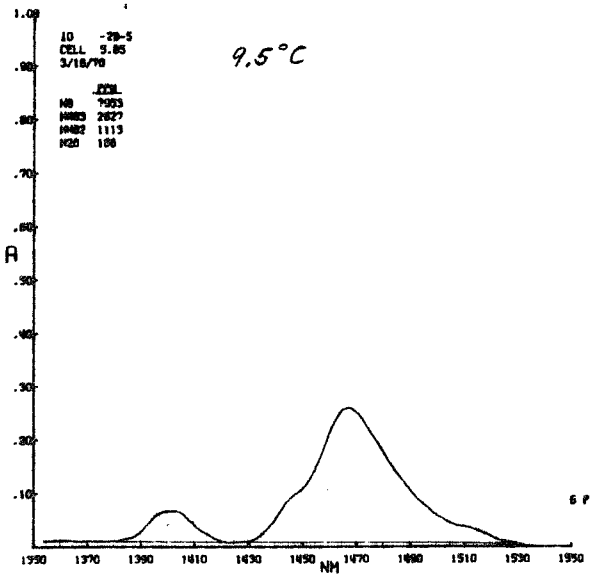

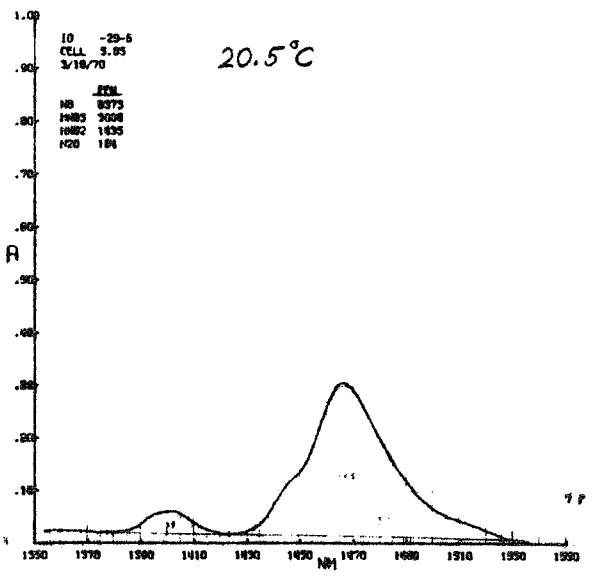

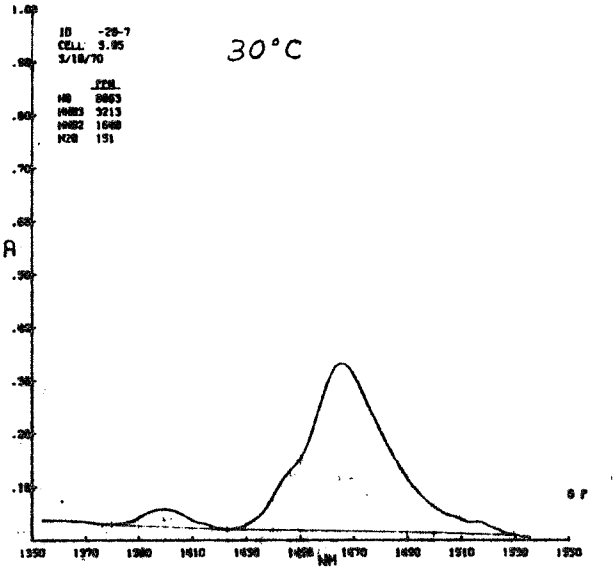

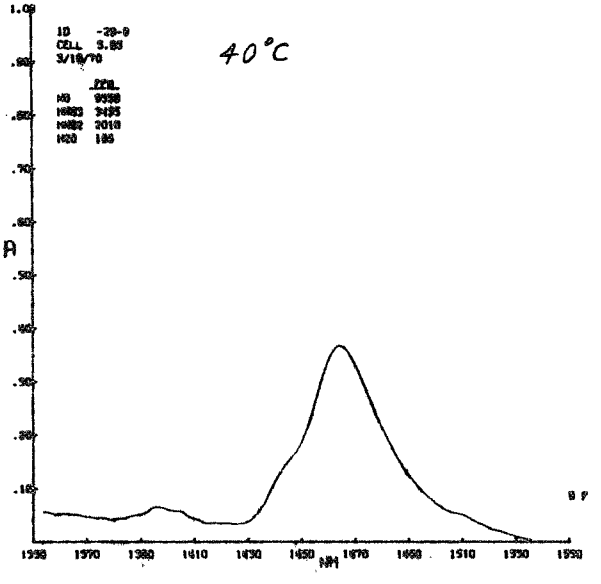

Table 12

Peak Position and Absorptivity of the 1470 nm. Band in RR N_2O_4 vs. Temperature

Sample	Temp., °C.	λ max.	a x 10^{-5} $cm.^{-1}$ $ppm.^{-1}$	Area (Arbitrary Units)
X16054-30-1	-11.5	1470	1.570	563
-27-1	-10.0	1470	1.572	563
-27-2	-5.0	1469	1.594	570
-30-2	-4.5	1469	1.585	555
-30-3	1.0	1469	1.591	555
-27-3	1.8	1469	1.621	570
-27-4	5.2	1468	1.621	567
-30-4	6.0	1468	1.619	560
-30-5	9.5	1468	1.619	555
-27-5	11.6	1468	1.638	564
-27-6	20.2	1467	1.670	567
-30-6	20.5	1467	1.649	565
-27-7	30.0	1466	1.691	569
-30-7	31.0	1466	1.682	563
-30-8	39.5	1465	1.787	591
-27-8	40	1465	1.790	588
-27-9	50	1464	1.835	592
-30-9	50	1464	1.807	597
-30-10	59	1464	1.831	581
-27-10	60	1463	1.946	642
-30-11	69	1463	1.795	587
-27-11	70	1462	1.958	621

$a = 1.602 \times 10^{-5} + 2.786 \times 10^{-8} \times t$ (-11.5 to 31.0°)

std. error of estimate = 0.0086×10^{-5}

Table 13

Summary of Spectrophotometric Data from G8 N_2O_4 at Various Temperatures

Sample	Temperature	ΔA (1470 nm.)	Area (1404 H_2O Band)
X16054-28-1	-11.0	.172	60
-29-1	-11.0	.177	63
-29-2	-6.0	.197	56
-28-2	-5.0	.195	54
-28-3	0.5	.214	47
-29-3	2.0	.225	45
-28-4	4.5	.230	45
-29-4	5.0	.236	42
-29-5	9.5	.252	39
-28-5	10.0	.250	38
-28-6	20.5	.285	27
-29-6	20.5	.292	28
-28-7	30.0	.320	23
-29-7	30.0	.315	23

correction for overlap of HNO_2 at the relative concentrations of this work is negligible. The relationship between the area of the H_2O band and the ppm. of H_2O was calculated from the standard spectrum of H_2O, Figure 7, and found to be 5.02 ppm. per unit area. This factor, of course, depends on the cell pathlength and the planimeter tracer arm setting, both of which were held constant throughout. These two relationships were used to calculate the ppm. of HNO_3 and H_2O in two samples of G8 N_2O_4 at a series of temperatures between -10° and 30°. The measured areas of the H_2O band were corrected for the spectrophotometric dilution caused by decreased density. The concentration of HNO_2 was calculated from the known total protons corrected for the contributions of HNO_3 and H_2O using the relationship: ppm. HNO_2 = $\left(\text{total ppm. protons} - \frac{\text{ppm. } HNO_3}{63} - \frac{\text{ppm. } H_2O}{9}\right) \times 47$. These results are summarized in Table 14 which also contains the ppm. of NO measured by the normal procedure and corrected for density changes as in the case of the H_2O measurement. The ppm. of N_2O_4 is 10^6 minus the sum of the other four components. Each of these concentrations in ppm. is converted to moles/liter from the relationship:

$$\text{moles/liter} = \frac{\text{ppm. x density x } 10^3}{\text{molecular weight}} \qquad (5)$$

Density at t degrees centigrade is calculated from the empirical equation

$$d = 1.4927 - 2.235 \times 10^{-3}\, t - 2.75 \times 10^{-6}\, t^2$$

The equilibrium constants K_1 and K_2 (equations 3 and 4) are listed

Table 14

Summary of Results of Analysis of G8 N_2O_4 vs. Temperature

X16054	Temp.,°C.	Density	ppm. NO	HNO_3	HNO_2	H_2O	$10^3/T$,°K.	$K_1 \times 10^3$	K_2	$K_3 \times 10^3$
-28-1	-11.0	1.5170	6770	1877	803	302	3.82	2.823	7.738	0.4172
-29-1	-11.0	1.5170	6929	1927	756	316	3.82	2.603	10.431	0.4302
-29-2	-6.0	1.5060	7139	2132	805	283	3.75	3.431	9.033	0.6040
-28-2	-5.0	1.5038	7208	2115	806	273	3.73	3.529	8.771	0.6209
-28-3	0.5	1.4916	7532	2315	859	240	3.66	4.694	7.533	0.8826
-29-3	2.0	1.4882	7638	2433	896	230	3.64	5.358	6.878	1.0284
-28-4	4.5	1.4826	8141	2483	801	231	3.60	4.874	11.150	1.1361
-29-4	5.0	1.4815	7776	2846	910	216	3.60	6.076	6.642	1.2205
-29-5	9.5	1.4712	8189	2718	881	202	3.54	6.720	8.041	1.5620
-28-5	10.0	1.4701	8135	2700	857	196	3.53	6.691	8.302	1.5771
-28-6	20.5	1.4457	8758	3060	935	142	3.41	11.369	6.025	2.9756
-29-6	20.5	1.4457	8773	3143	916	147	3.41	11.119	6.796	3.0566
-28-7	30.0	1.4232	9159	3438	815	122	3.30	12.983	9.430	4.5427
-29-7	30.0	1.4232	9220	3385	921	123	3.30	14.311	6.591	4.3953

in Table 14 as is a third constant, K_3, which represents the equilibrium:

$$3/2\ N_2O_4 + H_2O \rightleftharpoons 2HNO_3 + NO \qquad (6)$$

This equation is derived by eliminating HNO_2 between equations 1 and 2.

The thermodynamic relationship between the equilibrium constant and temperature is:

$$\frac{d\ \ln K_C}{dT} = \frac{\Delta H}{RT^2} \qquad (7)$$

where K_C is the equilibrium constant expressed in units of concentration, ΔH is the heat of reaction, R is the gas law constant, and T is absolute temperature. This relationship assumes constant pressure, but in the condensed phase the pressure effect is small. If ΔH is constant, which should be nearly true over this small temperature range, equation 7 can be integrated to give:

$$\ln K_C = -\frac{\Delta H}{RT} + \text{Constant} \qquad (8)$$

ΔH and the integration constant can be determined by plotting $\ln K_C$ vs. $1/T$ and measuring the slope and intercept. Table 15 summarizes the results of a linear regression analysis of the data from Table 14. The large error in the fit of K_2 is mainly a reflection of the fact that the concentration of HNO_2, the most difficult to measure, enters into the calculation as a third power.

Table 15

Summary of Least Squares Fit of ln K vs. 1/T

Parameter	K_1	K_2	K_3
Intercept	6.343	0.6187	9.824
Slope	-3203.7	407.1	-4602.1
Std. Error of Estimate*	0.0716	0.1633	0.0405
Heat of Reaction (cal.)	6366	-809	9144

*Std. deviation of measured values of ln K from least squares prediction.

Equation 8 and the values in Table 15 permit the calculation of the equilibrium constants at any temperature in the range -10° to 30°. The good linear fit (see Table 15) of the more easily determined constants K_1 and K_3 and the lack of any chemical or physical evidence to the contrary make extrapolation of these values of 70° seem reasonable. In addition, they can be used to good advantage at -10° as well to calculate the concentrations of HNO_2 and H_2O from measured concentrations of NO and HNO_3. The analysis for the latter two are more accurate because they are less subject to spectroscopic interferences, and in most samples of interest they are the predominant species. The inherent difficulties in measuring HNO_2 and H_2O plus their relatively low concentrations make the relative error very large. The indirect determination using the equilibrium relationships transfers the smaller relative error implicit in the determination of the major species to the minor species. In addition, it permits the calculation of concentrations

of HNO_2 and H_2O well below the limits of direct determination. The procedure for performing these calculations is outlined in Appendix IV.

The prediction of system composition at a specified temperature from analyses at another temperature is complicated by the fact that consecutive reactions are involved in the overall equilibrium. This situation prohibits expression of the system as a single, meaningful equation which includes all five species. The two reactions (equations 1 and 2) must be simultaneously at equilibrium. Briefly, the computational procedure which is used to satisfy this condition is the following. The equilibrium constants K_1 and K_2 are calculated from equation 8. The analysis at -10° is used as initial values in equation 3 and the number of moles which must be transferred, according to the stoichiometry of equation 1, in order to satisfy the equilibrium constant at the new temperature is calculated using an iterative procedure. Next, the new composition is used as initial values in equation 4 and the number of moles transferred is again determined by iteration. This computed composition is used in equation 3 and the cycle is repeated until the number of moles transferred is an acceptably small value. This procedure is described in detail in Appendix IV and forms the basis of the computer program called PPM which is written in BASIC language for a General Electric time-sharing computer.

D. Determination of Dissolved Oxygen at Elevated Temperatures

In the stress corrosion cracking mechanism, oxygen was suspected of playing a significant and detrimental role, even in low concentrations (<10 ppm.). Previously, analyses for oxygen in N_2O_4 were carried out at room temperature (24-28°C.) with singular success (1). By measurement of the oxygen in the gas phase and relating the amount found through the Henry's Law constant for oxygen solubilities in N_2O_4 (5), the concentration of oxygen in the liquid phase could be calculated to something less than 0.1 ppm. A measurement limit of 1-2 ppm. was encountered if the liquid phase was analyzed directly.

As a part of this program, an attempt was made to determine the concentration of O_2 in liquid N_2O_4 at the temperature used in the SCC test (74°C.). It was felt that such information might be of particular importance since evidence has been presented by other workers (6) that the equilibrium

$$NO_2 \rightleftharpoons NO + 1/2\ O_2$$

is shifted significantly to the right at temperatures about 60°C. In addition, it has been shown that the solubility of O_2 in liquid N_2O_4 increases with increasing temperature (5). Thus, it appeared possible that the concentration of dissolved O_2 might increase significantly during the course of a 72-hour test at 74°C.

In order to perform measurements at elevated temperatures, several changes in the gas chromatographic system were necessary. In addition, a pressure vessel was designed and constructed in which liquid N_2O_4 could safely be heated to elevated temperatures

and vapor phase samples taken for O_2 analysis. This work is described below.

1. Gas Chromatographic System

Chief modification in the gas chromatography system was replacement of the glove bag with a small Plexiglas dry box. This change was intended to provide better atmospheric control and to make more room for sample cylinders. In addition, the pressure vessel could be held inside the box. The dry box was also equipped with a sample port so that samples could be introduced with minimum disturbance of the low-oxygen atmosphere.

Figures 19 and 20 show the basic components of the gas chromatograph and the sampling system. Also shown, (Figure 20, Item 1) are the inlet and exit ports for the fluid used to maintain the pressure vessel at constant temperature. The approach of maintaining the vessel at constant temperature via circulation of an externally heated fluid was later abandoned in favor of a wrap-around heating mantle. Item 6, Figure 20, is the vacuum-flushing system used to control the atmosphere in the dry box and to fill the pressure vessel. A schematic representation of this system is shown in Figure 21 and a diagram of the cell-filling system is given in Figure 22. Not shown in Figures 19 and 20 is the sample port which can be installed on the dry box directly in front of the N_2O_4 trap (Item 2, Figure 20).

FIGURE 20

OXYGEN ANALYSIS APPARATUS - OVERALL VIEW

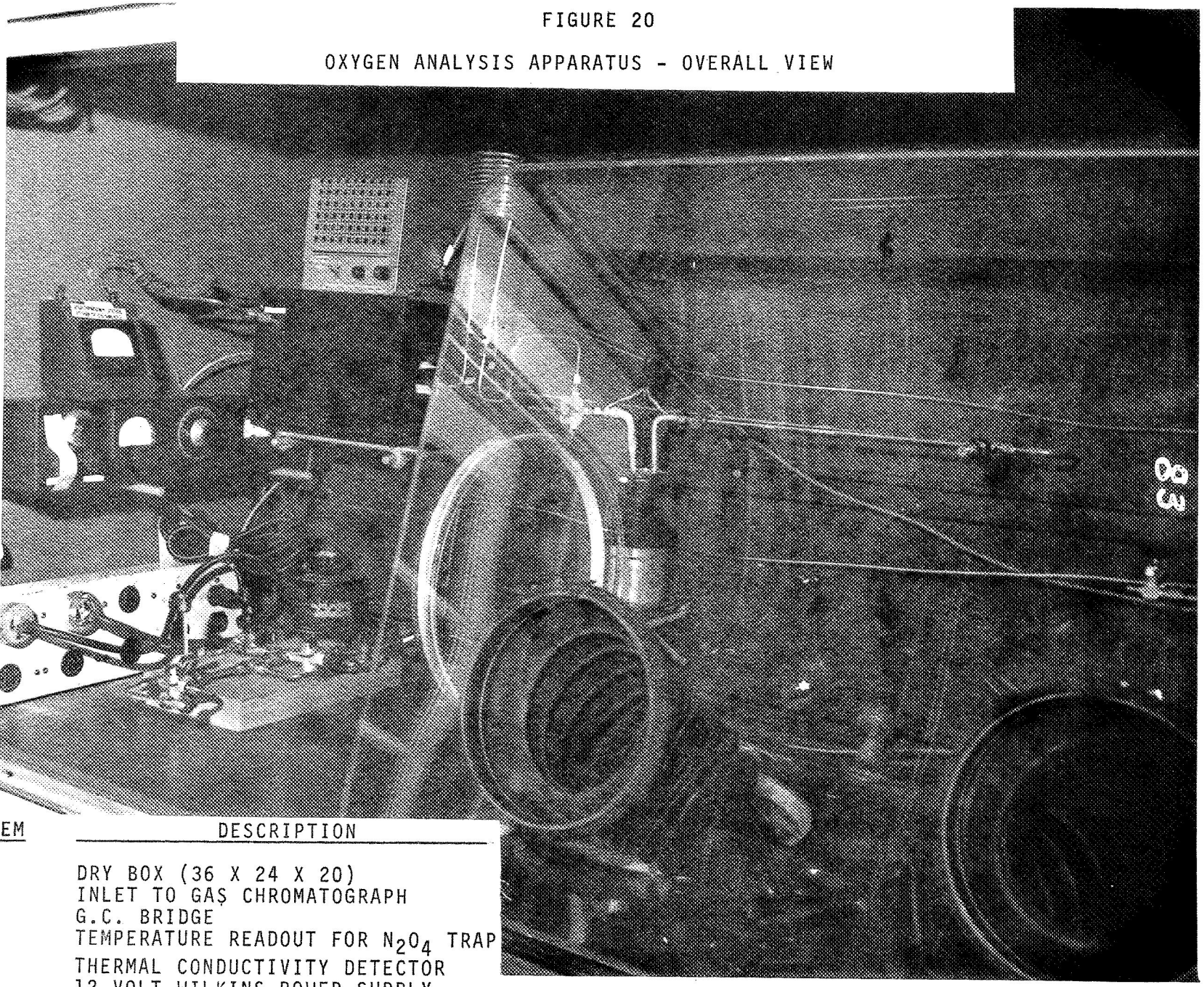

ITEM	DESCRIPTION
1	DRY BOX (36 X 24 X 20)
2	INLET TO GAS CHROMATOGRAPH
3	G.C. BRIDGE
4	TEMPERATURE READOUT FOR N_2O_4 TRAP
5	THERMAL CONDUCTIVITY DETECTOR
6	12 VOLT WILKINS POWER SUPPLY

FIGURE 21

CLOSE-UP OF GAS CHROMATOGRAPHY, DRY BOX, AND PRESSURE VESSEL FILLING SYSTEM

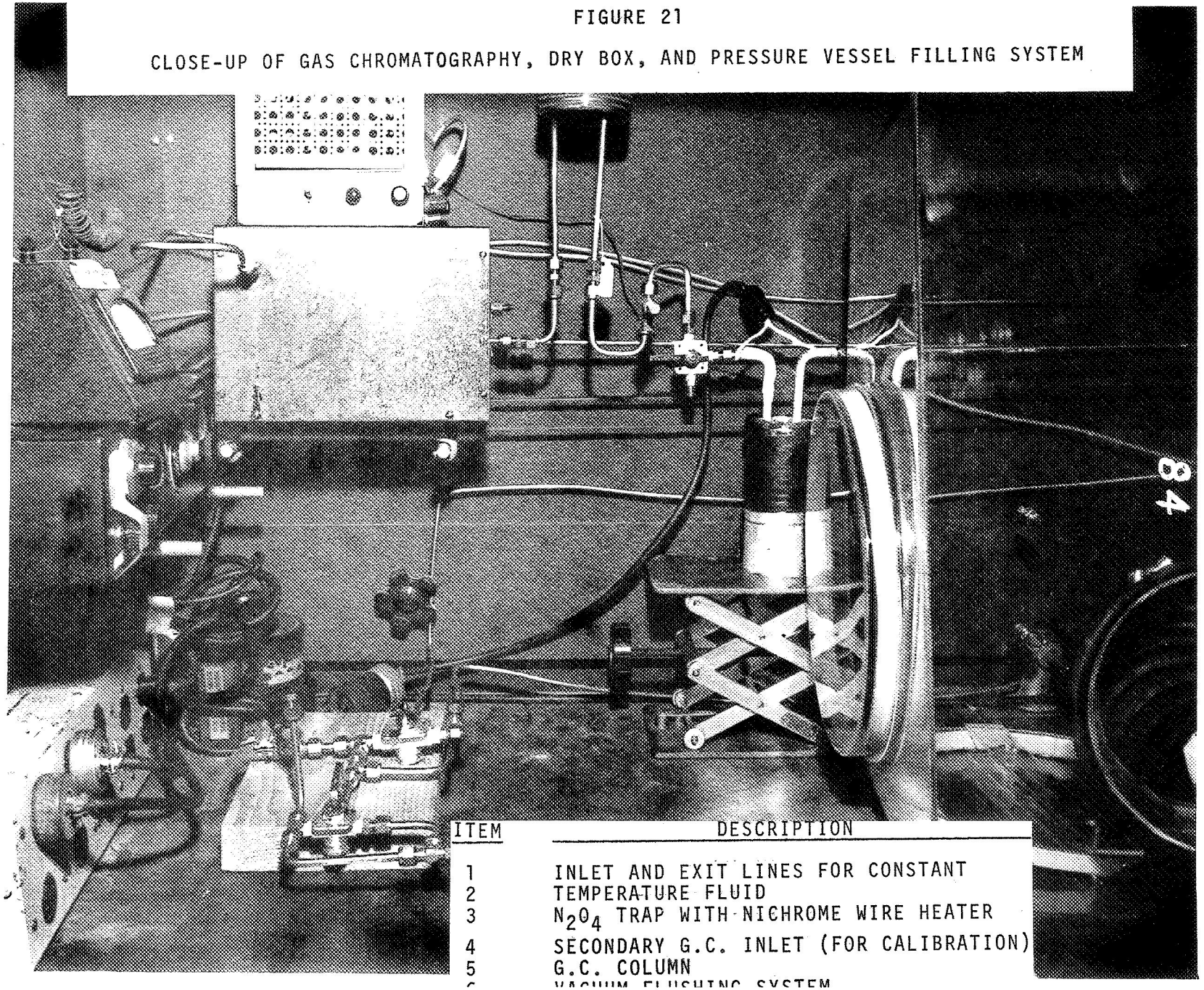

ITEM	DESCRIPTION
1	INLET AND EXIT LINES FOR CONSTANT
2	TEMPERATURE FLUID
3	N_2O_4 TRAP WITH NICHROME WIRE HEATER
4	SECONDARY G.C. INLET (FOR CALIBRATION)
5	G.C. COLUMN
6	VACUUM FLUSHING SYSTEM

FIGURE 22

VACUUM-FLUSHING SYSTEM FOR DRY BOX AND PRESSURE VESSEL

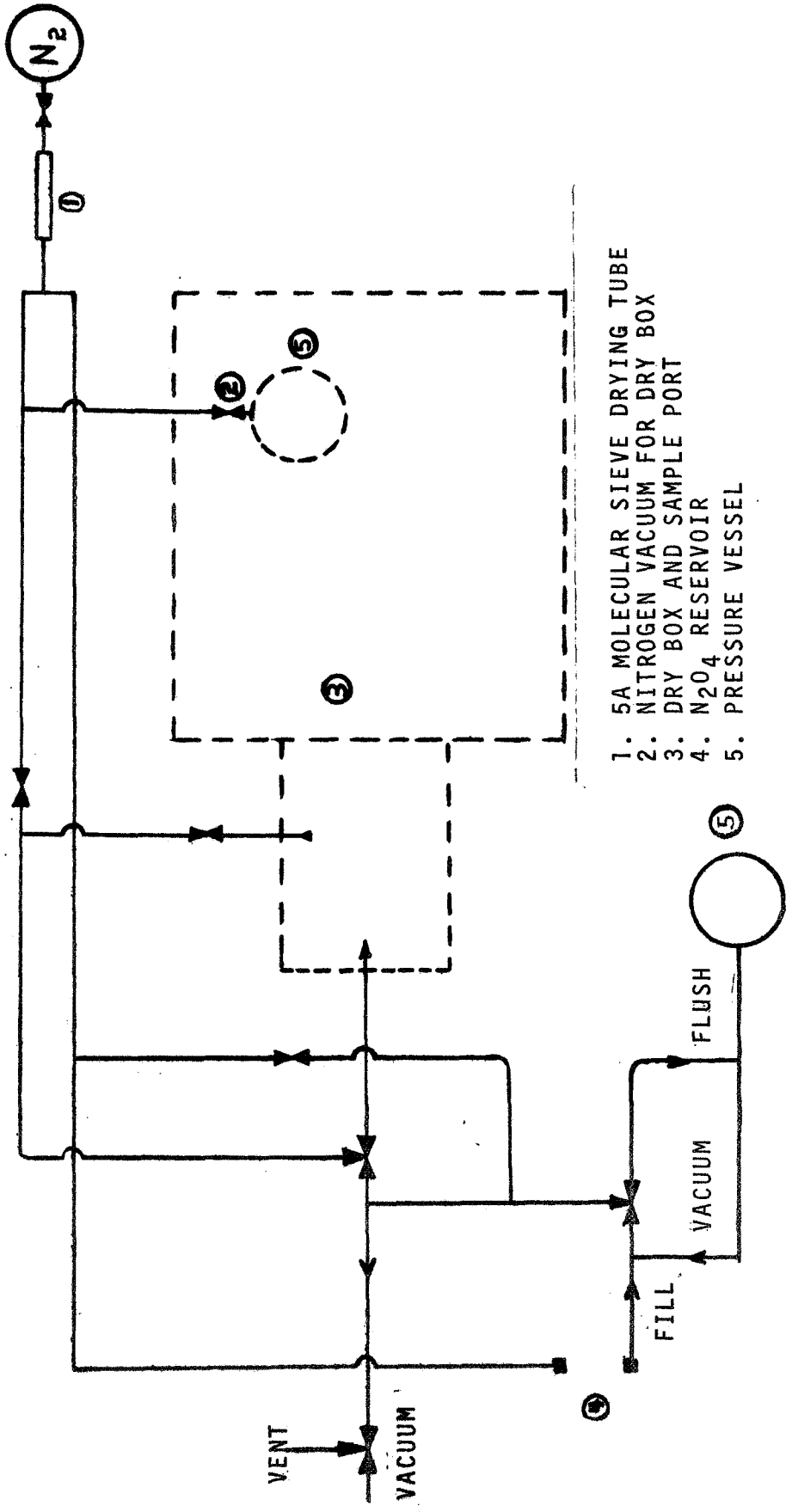

FIGURE 23

CELL-FILLING APPARATUS

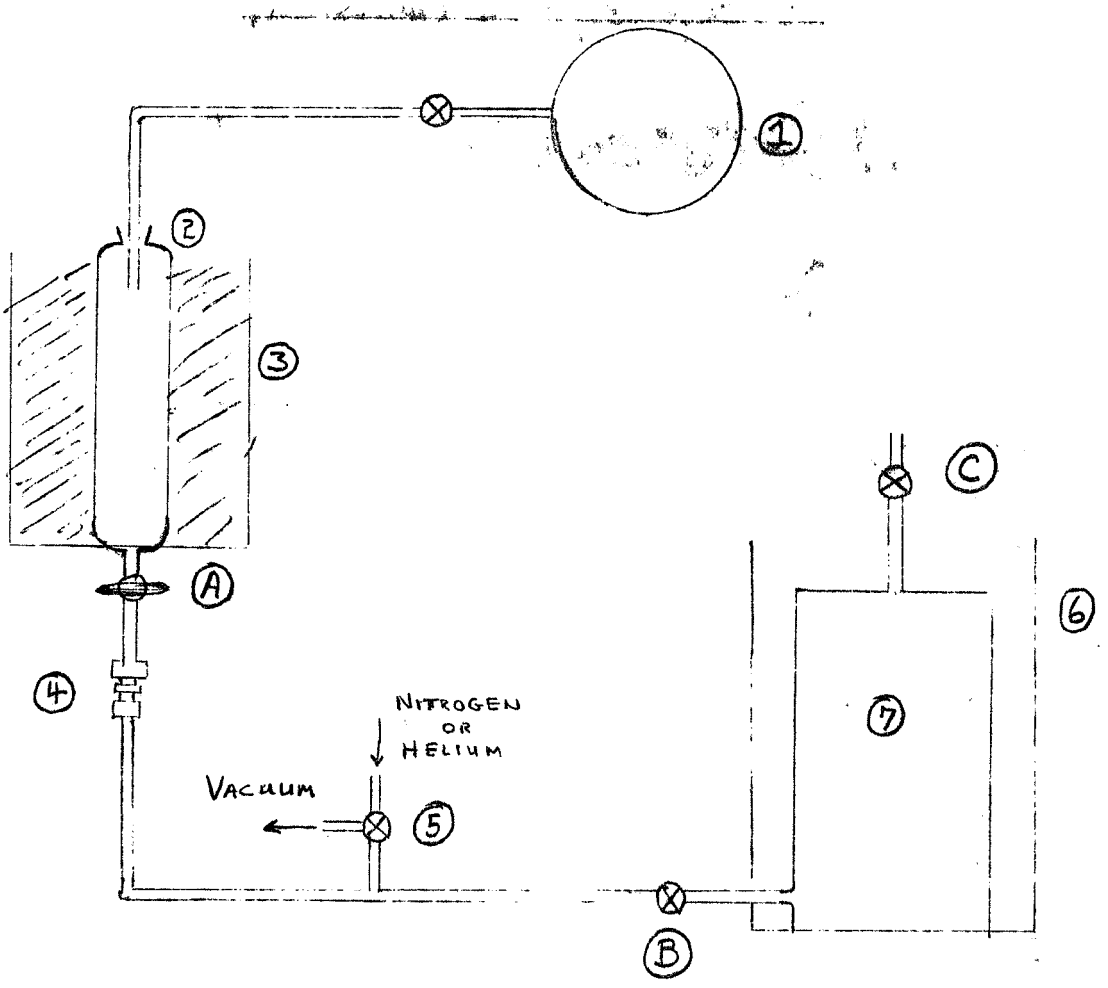

(1) N_2O_4 reservoir.

(2) 250 ml. calibrated dropping funnel.

(3) Cardboard box condenser filled with dry ice.

(4) 3/8-inch to 1/4-inch Swagelok reducing union.

(5) Three-way valve.

(6) Condenser jacket of reaction cell.

(7) Reaction cell.

2. Pressure Vessel

A detailed diagram of the pressure vessel with constant temperature jacket is shown in Figure 24. Construction was such that samples of both the liquid and gas phases could easily be taken. Other design features included a removable top so that U-bend specimens could be added, and a thermocouple encased in stainless steel for monitoring the vessel's inner temperature. Additional details of cell construction and associated fittings are given in the Appendix VI.

For initial experiments, the vessel was connected to a constant temperature bath located outside the dry box by means of Tygon tubing connected to the ports shown in Item 1 of Figure 20. It was soon found, however, that with the oil bath reservoir at 150°C., the maximum attainable temperature inside the cell was 60°C. Also, at the elevated temperatures, the prime of the circulating pump could not be maintained because of air dissolved in the oil. Replacement of the circulating pump with a bellows pump eliminated priming problems but did not provide a sufficiently fast flow rate to maintain the temperature required.

The outer jacket was removed and replaced with a sleeve-type heating mantle which was connected to a Guardsman temperature controller. This equipment is diagrammed in Figure 25. Temperatures were easily maintained with this experimental arrangement.

FIGURE 24

PRESSURE VESSEL FOR N_2O_4 EQUILIBRIUM STUDIES AT ELEVATED TEMPERATURES

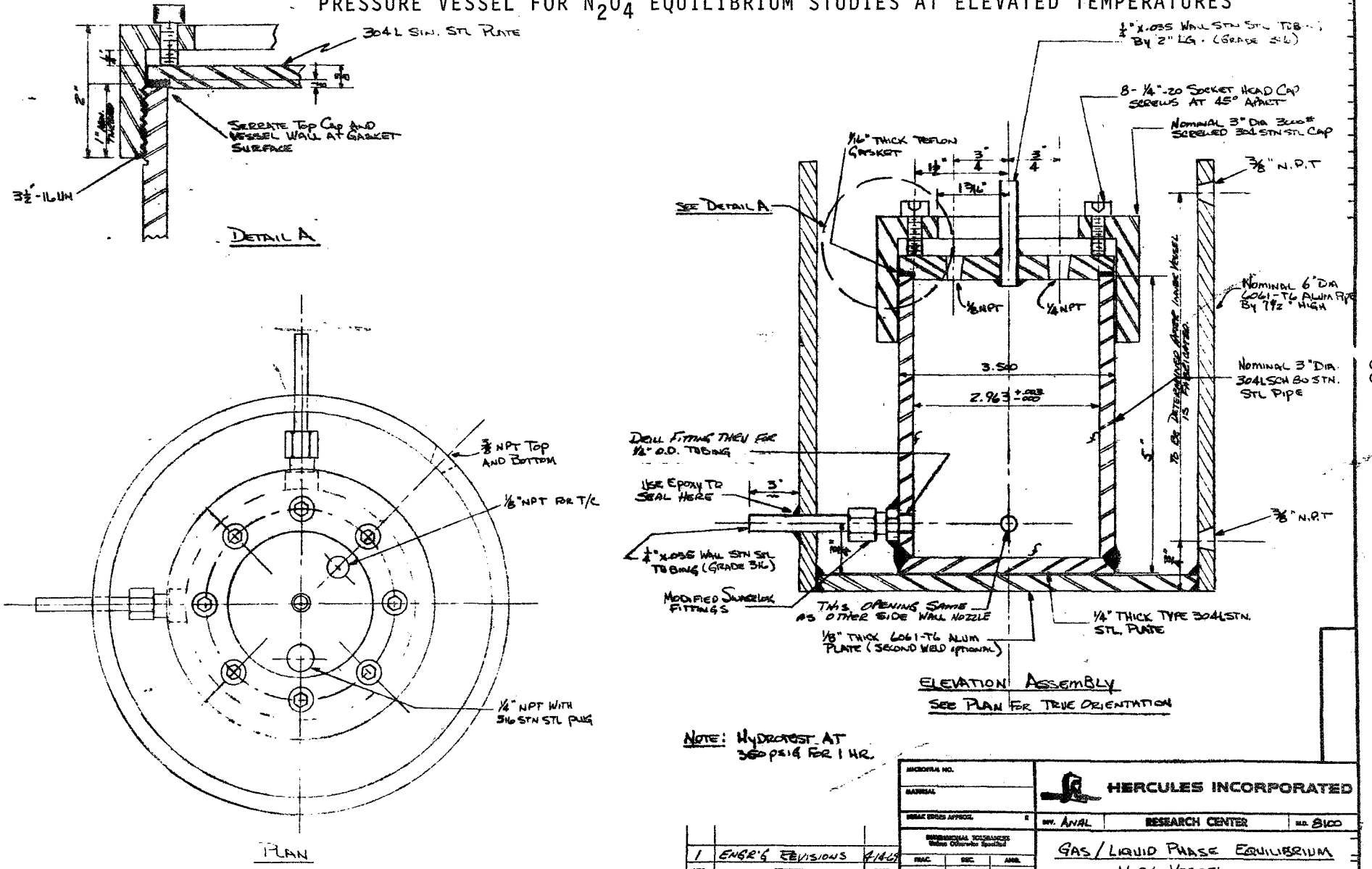

NOTE: HYDROTEST AT 360 psig FOR 1 HR.

NO.	MARK	DWG. NO., DESCRIPTION, MATL., ETC.	REMARKS

NO.	REVISION	DATE
1	ENGR'G REVISIONS	4/14/69

HERCULES INCORPORATED

DIV. ANAL | RESEARCH CENTER | BLDG. 8100

GAS / LIQUID PHASE EQUILIBRIUM WORK VESSEL

DRAWN D&A Morrow | DATE 4-11-69 | DWG. NO.

SCALE FULL | 32 | UNLESS NOTED

3. Experimental Results

The data obtained on the four runs attempted is given in Table 16. Little can be said about this data since most of the experiments (with the exception of Run 4) were terminated before conclusive data could be obtained.

In the initial work (Runs 1 and 2), primary problems involved the design of the temperature control apparatus. Specifically, pumping rates of hot oil from the reservoir to the vessel could not be maintained. Also, faults in the temperature read-out led to false conclusions about the adequacy of the heating system. For the remainder of the work, the oil bath and jacket were replaced by the heating system shown in Figure 25.

Other runs were beset with problems, the major one of which involved sampling at elevated temperatures. Withdrawal of hot (40-90°C.) N_2O_4 into a cool syringe produced instantaneous condensation in the barrel. Equipping the syringe with a heater so that it was operated at the temperature of the pressure vessel did not entirely eliminate the condensation problem. Thus, the data for all runs were considered to be suspect, primarily because of the possible recombination reaction

$$1/2\ O_2 + NO \rightleftharpoons NO_2.$$

The sampling problem might best be solved by use of a heated, high pressure, gas sampling valve. However, the problems associated with obtaining a truly representative sample of the gas phase would still be substantial.

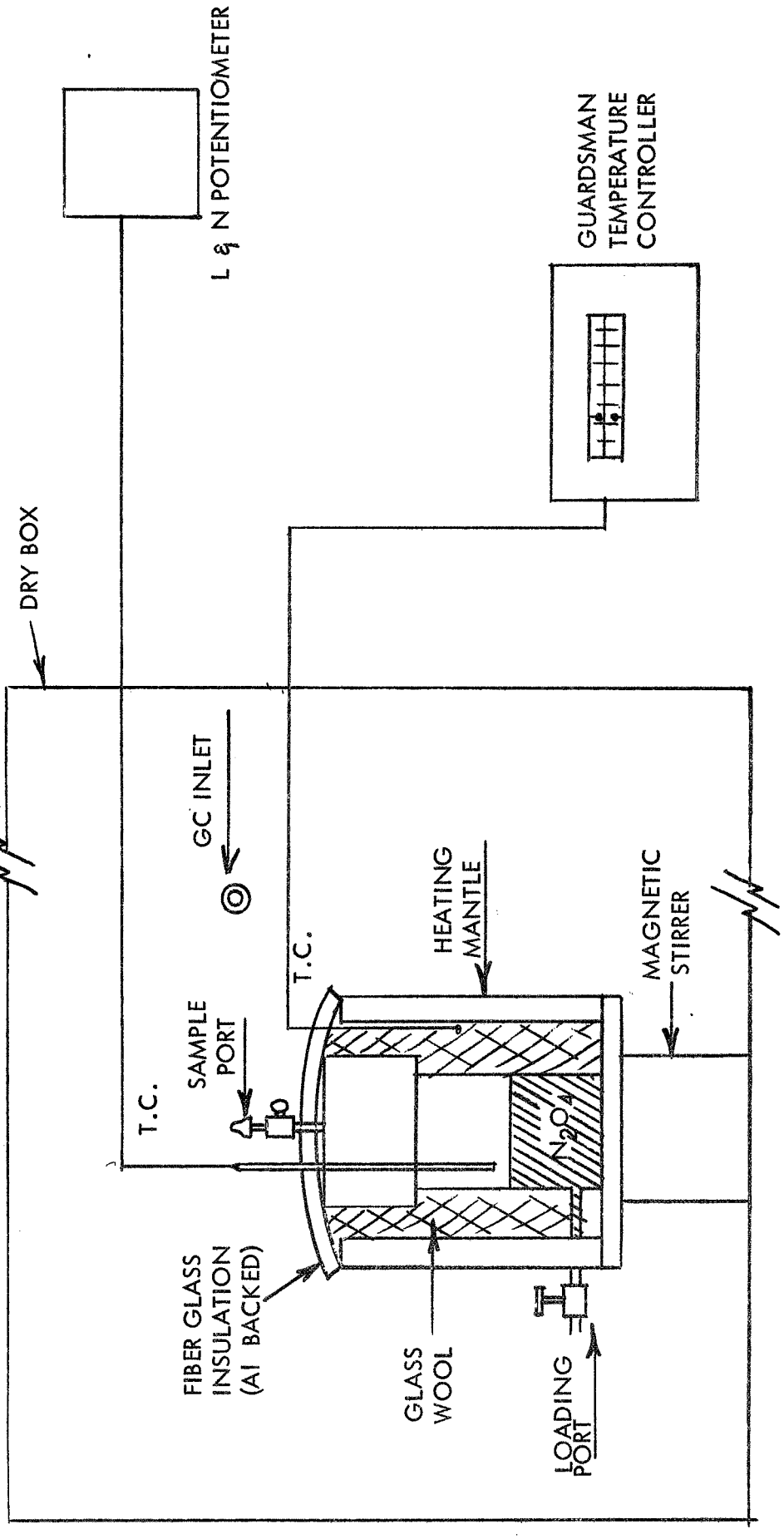

FIGURE 25 - TEMPERATURE CONTROL SYSTEM FOR PRESSURE VESSEL

Table 16 - Determination of Dissolved O_2 in Liquid N_2O_4 at Elevated Temperatures

Run No.	Hercules Designation	Time (Hrs.)	Temp. of N_2O_4 (°C.)	No. of Rep. Detns.	PO_2 Atmospheres	ppm. O_2 (Liquid)	s	% s	K x 10^3	Duration of Run (Hrs.)
1	X16852-24	0	25.2[a]	7	1.72×10^{-3}	0.61	0.033	5.4	1.017	
		2	72.5[a]	8	9.1×10^{-3}	3.8	0.20	5.4	1.191	10-12
2	X16852-31	0	25	Maximum Temp. Reached = 60°C. - See Text						
3	X16852-31	0	24.8	6	2.52×10^{-4}	0.09	0.011	12.2	1.017	
		288	60	-	-	-	-	-	-	288
4	X16852-33	0	25.2	5	2.43×10^{-4}	0.09	0.008	8.9	1.017	
		24	44	5	3.97×10^{-4}	0.15	0.02	13.3	1.092	
		48	59.5	7	2.51×10^{-4}	0.10	0.008	8.0	1.147	
		120	57.5	4	1.13×10^{-4}	0.04	0.01	25.0	1.140	
		144	93.0	2	1.00×10^{-4}	0.04	-	-	1.250	
		672	95.0	4	1.27×10^{-4}	0.06	0.005	8.3	1.263	672

[a]These temperatures were in error due to a depleted battery in the L&N potentiometer.

Run 4 was the best experiment performed. The data is, however, contradictory. No increase in oxygen level was observed over the 28-day duration of the experiment, most of it at elevated temperatures. However, the NO level was observed to increase drastically. In fact, NO was observed in all runs made, especially on elevation of the temperature. This suggests, particularly in the case of Run 4, that the run was contaminated with water. If this were the case, the large amount of NO generated would certainly inhibit the NO_2 decomposition reaction.

Because of the difficult problems associated with the apparatus, sampling, and possible water contamination during loading of the pressure vessel, significant data could not be obtained by this experimental approach. When it became apparent that the effect of oxygen at elevated temperatures could more readily be obtained through an empirical approach (see Phase B), this method was abandoned.

E. Electrical Properties

Pure liquid N_2O_4 is a medium of low dielectric constant ($\varepsilon = 2.4$) and very low electrical conductivity (specific conductivity $\approx 3.0 \times 10^{-13}$ ohm.$^{-1}$ cm.$^{-1}$ @ 24°C.). These values indicate that the concentration of ionic species in the pure liquid is extremely small. However, studies of organic and inorganic reactions involving N_2O_4 indicate that the reactive species in a great many of these reactions is either NO_2 free radical or NO^+ ion. In the case of most inorganic reactions, NO^+ ion has been shown to be the principal reactive species (7).

This evidence is supported by the fact that the degree of ionization and, consequently the reactivity of N_2O_4, is enhanced by the addition of liquids of high dielectric constant, e.g., nitromethane, HNO_3, H_2SO_4, HF. For example, in nitromethane ($\varepsilon = 37$) the electrical conductivity of N_2O_4 increases by a factor of 10^8. In dilute solutions in HNO_3, the dissociation of N_2O_4 into NO^+ and NO_3^- ions is complete, and the electrical conductivity of the solutions is comparable with that of alkali metal nitrates in HNO_3.

The electrical conductivity of N_2O_4 is also substantially increased by the addition of NO (to form N_2O_3) and/or NOCl, with the former exerting the greater effect. It has been shown that the presence of 10 mole % N_2O_3 increases the conductivity of N_2O_4 by a factor of 1400 times while the presence of an equivalent molar concentration of NOCl increases it by a factor of 350 (5). In view of these observations, it was felt that the electrical properties of several different N_2O_4 compositions should be measured for possible correlation with SCC behavior.

Three samples were examined:

(1) RR N_2O_4, containing about 5200 ppm. HNO_3.

(2) Above sample to which 1.0% NO was added.

(3) G8 N_2O_4, containing 7300 ppm. combined NO and 5000 ppm. protonated compounds (HNO_3, HNO_2, H_2O) calculated as HNO_3.

The dielectric constant (ε), dissipation factor (D), and specific conductivity (σ) were measured in a Balsbaugh 2TN50 liquid measuring cell as described in Appendix VII. The data are given in Table 17.

The A.C. measurements showed that all three samples had conduction type losses in the low frequency region. This could be due either to pure D.C. conduction by the ions present in the system, or to the Maxwell-Wagner effect which occurs in mixtures of very different conductivities, or to a combination of both effects. The fact that in all cases the loss increased by about a factor of 10 when the frequency was decreased from 1000 H_Z to 100 H_Z, indicated that the loss was wholly controlled by the D.C. conduction process. The magnitude of this loss in the case of ionic conduction is determined by the number of active ions present in the system and their charge and mobility. The measurements at 100 H_Z showed that the RR N_2O_4 sample had the lowest conduction loss while G8 N_2O_4 had the highest loss at this frequency. The D.C. resistivity measurements showed that the conductivity of RR N_2O_4 was much lower than that of the other two samples, and that the sample containing 1% combined NO was more conductive than the G8 N_2O_4 sample.

The high frequency loss (above 4 KH_Z) is most probably a relaxation type loss which can again be due to the relaxation part of the Maxwell-Wagner loss or to the conventional Debye

Table 17

Electrical Properties of N_2O_4 Compositions

	RR N_2O_4		RR N_2O_4 + 1% NO		G8 N_2O_4	
			A.C. Measurements			
Frequency, Hz	ε	D	ε	D	ε	D
10^2	2.37	0.0119	2.66	0.1444	2.59	0.0566
10^3	2.37	.0014	2.62	.0145	2.58	.0061
10^4	2.37	.0008	2.62	.0021	2.58	.0031
10^5	2.37	.0039	2.62	.0099	2.54	.0221
10^6	2.37	.0063	2.57	.0720	2.51	.0756
			D.C. Measurements			
	σ,ohm.$^{-1}$ cm.$^{-1}$		σ,ohm.$^{-1}$ cm.$^{-1}$		σ,ohm.$^{-1}$ cm.$^{-1}$	
	1.5×10^{-12}		2.5×10^{-11}		7.7×10^{-12}	

Loss arising from dipole moments. The results in this region also show that the loss was very low in RR N_2O_4 and higher in the other two samples.

The relationship of these measurements to the mechanism of stress corrosion cracking will be discussed in a later section.

Phase B - Stress Corrosion Cracking Tests

A. Facilities and Test Modifications

Considerable renovation and modification of the N_2O_4 handling and test facilities were required prior to the start of work under this contract. These changes are briefly discussed below.

1. N_2O_4 Delivery and Handling System

Preliminary maintenance required by the system involved the replacement of 10 valves and 50 ft. of stainless steel tubing, and a thorough check of the electrical system and hood exhaust fan to assure uninterrupted, full-time operation. An additional outside safety shower was also installed.

Disposal of waste N_2O_4 was a continual problem under NAS 8-21207, primarily because of pump failures. It was decided that for this work, all pumps would be eliminated and the movement of liquid N_2O_4 would be accomplished with N_2 gas pressure. To operate in this fashion, it was necessary to move the waste cylinder from the heated storage shed to an area where this cylinder could be cooled to reduce pressure build-up. Consequently, the cylinder was finally relocated out of doors, in a shaded area, and equipped with a water spray covering the entire surface of the cylinder for cooling during the summer months.

A new scrubbing system also was required so that the waste cylinder could be vented at relatively low pressures (1-2 psig.) to the atmosphere. In this system, venting occurred through two 4-gallon tanks connected in series to the vapor space in the waste

storage cylinder. The first tank was empty and served as a trap; the second tank contained ca. 3 gallons of 20% (wt.) caustic solution. N_2O_4 vapors from the storage cylinder passed through the empty tank over to the caustic tank and were dispersed and reacted in the caustic solution. Any unreacted N_2O_4 was exhausted to the atmosphere. As long as NaOH was available for reaction with N_2O_4, this scrubber produced little atmospheric contamination. A significant pH drop signaled the need to renew the caustic scrubbing solution. This scrubbing system performed as designed and permitted the venting of the waste N_2O_4 storage cylinder down to pressures of 1-2 psig. At these low pressures, no difficulty was experienced in transferring waste N_2O_4 from the hold tank to the waste storage cylinder. A diagram of the waste system is shown in Figure 26.

2. Stress Corrosion Cracking Test

In previous work, the stress corrosion cracking test was carried out by exposing 10 U-bend specimens of 6Al 4V ELI titanium sheet to liquid N_2O_4 for 72 hours at 165°F. (74°C.) in a glass-Teflon test cell (1). Approximately 3 liters of liquid N_2O_4 were required to perform each test including flushing and filling. The test gave extremely consistent results; the exposure of 200-300 U-bend specimens in 25-30 tests resulted in 100% consistency of failures or passes in every test.

For this investigation, the length of the Corgard glass-pipe, cell body was reduced from 12 inches to 6 inches in order to

FIGURE 26

N_2O_4 WASTE HANDLING SYSTEM

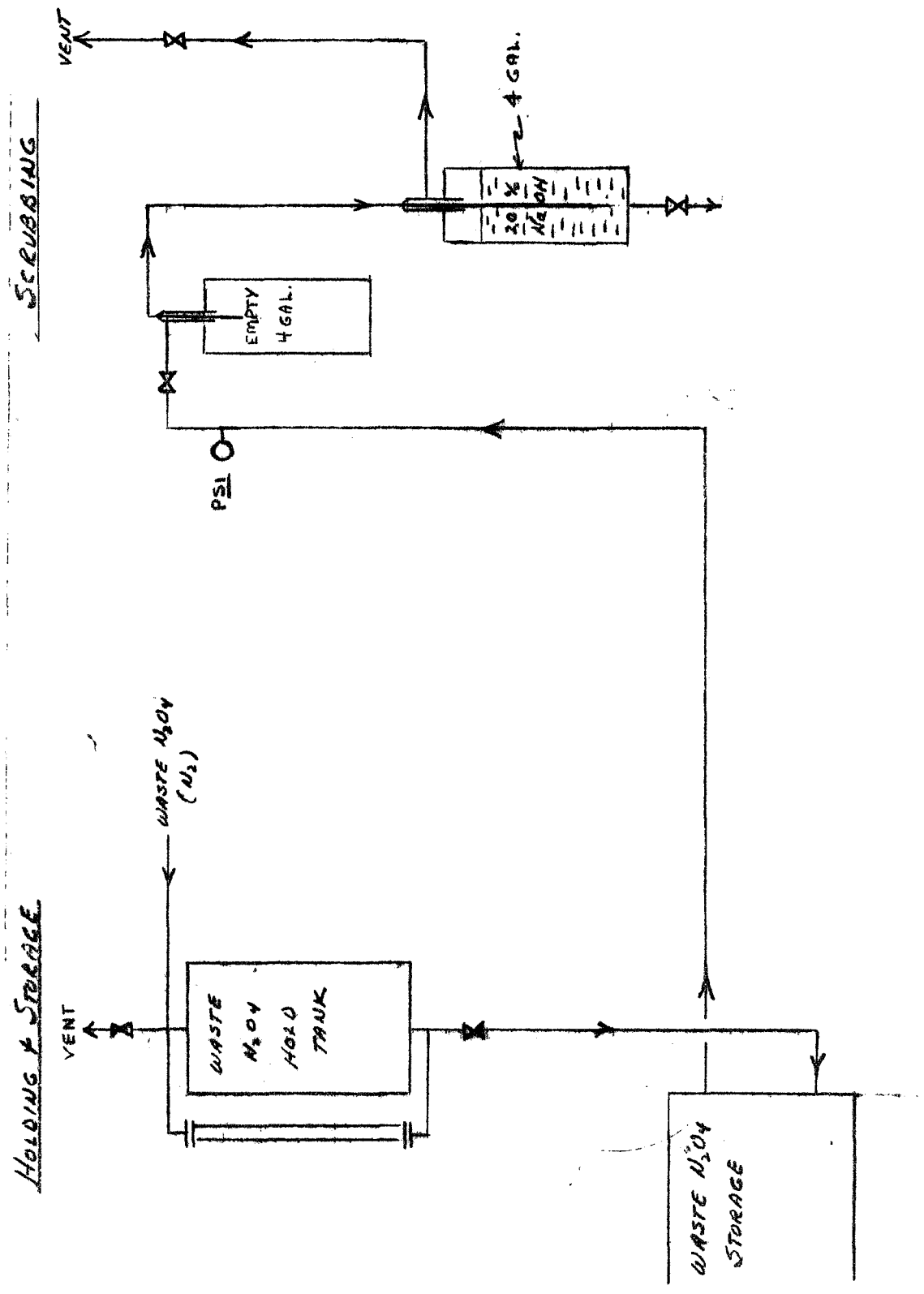

reduce the amount of N_2O_4 required per test. No other changes in the test cell design were necessary. Five of the smaller volume cells were constructed for this program and all performed satisfactorily.

Specimen preparation was the same as previously reported (1) with two minor exceptions. In all but a few cases, no attempt was made to deflect the specimens to an exact stress level. Instead, the pre-bent specimens were deflected to a constant leg separation of 2.10 cm. This ensured that all specimens were stressed well within the critical range for SCC to occur, i.e., 40-90% yield strength. This change in procedure eliminated the need for the tedious and time-consuming measurements and calculations required to obtain exact stress levels without sacrificing test reliability. A second minor procedural change involved the method of specimen loading. Under NAS 8-21207, the 10 U-bend specimens were loaded onto a rack and inserted into the test cell. In this work, the 4 or 5 specimens used per test were randomly placed in the test cell prior to pressure testing.

Finally, a new test oven was purchased, installed, and calibrated for this program. The oven and the modified cells were used in several preliminary tests with RR and G8 N_2O_4. In all cases, RR N_2O_4 caused all U-bend specimens to crack in half, while G8 N_2O_4 had no detectable effect.

B. Effect of Organic Compounds on Stress Corrosion Cracking

During the work performed under Contract No, NAS 8-21207 in 1968, it was postulated that the presence of organic compounds in N_2O_4 could inhibit SCC. This was based on the analysis and

testing of a sample of Red Nonreactive N_2O_4 obtained from Marshall Space Flight Center. It was theorized that the presence of organic compounds could cause inhibition in the following ways:

(1) Organic matter is more susceptible to oxidative attack than the alloy and functions as an antioxidant to react with oxygen or other attacking species.

(2) The oxidation of organic compounds by N_2O_4 almost always results in the generation of NO and/or HNO_2 which would further inhibit SCC.

(3) Highly polar products of the oxidation, such as carboxylic acids, might be strongly adsorbed or chemisorbed by any active metal surface thus limiting subsequent attack.

It was decided to conduct a limited study of the effect of organic compounds on the SCC reaction. The main purpose of this work was to gain insight into the basic mechanism of the attack on the titanium alloy.

1. Preliminary Work

In order to establish a reasonable concentration range for the study, the remaining portion of the MSFC N_2O_4 sample was analyzed quantitatively for organic matter. A value of 100-150 ppm. was obtained. The infrared spectrum of the isolated material was basically the same as that obtained during the original analysis. The principal features of the spectrum included bands characteristic of aliphatic C-H, carboxylic acid and salt, nitrate ester, and possibly carboxylic ester.

A group of inorganic compounds was then selected for testing. These included:

(1) Hexadecane: $H_3C-(CH_2)_{14}-CH_3$

(2) Squalane: $C_{30}H_{62}$

$$[(CH_3)_2CH-(CH_2)_3-\underset{\displaystyle CH_3}{CH}-(CH_2)_3-\underset{\displaystyle CH_3}{CH}-CH_2-CH_2-]_2$$

Aliphatic hydrocarbon containing high concentration of tertiary carbon atoms.

(3) Squalene: $C_{30}H_{50}$

$$[(CH_3)_2C = CH-(CH_2)_2-\underset{\displaystyle CH_3}{C}=CH-(CH_2)_2-\underset{\displaystyle CH_3}{C}=CH-CH_2-]_2$$

Unsaturated hydrocarbon containing high concentration of olefinic double bonds.

(4) Stearic acid: $CH_3(CH_2)_{16}COOH$

Straight chain, saturated monobasic acid.

(5) Sebacic acid: $HOOC(CH_2)_8COOH$

Saturated, dibasic acid.

(6) 2,6-Di-t-butyl-p-cresol:

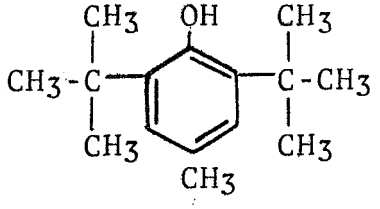

Hindered phenolic antioxidant.

(7) 2,4-Dinitrophenol:

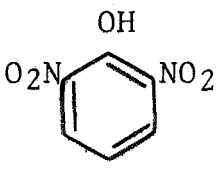

Nitrated phenol.

2. Solubility Tests

Initial add-back experiments required at least partial solution of the above organic compounds in RR N_2O_4. Solubility tests were carried out as follows:

A sample of the compound was weighed directly into a 250 ml. Erlenmeyer flask which was then cooled to 0°C. in an ice bath. RR N_2O_4 was cooled to 0°C. and the desired volume (usually 100 ml.) added to the flask. After initial observation, the mixture was stirred magnetically for up to 2 hours. Solubility was checked by periodic visual observations.

The results of these tests are summarized in Table 18.

3. Stress Corrosion Cracking Tests with Additives

A series of SCC tests was made primarily to assess the effects of various types of organic compounds on the cracking reaction. The test media were prepared by adding known amounts of the additives to a series of 1750 ml. stainless steel cylinders. The cylinders were then filled with RR N_2O_4 and the mixtures allowed to stand overnight to dissolve the additive. The test media were then used to flush and fill the test cells (see Appendix VIII). Tests were carried out in the usual way for about 70 hours at 165°-170°F. In addition to testing the organic additives listed above, five tests were conducted with inorganic additives. The test results are summarized in Table 19.

Table 18

Table 18 - Solubility Tests of Various Organic Compounds in RR N_2O_4 at 0°C.

Notebook Ref.	Additive	Wt., mg.	RR N_2O_4, ml.	Observations
X16910-2	Stearic Acid	10.8	80	Dissolved in 2 min.
	Sebacic Acid	10.1	70	Dissolved in 75 min.
	Hexadecane	12.1	70	Immediate solution without stirring
X16910-4	Squalane	16.9	100	An estimated 30-40% dissolved without stirring in 15 min. Remainder remained insoluble after 2 hrs.
	Squalene	19.6	100	Exothermic reaction on contact with N_2O_4 but only slight solubility after 2 hrs.
	Dalpac*	16.1	100	Dissolved in 10 min.
	2,4 Dinitrophenol	17.8	100	Dissolved in 10 min.
X16910-6	Boric Acid	20	100	Insoluble after 2 hrs.
	Phosphoric Acid	30	100	Insoluble after 2 hrs.

*2,6-Di-t-butyl-p-cresol

Table 19

Stress Corrosion Cracking Tests - Effect of Additives

Test No.	Additive	Amount, ppm.	Exposure Cond. Temp., °F.	Exposure Cond. Duration, Hr.	Failure Rate	Remarks
3	Hexadecane	150	170	70	5/5	2 spec. cracked completely in half; 3 showed large cracks in major stress areas
4	Stearic Acid	120	170	70	0/5	All 5 spec. exhibited a tarnish-like stain
5	Sebacic Acid	120	170	70	0/5	-
7	Squalane	95	165	70	0/5	-
8	Squalene	100	165	70	0/5	-
6	2,6-Di-t-butyl-p-cresol	100	165	70	0/5	-
13	2,6-Di-t-butyl-p-cresol	50	165	70	0/5	Combined NO: 110 ppm.
14	2,6-Di-t-butyl-p-cresol	25	165	70	5/5	All 5 spec. cracked completely in half. Combined NO: 32 ppm.
15	2,4-Dinitrophenol	84	165	69	0/5	-
11	2,4-Dinitro-phenol	43	165	71	5/5	2 spec. cracked completely in half; 1 spec. had 10-12 macro cracks and 10-12 micro cracks; 1 spec. had 10-12 micro cracks; 1 spec. had 1 macro crack at bolt hole

Table 19 - Contd.

Test No.	Additive	Amount, ppm.	Exposure Cond. Temp. °F.	Exposure Cond. Duration, Hr.	Failure Rate	Remarks
9	Boric Acid	103	165	71	5/5	All 5 spec. cracked completely in half
10	Phosphoric Acid	102	165	71	5/5	"
12	Copper Wire	60 in. 18 ga.	165	70	0/5	Copper wire dissolved in RR N_2O_4 leaving a light green precipitate that later evaporated in air. Combined NO: 1.3%
16	Platinum wire gauze	1-1/4 in. x 3 in.	165	69	5/5	All 5 spec. cracked completely in half
25	Platinized Pt gauze	1-1/4 in x 3 in.	170	70	5/5	Only 250 ml. of RR N_2O_4 used. All spec. had macro cracks, some cracked in half

4. Interpretation of Results

Organic compounds react with N_2O_4-NO_2 systems in a variety of ways depending on the structure of the organic compound and the reaction conditions. Predominant reactions include nitration, oxidation, and addition. Reaction products are usually numerous and frequently complex in nature. The test results indicated the following:

(1) Normal paraffins such as hexadecane (Test 3) are relatively difficult to oxidize or nitrate. Under the test conditions, the cracking reaction apparently could be initiated before reaction with the hydrocarbon could affect the system.

(2) Stearic and sebacic acids (Tests 4,5) would also be expected to be relatively resistant to attack by N_2O_4. Inhibition of SCC in these cases is probably due to adsorption or chemisorption on active titanium surfaces.

(3) The hindered phenolic antioxidant, 2,6-di-t-butyl-1-cresol (Tests 6,13,14), could conceivably inhibit SCC by all three proposed mechanisms, i.e., as a scavenger for active oxygen or highly oxidizing species, by generation of NO-HNO_2, and by adsorption of polar oxidation products on the metal surface. The first two mechanisms probably predominate in this case. Complete inhibition was obtained at the 50 and 100 ppm. levels; all specimens cracked at the 25 ppm. level.

(4) Squalane and Squalene (Tests 7,8) are examples of compounds that are readily oxidized or reacted with N_2O_4. Initial

oxidative attack would occur at the tertiary carbons of squalane and probably at carbon atoms α to the double bonds of squalene.

(5) Boric acid and phosphoric acid were tested to see if inorganic acids of varying strengths might passivate reactive titanium surfaces. The insolubility of these compounds complicated interpretation of the results. There was visual evidence that some of the boric acid did tend to adhere to the specimens in isolated spots.

(6) 2,4-Dinitrophenol (Tests 11,15) would be expected to react with N_2O_4 first to add a third nitro group and form picric acid. Test 11 was conducted to check for possible absorption or surface reaction of an acid phenolic group. Although all specimens cracked, the cracking behavior was so varied that interaction may have occurred. The initial additive level (43 ppm.) was lower than the other experiments because of the potential explosive hazard of picric acid. Test 15, conducted at a high concentration (84 ppm.), showed complete inhibition of the cracking reaction. Adsorption of the reaction products on the metal surface still appears to be the most likely explanation but oxidation of the 2,4-DNP cannot be ruled out. Unfortunately, an NO analysis was not obtained because of moisture contamination of the spectrophotometer cell.

(7) Pure N_2O_4 is reported to react very slowly, if at all, with copper at room temperature. Test 12 was intended to test the principle of adding a slightly more reactive surface to minimize attack on the titanium alloy. Apparently the combination

of higher temperature and HNO_3 present was sufficient to completely dissolve the copper wire and generate substantial quantities of NO, i.e., 1.3%. At this level of combined NO, no specimen cracked.

(8) A platinum surface is quite effective in decomposing hydrogen peroxide and some other oxidizing species. The presence of a piece of bare platinum gauze had no effect on the SCC test in Test 16; platinizing the gauze and reducing the volume of N_2O_4 in the test likewise had no effect (Test 25).

C. Effect of Dissolved Oxygen - Liquid Phase Tests at 40°C.

In a limited series of tests performed under NASA Contract No. 8-21207, the effect of dissolved oxygen on the SCC test was investigated. It was found that samples of RR N_2O_4 containing <1 to 20 ppm. dissolved O_2 caused cracking in test specimens at the normal test temperature of 165°F. (74°C.). However, two 76-hour runs at 70°-80°F. showed that a RR N_2O_4 sample containing about 20 ppm. dissolved O_2 caused 50-100 times more cracking (100-800 cracks/cm.^{2}) than a sample whose O_2 content had been reduced to about 1 ppm. (2-8 cracks/cm.^{2}). This observation was sufficiently important to initiate a series of experiments designed to establish the effect of dissolved O_2 on SCC.

1. Preliminary Work - Ambient Temperature

For preliminary testing, a single-position oxygen pressure system was assembled (Figure 27). A test cell was flushed with 1 cell-volume of N_2O_4, emptied, and filled again. Approximately 100 ml. of N_2O_4 was then removed and the cell attached to the

FIGURE 27

OXYGEN PRESSURE SYSTEM

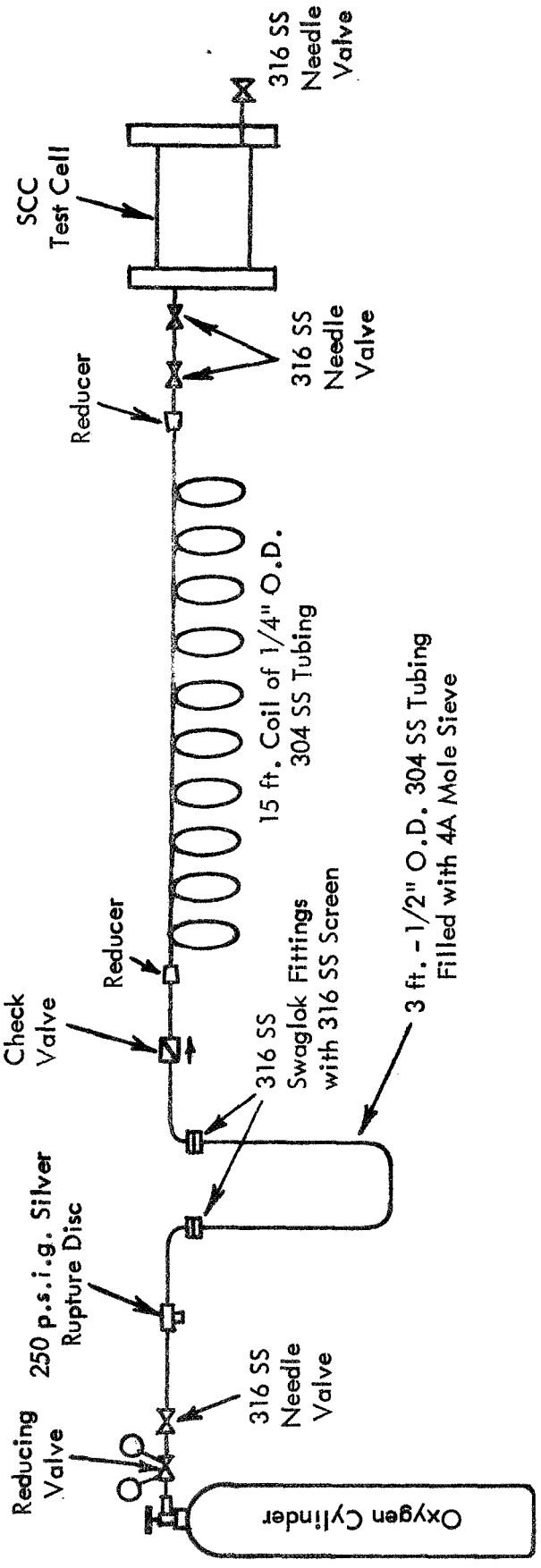

oxygen pressure system. The oxygen pressure was set and maintained constant throughout the run by means of the tank reducing valve. It was hoped that the behavior of the test media could be evaluated by crack density measurements.

A number of preliminary tests were made to see if a consistent relationship between crack density and O_2 partial pressure could be observed at ambient temperature. This series of experiments was hampered by wide ambient temperature fluctuations during a given day and between days, as well as by the fact that all of the observed cracks were micro in nature, requiring microscopic examination at 200X. In general, the results tended to confirm the oxygen effect previously observed. However, sufficient anomalies were encountered to show that the experimental conditions were not adequately under control. The most important variable appeared to be the test temperature.

2. Dissolved Oxygen Tests at 40°C.

All subsequent testing was performed at a constant temperature of 40°C. in a large capacity, incubator-type oven. Four U-bend specimens of 6Al 4V Ti alloy were used per test. The cell flushing and filling procedure was the same as described above. Oxygen pressure was maintained on the cells throughout the duration of each 70-hour test. The original method of measuring and reporting crack density was revised. The developed procedure employed a Balphot Metallograph which was used to count all of the cracks in the area of maximum stress on both sides of the U-bend specimen. The average of the two results

was reported. The area of maximum stress is defined as the edge area of the curved portion of the U-bend specimen. Magnifications of 100X and 200X were commonly employed. The test results obtained at 40°C. are summarized in Table 20.

The test data showed that tests conducted in the presence of oxygen produced more cracking than the control tests in 7 out of 8 cases. The experimental evidence did not indicate that the crack density was directly proportional to oxygen pressure. Application of some non-rigorous statistical tests indicated that at least 5 out of the 7 positive differences between the means of the control and O_2 tests were statistically significant. Although the precision of the crack density measurements was poor by analytical standards (relative standard deviation of 10-30%), it was judged to be adequate for the purpose of establishing trends or rough correlations. It was apparent, from the variability in the control values and the higher crack densities obtained in the later tests (Tests 58-65), that all of the test variables were not under control. Specimen variability was the prime suspect.

3. Crack Density Measurements

The potential value of the crack density measurements in the oxygen study was diminished by the variability of the test results. Several aspects of this problem were briefly investigated.

a. Edge Effects

Since the crack counting was performed microscopically on the edges of the specimens, it was felt that the nature of the edge finish might be adversely affecting the reproducibility of the measurements. A test was set up and carried out with RR N_2O_4

Table 20

Stress Corrosion Cracking Tests - Effect of Dissolved Oxygen

RR N_2O_4 - 40°C. - 70 Hours

Test No.	39	40	44	45	50	51	58	59	60	61	62	63	64	65
O_2 Pressure, psig.	-	30	-	50	-	100	-	5	30	100	-	-	5	5
Crack Density (200X)	380	550	275	500	0	250	630	640	1520	1975	950	560	880	1660
	400	500	150	550	0	370	1130	450	1820	1945	670	460	1500	1840
	400	525	150	550	1	480	840	430	1370	2140	1120	481	1260	1970
	420	650	250	450	7	550	900	375	1410	1450	820	260	1240	1030
Av.	400	556	206	512	2	412	875	474	1530	1880	890	440	1220	1625
Δ		+156		+306		+410		-401	+655	+1005	Δ average		+555	+960
											Δ high value		+330	+735
Std.Deviation, s	16	66	66	48	-	131	206	115	204	298	191	128	256	416
Relative Std. Deviation, %	4.1	11.8	31.9	9.3	-	31.8	23.5	24.3	13.3	15.8	21.5	29.0	21.0	25.6

Pooled standard deviation, controls, s_p^c = 141 d.f. = 15

Pooled standard deviation, O_2 tests, s_p^t = 225 d.f. = 24

Overall pooled standard deviation, s_p = 197 d.f. = 39

Confidence interval, average of four replications, 95% confidence level, $L_{1/2} = \pm 199$.

for 70 hours at 40°C. to evaluate this effect. Four U-bend specimens were employed representing a range of edge finishes from standard machining to 600 grit (produced by wet silicon carbide paper). The results are shown in Table 21. It did not appear that the nature of the edge finish had a significant effect on the crack density.

Table 21

Effect of Edge Finish on Crack Density
Test 67
RR N_2O_4 40°C. 70 Hrs.

Specimen	Edge Cracks[1] Max. Stress Area	Edge Cracks[1] Beyond Max. Stress Area	Surface Finish of Edge	Remarks
UY	36	3.2	Standard - as machined	Standard stressing procedure
UZ	46	4.7	120 Grit - Wet SiC	
VA	52	6.7	240 Grit - Wet SiC	
VB	31	8.5	600 Grit - Wet SiC	

[1] The cracks on the edges were too numerous to count between tangent scribes. The values reported above represent the average number of cracks per field of view at 200X. Four areas were counted to determine the averages in each case.

b. Measurements on the Plane of the Specimen

An attempt was also made to confirm the crack densities obtained from edge measurements with measurements across the plane of the U-bends. A single microscope field width (200X) scan was made from tangent scribe to tangent scribe across the entire width of U-bend specimens selected from Tests 57-65. It was found to be extremely difficult to determine whether scanning was being done at the actual tangent point, i.e., the point of maximum stress. The crack densities were found to vary widely just 1 or 2 field diameters (200X) on either side of the scan line. Crack density was also observed to be less in the center of the scan than at either side. This observation tends to correspond to the dishing effect produced in the center of the width around the radius of the bend. It appeared that there might be some areas of the bend approaching a compression state. It was concluded that measurements of crack density on the plane of the specimen were not practical.

c. Effect of Stress Level

It is well known that stress level is a critical factor in SCC. However, it was not known how critically the crack density was affected by stress level. In the early work done under Contract No. NAS 8-21207, stress level was investigated but only with regard to whether cracking was produced or not. No crack density measurements were attempted, and it was found that cracking occurred at any stress level above 30% of yield strength (the lowest level tested).

An orienting test run was made (Test 66) in which 2 standard U-bends were unbolted before exposure (RR N_2O_4, 40°C., 60 hrs.) and 2 unstressed, straight blanks were exposed. The results are shown in Table 22. The previously stressed and unbolted specimens showed a crack density of 4-5 cracks/field of view compared to a range of 30-50 cracks/field of view for normally stressed U-bends (see Table 21). The unstressed blanks showed no edge cracks but numerous cracks were observed in and around the stamped letters and bolt holes.

Table 22

Effect of Stress Level on Crack Density
Test 66
RR N_2O_4 40°C. 70 Hrs.

Specimen	Description	Crack Density[1] Max. Stress Area	Outside Max. Stress Area	Other
UI	Previously stressed U-bends, unbolted	5	0	-
UJ		4	0	-
VC	Unstressed blanks	0	0	20 - cracks around lettering 15 - cracks around bolt hole
VD		0	0	65 - cracks around lettering 13 - cracks around bolt hole

[1] These values represent the average number of cracks per field of view at 200X. At least 4 areas were counted and averaged in each case.

Two additional runs were conducted to investigate the sensitivity of crack density to variations in normal prebending and stressing procedures. Variations can occur principally in the prebend angle and in the final spacing of the U-bend arms. It has been observed that, on occasion, the prebend angles varied significantly. For this work, prebends were sorted to obtain 10 specimens with very similar prebend angles. The prebends were then stressed with bolts to different degrees of final deflection and thus different stress levels. They were then exposed to RR N_2O_4 at 40°C. for 70 hrs. The results are shown in Table 23.

Table 23

Effect of Applied Stress Level on Crack Density
Tests 68 and 69
RR N_2O_4 40°C. 70 Hrs.

Test No.	Distance Between Arms, cm.	Edge Crack Density
68	1.94	2200
	2.02	2100
	2.10	1490
	2.18	900
	2.26	980
69	1.47	2460
	1.78	2380
	2.10	1430
	2.42	630
	2.74	390

The data showed that the crack density is quite sensitive to changes in applied stress. A difference of about 1 mm. in the spacing of the arms could cause a variation of 200-500 cracks. Variability in the prebend angle would also enhance the variance of the crack density.

4. Dissolved Oxygen Tests - Controlled Stress Level

In view of the above work, a series of tests was run in an attempt to measure the dissolved oxygen effect at a higher level of precision than previously attained. Specimens for 4 tests were prepared so that each specimen was finally stressed to about 70% of yield strength as calculated by the Blake formula (1, pp. 90-92). The specimens were then loaded into test cells and tested with RR N_2O_4 at 40°C. for 70 hours under 3 different pressures of oxygen. The results are shown in Table 24. These data did not show a significant improvement in precision over previous data. As before, the tests made in the presence of oxygen showed a higher average crack density than the control. Only one of these differences ($\bar{X}_{71} - \bar{X}_{73}$) was statistically significant. Once again the increase in crack density was not directly proportional to the O_2 pressure. It appears that the basic variability of crack generation and measurement requires the use of statistical methods for useful interpretation.

Table 24

Stress Corrosion Cracking Tests - Effect of Dissolved Oxygen

RR N_2O_4 40°C. 70 Hrs.

Test No.	71	72	73
O_2 Pressure, psig.	35	110	-
Crack Density (200X)	1880	2320	960
	1790	1040	925
	1610	1050	1360
	1580	1340	1240
Av.	1715	1438	1121
Δ	+594	+317	-
Std. Deviation, s	144	604	212
Relative Std. Deviation, %	8.4	42.0	18.9

D. Effect of Nitric Acid - Liquid Phase Tests at 40°C.

Another impurity in N_2O_4 that might have a possible positive effect on SCC is nitric acid. Accordingly, several 40°C. tests were run to evaluate the effect of HNO_3 concentration. Test media were prepared in 1650 ml. stainless steel sample cylinders. A cylinder was first filled to about 75% of its capacity with RR N_2O_4. Next, selected volumes of 99% HNO_3 were added by pipet. The cylinder was then filled with additional RR N_2O_4 and mixed thoroughly. The resulting solution was used to flush and fill an SCC test cell in the usual way. The starting level of HNO_3 concentration in the RR N_2O_4 was approximately 5300 ppm. Addition of 99% HNO_3 to the cylinder was at two levels, i.e., 5 ml. and

20 ml., corresponding to final HNO_3 concentration levels of ca. 0.8% and 1.8%. After preparation, analysis of the initial two mixtures gave values of 0.8% and ~1.5% HNO_3, respectively. The higher value could not be accurately determined because it was considerably outside of the calibration range of the near-infrared spectrophotometric analysis method. Both mixtures were found to contain a very small amount of combined NO after preparation, i.e., 16-17 ppm. This concentration level is about at the limit of detection of the method and is of questionable accuracy. From all previous work, this low level of NO is insufficient to cause inhibition of SCC. However, in subsequent runs the test media were pressured with oxygen before the tests. The results are summarized in Table 25.

The data indicated an actual inhibition of SCC when HNO_3 was added to the RR N_2O_4 up to the 0.8% and 1.8% levels. Identical results were obtained when the test mixtures were treated with 5 psig. oxygen after the additions of HNO_3. Only when a drastic O_2 treatment was employed after HNO_3 addition did the test mixtures show SCC crack densities similar to the control. It was concluded that, as a separate entity, HNO_3 does not have any positive effect on SCC. The experimental evidence indicated that increasing the amount of HNO_3 can either cause inhibition or can result in enhanced inhibition by interaction with other species present, e.g., NO. (See Section II-F, Critical Composition Level Tests.)

Table 25

Stress Corrosion Cracking Tests - Effect of HNO_3 Concentration

RR N_2O_4 - 40°C. - 70 Hours

Test No.	46	47	55	56	57	53	52	54
RR N_2O_4, ml.	1645	1630	1645	1630	1650	1645	1630	1650
99% HNO_3, ml.	5	20	5	20	-	5	20	-
O_2 Treatment	-	-	5 psig.(1)	5 psig.(1)	-	50 psig.(3)	50 psig.(3)	-
NO, ppm.	16	17	-	-	-	12	-	-
HNO_3, ppm.	8330	~15300	-	-	-	8840	-	-
Crack Density (200X)	3	0	4	0	>700	525	590	425
	5	0	6	0	>700	500	600	420
	7	0	8	0	>700	525	600	375
	10	0	5	0	>700	525	620	500
Av.	6	0	6	0	>700(2)	519	602	430

Notes: (1) After removal of 300 ml., sample cylinder was pressured to 5 psig. with O_2 and then shaken periodically for 2 hours. The O_2 pressure was vented to atmospheric pressure and allowed to stand overnight at ambient temperature.

(2) 400-500 of these cracks were very tiny and difficult to count.

(3) After removal of 300 ml., sample cylinder was pressured to 50 psig. with O_2 and then disconnected from the O_2 source. Stood overnight at ambient temperature. Vented to atmospheric pressure and used to load cell.

E. Interaction of NO_2 and O_2 - Vapor Phase Tests

A number of preliminary vapor phase SCC tests were carried out to help clarify the SCC mechanism by investigating any possible interaction of NO_2 and O_2 that might be related to SCC. The results are shown in Table 26. In Tests 24 and 26, the cells containing the specimens were filled with liquid N_2O_4, emptied, and filled again. The cell was again drained, leaving only a very small amount of liquid and essentially one atmosphere pressure of NO_2 vapor. When heated to the test temperature (74°C.), the specimens would be in contact solely with NO_2 vapor. One of these two test cells was then pressured to 30 psig. with oxygen.

In Test 24, all specimens remained unchanged. However, in Test 26 where 30 psig. of O_2 was added, all specimens developed a large number of macrocracks. Many of these cracks had a "burned" appearance, possibly due to a variety of oxide colors within the cracks. This is the first time that this type of crack appearance had been observed. These results lead to a series of runs (Tests 28-33) in which oxygen was used as the main test medium and varied amounts of NO_2 were added by injecting measured volumes of liquid N_2O_4. The N_2O_4 was converted to NO_2 vapor at the test temperature. None of these tests caused the alloy specimens to crack. The main experimental difference in this series of tests was that the specimens had never been in contact with liquid N_2O_4.

Table 26

Stress Corrosion Cracking Tests - RR N_2O_4 Vapor + O_2

Test No.	Test Medium	Amount	Temp., °C.	Duration, Hr.	Failure Rate	Remarks
24	RR N_2O_4 Vapor (after liquid drain)	1 atm.	77	70	0/5	-
26	Same as No. 24 Oxygen	1 atm. 30 psig.	74	70	5/5	All spec. had many macrocracks; varied oxide colors in cracks.
28	RR N_2O_4 vapor Oxygen	0.5 ml. Liq. 15 psig.	74	70	0/4	-
29	RR N_2O_4 vapor Oxygen	1.0 ml. Liq. 15 psig.	74	70	0/4	
30	No N_2O_4 Oxygen	- 15 psig.	74	70	0/4	-
31	RR N_2O_4 vapor Oxygen	0.5 ml. Liq. 30 psig.	74	70	0/4	-
32	RR N_2O_4 vapor Oxygen	1.0 ml. Liq. 30 psig.	74	70	0/4	-
33	No N_2O_4 Oxygen	- 30 psig.	74	70	0/4	

In addition, it appeared likely that the nitrogen used to purge the cells after cleaning had not been completely flushed out with oxygen. Thus, the test medium really consisted of a mixture of N_2 + O_2 instead of pure O_2.

Since it appeared possible that contact with liquid N_2O_4 prior to vapor phase testing might be critical, this technique was used in an additional series of tests. The test conditions and results are shown in Table 27. Tests 35 and 41 were essentially repeats of Test 26; Test 34 was a control. In Test 36, two of the four specimens were immersed in liquid N_2O_4 for 10 minutes before placing them in the test cell under 30 psig. O_2 pressure. The remaining two specimens in the test were handled normally. None of the specimens in the above tests developed cracks with the possible exception of Test 41 where a few possible incipient microcracks were observed at 400X.

Five additional vapor phase tests were then performed. Tests 42 and 43 were run to check the effect of higher O_2 pressures. Test cells containing the U-bend specimens were filled, emptied, and filled again with RR N_2O_4. The cells were then emptied again and vented to atmospheric pressure. Oxygen pressure was then applied, the cells sealed, and the test carried out. Neither test gave any evidence of cracking; specimens were examined up to 400X magnification.

Table 27

Stress Corrosion Cracking Tests - Vapor Phase

Test No.	Test Medium	Amount	Temp., °C.	Duration, Hours	Failure Rate	Remarks
34	RR N_2O_4 vapor (After liquid drain)	-	74	70	0/4	-
35	RR N_2O_4 vapor Oxygen	- 30 psig.	74	70	0/4	-
36	Oxygen	30 psig.	74	70	0/4	Two specimens were immersed in liquid N_2O_4 for 10 min. before exposure in cell; remaining 2 spec. untreated. No cracking detected.
41	RR N_2O_4 vapor Oxygen	- 30 psig.	72	71	0/4	Possible incipient cracks observed at 400X. Very few in number.
42	RR N_2O_4 vapor Oxygen	- 50 psig.	72	70	0/4	-
43	RR N_2O_4 vapor Oxygen	- 100 psig.	72	70	0/4	
48	RR N_2O_4 liquid	-	25	24		
	RR N_2O_4 vapor	-	72	70	0/4	
49	RR N_2O_4 liquid	-	25	24		
	RR N_2O_4 vapor Oxygen	- 50 psig.	72	70	0/4	

During the above test preparation, the specimens were actually in contact with liquid RR N_2O_4 for only about 5 minutes. It was felt that a longer contact with the liquid might alter the oxide coating of the specimens sufficiently to permit subsequent attack by O_2. Accordingly, in Tests 48 and 49, the specimens were allowed to remain in contact with RR N_2O_4 for 24 hours at ambient temperature. The liquid was then drained, Test 49 pressured to 50 psig. with O_2, and the tests carried out for 70 hours at 72°C. No cracking occurred.

The unusual results observed in Test 26 remained anomalous; no other vapor phase test showed any significant evidence of cracking.

F. Critical Composition Level Tests

One of the major objectives of this program was to establish the concentration levels of the important minor constituents of N_2O_4 that are critical to their respective actions. In order to carry out this work, the following procedures were required:

(1) Analytical methods for quantitatively determining the important minor constituents in the concentration range of <10 ppm. to 1% (4 orders of magnitude).

(2) Procedures for adjusting the composition of liquid N_2O_4 with respect to the minor constituents, and for loading SCC test cells with the resulting material.

(3) A sensitive and statistically reliable SCC test.

The development of the analysis procedures has previously been described in Section I.B. Combined NO is measured spectrophotometrically in the visible spectral region; HNO_3, HNO_2 and H_2O are measured spectrophotometrically in the near-infrared region. Because of the complexity of the spectra, the absorbances are digitized and the concentrations calculated by digital computer. Alternately, concentrations of the species that are particularly difficult to determine, i.e., HNO_2 and H_2O, can be calculated from the measured NO and HNO_3 concentrations by use of experimentally determined equilibrium constants (see Section I.C.). At this point several important facts should be emphasized. First of all, the N_2O_4 systems studied in this work are composed of some or all of the following molecular species in equilibrium: N_2O_4, NO_2, N_2O_3, HNO_3, HNO_2, and H_2O. In an inert, closed system, at constant temperature, equilibrium is established and maintained. These conditions are obtained in the high pressure, temperature-controlled cell used for spectrophotometric analyses, and in the SCC test cells in the absence of significant amounts of reactive species. However, if the temperature changes, or the system volume changes, or adventitious contamination occurs, e.g., H_2O pick-up, or reaction takes place, the composition will change significantly. Essentially all of the analyses performed during this program were carried out at -10°C. This temperature was selected in order to simplify the spectral interpretation and calculations. On the other hand, all of the critical composition SCC testing was performed at 70-74°C. During this work, an attempt

was made to determine the variation of equilibrium constant with temperature. Although some success was achieved in this effort, the majority of the critical compositions were determined in terms of the analyzed compositions at -10°C.

The composition of N_2O_4 systems can be adjusted in a variety of ways. For example, protons can be added as 100% HNO_3 or as H_2O. In the latter case, particularly, time must be allowed for solution and reaction of the H_2O. As previously described, protonated species can be removed by batch contact with Type 3A Molecular Sieve. Composition can also be adjusted by the addition of gaseous reactants such as NO and O_2. NO dissolves and reacts very rapidly to form N_2O_3; O_2 solution and reaction is much slower. A range of liquid compositions can also be obtained by blending liquid samples. The majority of the compositional adjustments were performed by the addition of NO gas directly to SCC test cells containing liquid N_2O_4 whose HNO_3 content ranged from 50 to 6000 ppm. Samples were usually taken and analyzed for combined NO, HNO_3, HNO_2, and H_2O before and after each SCC test. The NO was initially injected through silicone rubber septa into the cells by means of large (50-100 ml.) hypodermic syringes. Later, the NO was added by pressurizing a small (90-150 ml.) stainless steel sample cylinder to a known pressure with NO and then connecting to the test cell. The apparatus is shown in Fig. 28.

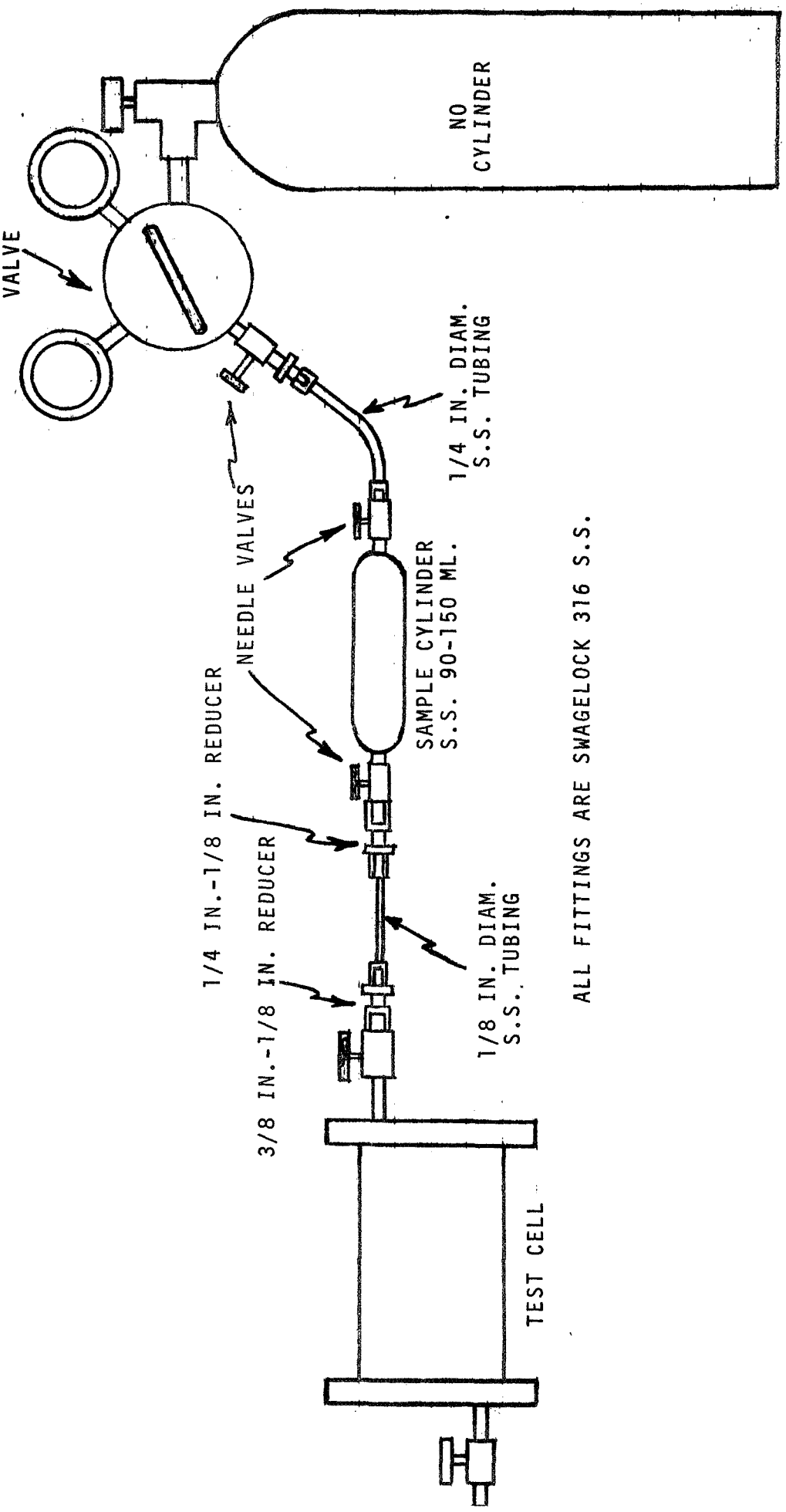

FIGURE 28

APPARATUS FOR ADDITION OF NO TO SCC TEST CELLS

With regard to the third requirement, a satisfactory SCC test was developed under the previous contract (1). A modified version of this test, employing a smaller volume cell and fewer U-bend specimens, was used in this work (see Section II.A).

1. Addition of NO to RR N_2O_4

The objective of the initial critical level testing was to establish the minimum amount of NO that would inhibit SCC in RR N_2O_4. The HNO_3 content of the starting material was approximately 5200 ppm. Ranging experiments were performed by adding varying amounts of NO to test cells containing RR N_2O_4 and then testing for 70 hours at 74°C. Contents of the test cells were analyzed before and after each test. Initial results showed that the critical level of combined NO was between 110 and 215 ppm. The addition of NO to achieve this level, reduced the HNO_3 content of the test mixtures to 4725 and 4450 ppm. respectively. A series of 4 tests was then made to explore the above narrow region of combined NO levels. The results are shown in Table 28. The data showed that 150 ppm. combined NO is a borderline condition for SCC, and that the minimum NO level for complete inhibition in RR N_2O_4 under the test conditions is between 150 and 190 ppm.

2. Effect of the Distribution of Minor Constituents on Stress Corrosion Cracking

Work under the previous contract (NAS 8-21207)showed that stress corrosion cracking in the N_2O_4-Ti alloy system under study could be drastically influenced by very minor changes in

Table 28

Stress Corrosion Cracking Tests - RR N_2O_4 + NO

Test No.	NO, ppm. Before	NO, ppm. After	HNO_3, ppm. Before	HNO_3, ppm. After	HNO_2, ppm. Before	HNO_2, ppm. After	H_2O, ppm. Before	H_2O, ppm. After	Failure Rate	Remarks
86	96	95	4632	4737	12	16	48	46	4/4	All specimens cracked in half.
	96		4684		14		47			
87	148	136	4504	4610	41	31	63	63	4/4	3 specimens cracked in half; 1 spec. had macro cracks
	142		4557		36		63			
88	146	148	4500	4610	27	23	69	66	2/4	1 specimen cracked in half; 1 spec. had macro cracks; 2 spec had no cracks (200X)
	147		4555		25		68			
89	192	182	4399	4520	36	54	80	76	0/4	No cracks (400X).
	187		4460		45		78			

composition. These changes could be brought about by the addition of normal constituents and/or foreign additives. Such additions, along with changes in temperature, pressure, or vapor space, can cause shifts in the equilibrium composition and influence SCC. In previous sections, the effects of organic additives, oxygen, and nitric acid have been evaluated. In this section, the effects of combined NO and the distribution of protonated species will be described.

One of the more interesting discoveries made earlier was that lower total proton levels in the N_2O_4 required the addition of larger amounts of NO in order to achieve inhibition of SCC. This behavior indicated that species produced by the interaction of HNO_3 and N_2O_3, i.e., HNO_2 and H_2O, were critically involved in the characterization of a non-cracking system. Consequently, it was planned that this phenomenon would be further investigated in the current program. Instead of adding known amounts of HNO_3 or H_2O to previously deprotonated N_2O_4, it was decided to combine the deprotonation study previously described (Section I.A. 2.c) with the composition-SCC experiments. As previously mentioned, the deprotonation by batch contact with AR 12-22 Molecular Sieve is a slow process and NO addition experiments could readily be performed while the proton level was decreasing with time. Attempts were made to cover concentration ranges of 0-1000 ppm. combined NO and 0-6000 ppm. HNO_3 (composition at -10°C.). Throughout the course of this program, it has been demonstrated that these two constituents could be determined with excellent sensitivity,

accuracy, and precision. The direct determinations of trace levels of HNO_2 and H_2O were much more susceptible to error and other types of secondary correlations were attempted.

Basically the SCC tests were performed under standard conditions (70 hrs. at 74°C.) after the composition of the N_2O_4 had been adjusted by the addition of gaseous NO to the test cells and samples had been taken for analysis. Upon completion of the tests, the oven was shut off and the cells allowed to cool to room temperature. In most cases, an additional analytical sample was taken from each cell. The data from 31 test runs are given in Table 29 and are plotted in Figure 29. Values from the previous contract work (7 tests) are included in the plot. The principal values presented in the table were determined spectrophotometrically; the values for HNO_2 and H_2O in parentheses were calculated from the determined equilibrium constants.

In general, the composition data exhibited the following characteristics:

(1) Replicate NO and HNO_3 determinations showed excellent precision.

(2) Agreement of "Before" and "After" values for NO and HNO_3 was considered to be very good in 17 of the 22 cases in which both analyses were made. The main sources of variability were sampling the test cell before room temperature equilibrium was re-established, and possible moisture contamination.

Table 29

Critical Composition Level SCC Tests

(Compositions Determined at -10°C.)

Test No.		ppm., By Weight NO A	NO B	HNO_3 A	HNO_3 B	HNO_2 A	HNO_2 B	H_2O A	H_2O B	Failure Rate
78		19	85	5086	4938	7	-	13	28	
		27	85	4990	4927	24	-	13	28	
		27		5000		38		19		
		24	85	5025	4932	23		15	28	
	Av.	54		4978		23 (16)		17 (15)		4/4 X
79		106	111	4714	4725	9	7	54	48	
		107	112	4703	4756	27	32	54	51	
		108		4713		25		54		
		107	112	4710	4740	20	20	54	50	
	Av.	110		4725		20 (30)		52 (27)		4/4 X
80		218	212	4374	4511	6	60	81	87	
		222	213	4385	4511	4	60	84	90	
		214		4406		0		81		
		218	212	4388	4511	3	60	82	88	
	Av.	215		4450		7 (56)		85 (47)		0/4 0
81		292	286	4214	4340	49	74	114	102	
		288	286	4235	4319	61	77	113	105	
			288		4320		62		99	
		290	287	4225	4325	55	71	114	102	
	Av.	288		4275		63 (72)		108 (59)		0/4 0
86		96	94	4622	4737	-10	16	51	45	
		96	96	4642	4737	33	16	45	48	
		96	95	4632	4737	12	16	48	46	
	Av.	96		4684		14 (26)		47 (23)		4/4 X
87		147	134	4504	4600	41	25	66	63	
		149	138	4504	4621	41	37	60	63	
		148	136	4504	4610	41	31	63	63	
	Av.	142		4557		36 (38)		63 (33)		4/4 X
88		143	149	4505	4610	26	23	66	66	
		148	147	4494	4610	28	23	72	66	
		146	148	4500	4610	27	23	69	66	
	Av.	147		4555		25 (39)		68 (34)		2/4 0
89		191	180	4389	4515	30	55	78	78	
		192	185	4409	4525	42	53	81	75	
		192	182	4399	4520	36	54	80	76	
	Av.	187		4460		45 (48)		78 (41)		0/4 0
90		0	20	2668	2657	50	67	7	10	
		0	22	2678	2678	63	63	10	10	
		0	21	2673	2668	56	65	8	10	
	Av.	10		2670		60 (2)		9 (1)		4/4 X
91		0	182	2678	2708	79	136	7	49	
		0	181	2658	2687	51	139	7	43	
		0	182	2668	2698	65	138	7	46	
	Av.	91		2683		102 (14)		26 (7)		4/4 X
92		85	-	2594	-	62	-	13		
		85	-	2594	--	47	-	13		
		85		2594		54		13		
	Av.	85		2594		54 (13)		13 (6)		4/4 X
93		345	335	2405	2436	33	59	25	28	
		343	336	2404	2404	64	49	25	25	
		344	336	2404	2420	48	54	25	26	
	Av.	340		2412		51 (48)		26 (22)		0/4 0
94		23	45	2204	2172	52	42	11	14	
		23	46	2108	2088	69	41	8	11	
		23	46	2156	2130	60	42	10	12	
	Av.	34		2143		51 (4)		11 (2)		2/2 X
95		223	226	2003	2035	56	66	14	14	
		221	225	1993	2045	58	64	14	14	
		222	226	1998	2040	57	65	14	14	
	Av.	224		2019		61 (26)		14 (10)		2/2 X
96		360	374	1929	1971	53	77	17	20	
		359	375	1940	1982	67	75	17	20	
		360	374	1934	1976	60	76	17	20	
	Av.	367		1955		68 (42)		18 (16)		0/2 0
97		445	479	1939	1961	83	64	17	14	
		450	472	1929	1937	69	-	20	26	
		448	476	1934	1949	76	64	18	20	
	Av.	462		1942		70 (52)		19 (19)		0/2 0
98		382	393	462	484	75	36	14	5	
		384	392	462	501	75	23	11	4	
		383	392	462	492	75	34	12	4	
	Av.	388		477		54 (11)		8 (1)		2/2 X
99		500	-	452	-	77	-	14	-	
		500	-	440	-	32	-	4	-	
		502		465		56		7		
		501		452		55		8		
	Av.	501		452		55 (13)		8 (1)		2/2 X
100		534	479	442	494	38	40	5	4	
		525	468	442	493	34	37	5	4	
		530	474	442	494	36	38	5	4	
	Av. (3)	530		442		36 (14)		5 (1)		0/2 0
101		619	539	436	535	27	39	7	5	
		623	548	437	525	25	47	7	5	
		621	544	436	530	26	43	7	5	
	Av. (3)	621		436		26 (16)		7 (1)		0/2 0
102		86	139	168	204	31	35	5	6	
		85	139	178	196	34	27	6	6	
		86	139	173	200	32	31	6	6	
	Av.	112		187		32 (1)		6 (0)		2/2 X
103		163	182	123	158	27	30	6	6	
		164	214	129	166	22	33	6	5	
		164	198	126	162	24	32	6	6	
	Av.	181		144		28 (2)		6 (0)		2/2 X
104		280	280	140	179	21	36	6	6	
		280	280	140	174	32	29	7	5	
		280	280	140	176	26	32	6	6	
	Av.	280		158		29 (3)		6 (0)		2/2 X
105		358	358	114	170	27	37	5	6	
		357	359	113	166	33	29	6	5	
		358	358	114	168	30	33	6	6	
	Av.	358		141		32 (3)		6 (0)		2/2 X

Test No.		NO A	NO B	HNO_3 A	HNO_3 B	HNO_2 A	HNO_2 B	H_2O A	H_2O B	Failure Rate
106		-	336	-	4124	-	61	-	117	
		-	333	-	4135	-	59	-	114	
	Av.		334		4130	60	(80)	116	(63)	0/2 0
114			154		4622		-10		63	
			177		4516		-7		69	
			182		4527		-9		69	
	Av.		171		4555	-9	(45)	67	(39)	4/4 X
115			386		1781		95		18	
			387		1707		92		18	
	Av.		386		1744	94	(39)	18	(13)	4/4 X
116			799		86		30		5	
			803		62		23		5	
	Av.		801		74	26	(3)	5	(0)	0/4 0
117			1134		67		27		7	
			1140		53		20		6	
	Av.		1137		60	24	(4)	6	(0)	1/4 0
119			220		3555		20		50	
			224		3512		58		50	
			222		3513		43		47	
	Av.		222		3527	40	(45)	49	(31)	0/4 0
120			344		2435		74		28	
			343		2415		47		25	
	Av.		344		2425	60	(48)	26	(22)	2/4 0

(1) A values determined before SCC test; B values determined after SCC test. - (2) Values in parentheses were calculated from equilibrium constants using average NO and HNO_3 values. - (3) B samples were taken before equilibrium was re-established; A values used instead of average.

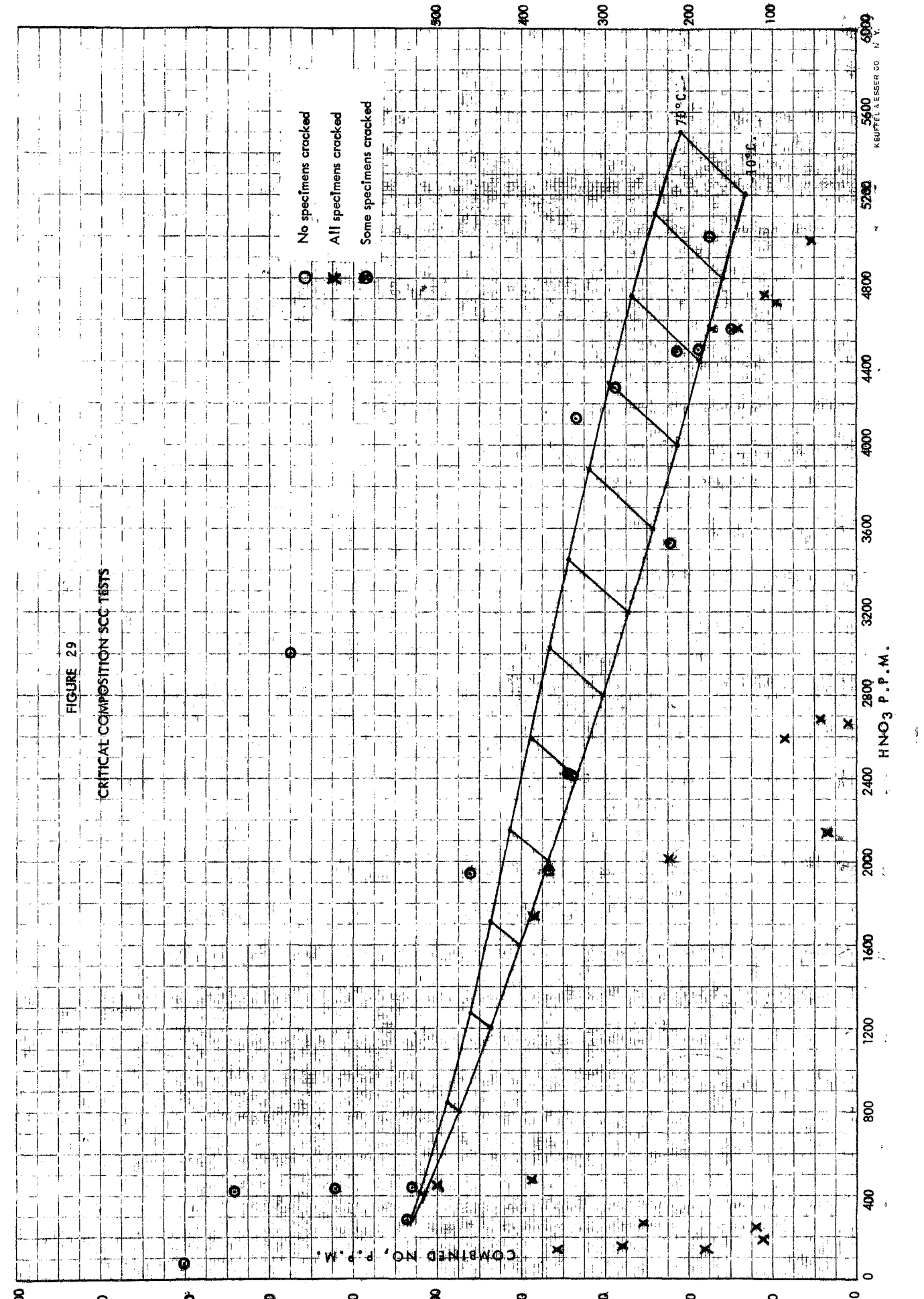

FIGURE 29

CRITICAL COMPOSITION SCC TESTS

(3) HNO_2 and H_2O values, while exhibiting satisfactory precision and "Before" and "After" agreement in most cases, must be considered as much more doubtful on an absolute basis. Agreement with the values calculated from the equilibrium constants was frequently poor. Essentially all of the HNO_2 and H_2O values are considered to be outside of the range of concentrations at which the computerized spectrophotometric procedure performs satisfactorily. The main limitations of the method appear to involve spectrophotometric and digitizing variability, and temperature stability during analysis.

The lower curve in Figure 29 represents the critical composition line as measured at -10°C. Compositions lying below the line caused cracking while compositions above the line did not. The upper line represents the actual composition of the N_2O_4 system at a temperature of 70°C. The tie lines connect corresponding compositions at the two different temperatures. The critical composition data at -10°, 40°, and 70°C. are given in Table 30. It can be seen that, as the temperature rises, the amounts of N_2O_3 and HNO_3 increase at the expense of the HNO_2 and H_2O. In all of the critical compositions at 70°C., the HNO_2 level has dropped to 20 ppm. or less and the H_2O level to about 1 ppm. or less.

Table 30

Critical Compositions at Different Temperatures

Temp., °C.	ppm.				
	N_2O_4	NO	HNO_3	HNO_2	H_2O
-10	999072	515	400	12	0.9
40	999059	520	414	6	0.1
70	999058	521	416	4	0.03
-10	998701	474	800	22	3.4
40	998665	487	838	10	0.2
70	998661	489	843	7	0.1
-10	998327	436	1200	30	7
40	998261	457	1267	14	0.5
70	998254	461	1275	10	0.2
-10	997949	402	1600	37	11
40	997848	432	1701	18	0.8
70	997839	437	1712	12	0.2
-10	997573	368	2000	43	16
40	997436	407	2135	21	1.2
70	997423	413	2150	14	0.4
-10	997197	335	2400	47	21
40	997023	383	2569	23	1.6
70	997006	389	2588	16	0.5
-10	996821	303	2800	49	26
40	996612	359	3002	26	2.1
70	996592	366	3023	18	0.6
-10	996447	272	3200	51	31
40	996207	334	3430	27	2.6
70	996184	343	3454	19	0.7
-10	996071	243	3600	51	35
40	995804	311	3854	29	3
70	995779	320	3881	20	0.9
-10	995698	214	4000	50	38
40	995411	285	4271	29	3.4
70	995384	295	4300	20	1.0
-10	995326	186	4400	48	40
40	995029	259	4680	29	3.7
70	995000	269	4710	20	1.1
-10	994956	159	4800	44	41
40	994657	231	5080	28	3.9
70	994627	241	5111	19	1.1
-10	994588	132	5200	40	40
40	994300	201	5469	26	3.9
70	994271	210	5499	18	1.1

G. Special Tests Related to SCC Mechanism

A number of miscellaneous SCC tests were performed in an effort to clarify certain aspects of the SCC mechanism.

1. Passivation Experiment

G8 N_2O_4, i.e., green N_2O_4 containing 0.8% combined NO, does not cause SCC in 6Al 4V Ti alloy. This behavior may be due either to a passivating reaction with active alloy surfaces to prevent attack, or to the fact that the principal attacking species may not be present. In order to assess the surface passivation hypothesis, a test was conducted in which 4 U-bend specimens were first exposed to G8 N_2O_4 for 70 hours at 74°C. The G8 N_2O_4 was then replaced with RR N_2O_4 and the specimens exposed for an additional 70 hrs. at 74°C. If the G8 N_2O_4 passivated the surfaces of the specimens adequately, cracking should not occur.

At the completion of the test, all 4 U-bend specimens had cracked in half. Initially it was felt that the surface passivation hypothesis had been disproven. However, at the high level of stress present in the U-bends, it appears probable that fresh surfaces would continue to be formed at slip-planes and oxide layer cracks during the 70-hour exposure to RR N_2O_4. Thus, even if the initial fresh surfaces were passivated by the G8 N_2O_4, the new surfaces exposed to the RR N_2O_4 during the second 70 hours could lead to cracking.

2. Brittle-Film Formation

One theory of mechanical crack propagation in SCC involves the initial formation of an embrittled surface layer that then undergoes brittle fracture in the presence of tensile stress (8). The resulting crack is arrested by plastic deformation when it enters the ductile substrate. The distance to which it propagates in the substrate depends on such factors as dislocation mobility and availability of slip systems. Further film formation occurs at the clean surfaces exposed by the fracture stage and, at a critical film thickness, film rupture again occurs. The crack propagation thus proceeds discontinuously by repeated cycles of the formation and rupture of the film.

An interesting feature of the brittle-film model is that it does not require the simultaneous action of stress and exposure to the environment, and it predicts that cracking should result from the exposure of unstressed specimens to the cracking environment followed by stressing in the absence of the environment. This has been confirmed experimentally in some systems (9).

This mechanism was tested by first exposing 4 drilled Ti alloy flats, and 4 pre-bend specimens to RR N_2O_4 for 70 hours at 74°C. Examination of the specimens showed that the drilled flats had developed some micro-cracks at the identification stampings and at the bolt holes but nowhere else. The pre-bends developed micro-cracks in the maximum stress area.

All of the specimens were then fully stressed by bolting and the crack patterns examined over a 2-week period. There was no change in the number or appearance of the cracks. The brittle-film mechanism thus does not appear to apply to the 6Al 4V Ti alloy-N_2O_4 system.

3. Applied Potential Test

In many aqueous systems, cathodic protection has proved to be an effective means of preventing stress corrosion cracking in alloys of magnesium, aluminum, copper, mild steel, and stainless steel. Cotton (10) found that the application of 1.5 volts, anodic, to titanium specimens greatly reduced the rate of normal corrosion. A simple experiment was performed in an effort to assess the effect of applying a fixed potential to stressed U-bend specimens in the nonaqueous N_2O_4 test system. Two U-bend specimens were attached to two conductive stainless steel rods and stressed in place by means of titanium alloy nuts (Figure 30). Each rod with its attached specimen was screwed through a tapped hole in the Teflon end plates of a test cell. The cell was then assembled and pressure tested in the usual way. A 1.5-2.0 volt battery was then connected between the two specimens, and the cell was flushed and filled with RR N_2O_4. After 70 hours at 74°C., both specimens had cracked in half. A check of the battery voltage showed that it had not lost its charge.

It thus appeared that neither anodic or cathodic polarization had any effect on SCC. However, the conductivity of N_2O_4 is very low and other levels of potential or current density might be required.

FIGURE 30

TEST CELL ENDPLATE AND SPECIMEN HOLDER
FOR APPLIED POTENTIAL TEST

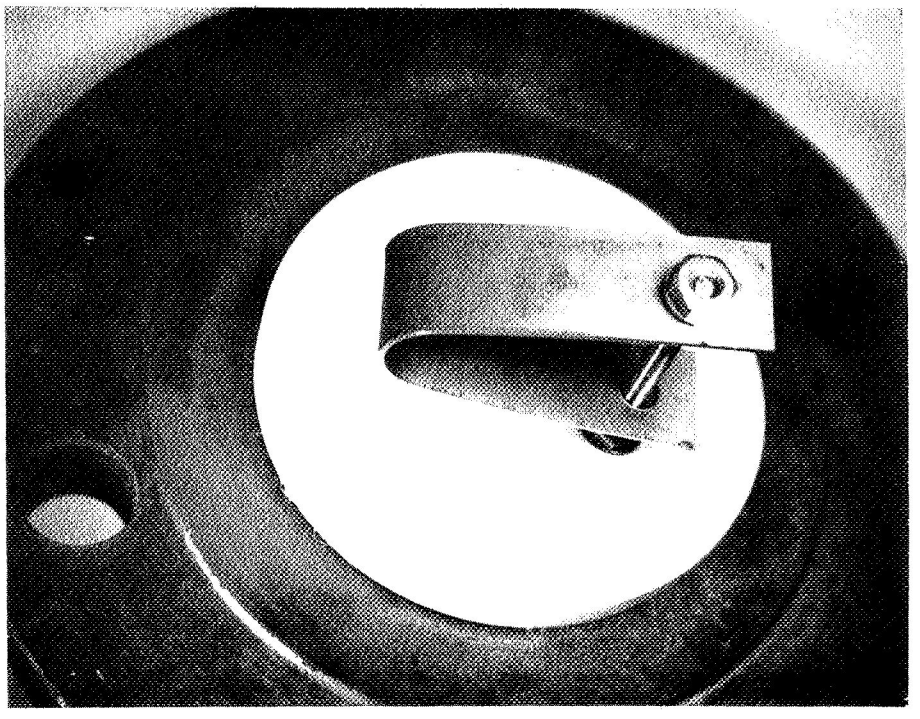

SUMMARY

I. NAS 8-21207

Substantial progress toward the overall goals of this program was achieved during the first year's work under Contract No. NAS 8-21207. The more important aspects of this work have previously been reported in detail (1), and described briefly in the Introduction of this report. The principal experimental accomplishments were as follows:

(1) A satisfactory stress corrosion cracking test was developed.

(2) Six new analytical methods for the analysis of liquid N_2O_4 systems were developed.

(3) A study of the near-infrared spectral region resulted in the elucidation of the nature and approximate distribution of the proton-containing compounds in liquid N_2O_4 systems for the first time.

(4) Techniques were developed for the quantitative adjustment of the minor constituent composition of liquid N_2O_4 systems.

(5) The SCC behavior of 6Al 4V titanium alloy stressed U-bend specimens in a wide variety of liquid N_2O_4 compositions was established.

The following information was derived from the above experimental program.

Composition

It was found that the principal differences between "red" and "green" N_2O_4 were that "red" N_2O_4 contained NO_2, HNO_3, and O_2 as minor constituents in solution, while "green" N_2O_4 contained NO_2, N_2O_3, HNO_3, HNO_2, and H_2O. Typical so-called Red Reactive (RR) N_2O_4 (MIL-P-26539A) contained ∿6000 ppm. HNO_3 and ∿10 ppm. dissolved O_2. Typical G8 N_2O_4 (MSC-PPD-2A), manufactured to contain ∿8000 ppm. combined NO, contained about 2000-3000 ppm. HNO_3, even though the total proton content calculated as H_2O or HNO_3 was almost identical to that of the RR N_2O_4. The remainder of the protons was present as HNO_2 and H_2O, but quantitative measurements could not be made at this time.

Corrosion Rates

Typical RR N_2O_4 attacks unstressed 6Al 4V ELI Ti Alloy to a small but measurable degree at 72-74°C., i.e., 0.8-0.9 mils/year. At room temperature the rate of attack is negligible, i.e., <0.06 mils/year.

G4 and G8 N_2O_4 showed no evidence of corrosive attack at 72-74°C., i.e., <0.06 mils/year. At the same temperature, RN N_2O_4 containing 500 ppm. combined NO showed a corrosion rate of 0.14 mils/year.

Stress Corrosion Cracking Behavior

Normal SCC testing was carried out in a glass-Teflon test cell at 72-74°C. for 72 hrs. using 10 U-bend specimens per test. During the development of this test, the SCC behavior of RR N_2O_4 was established.

(1) Cracking occurred at stress levels of 30% of yield strength or above (lowest level tested).

(2) Some cracks developed at all test temperatures between ambient and 74°C.

(3) Cracks developed in <24 hrs. at 74°C.

(4) Under normal test conditions, all specimens usually cracked in half. Under some less drastic conditions of temperature, stress, or exposure time, macro and micro cracks developed in the area of maximum stress. In addition, cracks routinely occurred at identification stampings, sheared edges, and edges of drilled holes.

In the case of G8 N_2O_4, no cracks developed in the U-bend specimens under the most drastic test conditions used. This was also true of G4 N_2O_4 (0.4% combined NO).

Red Non-reactive (RN) N_2O_4 was considered in this program to be N_2O_4 that is visually indistinguishable from RR N_2O_4 at 0°C. and which does not cause SCC in the standard test. Samples of N_2O_4, having a normal proton content of 5000-6000 ppm. as HNO_3, to which 150-500 ppm. NO was added qualified as RN N_2O_4. As much as 800 ppm. NO could be added to RR N_2O_4 before a green cast could be visually observed at 0°C.

Metal Solubility in N_2O_4

The trace metals content of the RR and G8 N_2O_4 used in this work was extremely low. Iron was the major contaminant, being present to the extent of 0.3-0.4 ppm. in RR N_2O_4 and 0.8-1.0 ppm. in G8 N_2O_4. No Ti, Al, or V was detected in these materials.

After SCC tests with RR N_2O_4, significant amounts of metals were found in solution, i.e., 10-37 ppm. Ti, 0.4-0.9 ppm. Al, and 2-9 ppm. V. Based on the average corrosion rate (0.85 mils/year), the expected total concentration of dissolved metals would be 26 ppm. The average weight ratio of Al/Ti in solution was found to be 0.024 compared with 0.067 in the alloy; the V/Ti ratio in solution was 0.26 compared with 0.044 in the alloy. The combined chlorine level of the N_2O_4 did not change significantly during the SCC tests.

Effect of Composition on SCC

In the system under study, it was shown that stress corrosion cracking behavior could be drastically influenced by certain very minor changes in composition of the N_2O_4 medium. For example, the presence of as little as 150 ppm. combined NO in typical RR N_2O_4 was sufficient to inhibit SCC. However, when the HNO_3 level was reduced by adsorbent treatment from ∿6000 ppm. to 250-350 ppm., the combined NO content had to be raised to above 500 ppm. to achieve inhibition. This behavior indicated a definite critical interdependency between N_2O_3 and protonated species concentrations with regard to SCC behavior. It pointed to the presence of HNO_2 and H_2O as the main critical indicators of a non-reactive system.

Other pertinent observations indicated the possibility that the level of dissolved O_2 in RR N_2O_4 influenced the rate of cracking at room temperature but not at 74°C. The analysis of a sample of Red Nonreactive N_2O_4 from the Marshall Space Flight Center indicated that contamination with organic matter could inhibit SCC.

Mechanism

The available evidence appeared to favor the hypothesis of an oxidative attack mechanism that was inhibited by the presence of critical concentrations of HNO_2 and/or H_2O. The specific nature of the attacking species, and the mode of SCC inhibition were not established.

II. NAS 8-30519

The work performed under this contract had the same overall goals as NAS 8-21207 but with modifications and extensions of the experimental program (see Introduction). The experimental accomplishments relative to the specific objectives of the program were as follows:

(1) A process was developed that was capable of reducing the total proton content of liquid N_2O_4 to below the current analytical limit of detection, i.e., $\lesssim$ 10 ppm. as HNO_3. The process consists of batch contact of liquid N_2O_4 with Davison Acid-Resistant Type 3A Molecular Sieve (AR12-22) at a ratio of approximately 200 g./liter, preferably under O_2 pressure.

(2) A major success was achieved in the development of spectrophotometric methods for the qualitative and quantitative characterization of the liquid N_2O_4 system. This success was made possible by computer analysis of the complex digitized spectra in the visible and near-infrared regions.

(3) The above system was used to study the composition of the proton - containing compounds in liquid N_2O_4. Changes of composition with the addition of H_2O, NO, and O_2 were measured and equilibrium constants for the system N_2O_4-NO-H_2O calculated. In order to relate measured equilibrium compositions at -10°C. with those actually present at the SCC test temperature, the effect of temperature on the equilibrium was determined.

(4) Methods were developed by which the composition of liquid N_2O_4 systems could be adjusted with respect to the composition of the minor constituents. This was most effectively accomplished by the addition of NO gas to liquid N_2O_4 that had been contacted with Type 3A Molecular Sieve to reduce the total proton level.

(5) The above developments were used to establish basic correlations relating the composition of the N_2O_4 system with stress corrosion cracking behavior. The effects of trace organic impurities, dissolved O_2, and HNO_3 addition on SCC were first investigated. After a previously observed interdependency between combined NO and proton level was confirmed, the composition range between NO/HNO_3 ratios of 10/1 to 1/100 was tested for SCC behavior and a basic correlation curve established.

(6) Several experiments were performed in an effort to clarify certain aspects of the SCC mechanism. These included measurement of the change of dielectric constant, electrical

conductivity, and dissipation factor with increasing NO content. A limited number of SCC tests related to surface passivation, brittle-film formation, and effect of applied potential were performed.

(7) A substantial experimental effort was made to study the thermal dissociation of NO_2 to form NO and O_2 at the SCC test temperature. A previously developed gas chromatography method for the determination of dissolved O_2 was employed. The work was unsuccessful due to the severe sampling problems encountered at elevated temperatures.

As a result of the above experimental work, sufficient information was obtained to accomplish the specific objectives of this program. The observations leading to this conclusion are summarized below:

RR N_2O_4 + NO

In oxygen-treated N_2O_4, HNO_3 is the only proton-containing compound detected by current methods. When NO gas is added to this material, it reacts very rapidly with equilibrium amounts of NO_2 present to form N_2O_3. At the same time, the HNO_3 level drops rapidly, the H_2O level rises rapidly, and the HNO_2 levels begins to rise slowly. The shapes of the composition curves (Figure 13) are typical of a series of consecutive reactions.

Oxygen treatment of the resulting mixture quantitatively converts all of the protonated species back to HNO_3. This reaction is slower, the rate determining step probably being the rate of solution of O_2 in the N_2O_4.

Proton-free N_2O_4 + H_2O

The initial addition of H_2O to essentially proton-free N_2O_4 resulted in the formation of N_2O_3 and almost complete conversion of the H_2O to HNO_3 and HNO_2 in the approximate mole ratio of about 14/1. With successive additions of water, the rate of increase of HNO_3 leveled out, that of H_2O increased, and the HNO_2 level increased at a slow constant rate (Figure 15). All of the added protons were accounted for by the determination of these three species.

Effect of Temperature on Equilibrium

When a sample of liquid N_2O_4 containing N_2O_3, HNO_3, HNO_2, and H_2O is heated, the equilibrium shifts to increase the concentration of N_2O_3 and HNO_3, and decrease the concentration of HNO_2 and H_2O

Effect of NO on Electrical Properties

The addition of NO gas to RR N_2O_4 causes a significant increase in the dielectric constant and electrical conductivity of the medium. For example, the addition of 1% NO by weight to

RR N_2O_4 increased the dielectric constant from 2.37 to 2.62 and the conductivity from 1.5 X 10^{-12} to 2.5 X 10^{-11} ohm^{-1} $cm.^{-1}$. It is postulated that the presence of N_2O_3 increases the extent of self-ionization of N_2O_4 to form NO^+ and NO_3^- ions.

Effect of Organic Impurities

The presence of as little as 50-150 ppm. of organic impurity in N_2O_4 can inhibit SCC. It is postulated that inhibition occurs either by reaction of the organic compound with the corrosive species, or by the generation of other inhibitors, e.g., HNO_2, H_2O, during normal oxidation. Adsorption or reaction of polar oxidation products on active metal surfaces is also a possibility. Antioxidants and others readily oxidized compounds appeared to be the best inhibitors, and straight chain saturated hydrocarbons appeared to be the least effective.

Effect of Dissolved O_2

The dissolved O_2 content of the RR N_2O_4 used in thus work was of the order of 10 ppm. as delivered from the cylinder. This material can cause SCC at room temperature and above in stressed U-bend specimens. Previous work suggested that lower O_2 levels led to less cracking. In this work, pressurization of

the SCC test cells with O_2 produced significantly more cracking at 40°C. than the controls. The crack density was not proportional to the O_2 pressure.

Effect of HNO_3 Concentration

Normal RR N_2O_4 contains 0.5-0.6% by weight HNO_3. Addition of 100% HNO_3 to increase the concentration to 1 and 2% caused significant inhibition of SCC at 40°C. At 1% HNO_3 the cracking density was greatly reduced; at the 2% HNO_3 level, no cracking occurred after 70 hrs. Retesting after oxygen treatment of the samples confirmed these observations. More drastic O_2 treatment caused cracking comparable to the control.

Vapor Phase Tests

Except for one anomalous test, SCC could not be induced in stressed U-bend specimens by vapor phase contact with mixtures of NO_2 and O_2 at 74°C. Immersion of the test specimens in RR N_2O_4 at room temperature for periods up to 24 hrs. prior to the vapor phase tests had no effect.

Critical Composition Level Tests

This work confirmed the previously established observation that the SCC behavior of liquid N_2O_4 systems was drastically affected by the concentration and distribution of the following

minor constitutents, i.e., N_2O_3, HNO_3, HNO_2, and H_2O. The addition of NO to N_2O_4 containing various levels of HNO_3 produced a range of compositions that could be tested for SCC behavior. From the results of these tests, it was possible to construct a critical concentration level plot of NO versus HNO_3 concentrations (Figure 29). This plot showed that lower concentrations of HNO_3 required higher levels of NO addition to achieve inhibition of SCC. The extremes of the curve corresponded to 515 ppm. combined NO at 400 ppm. HNO_3 and 132 ppm. combined NO at 5200 ppm. HNO_3 (compositions measured at -10°C.). Conversion of these critical compositions as measured at -10°C. to predicted composition at 70°C. indicated that the HNO_2 level was 20 ppm. or less and the H_2O about 1 ppm. or less at every point on the curve.

Special SCC Tests

A test to assess the passivation of active metal surfaces by contact with N_2O_4 containing 0.8% combined NO proved to be inconclusive.

An experiment designed to test a brittle-film mechanism of crack propagation indicated that the model did not apply to this sytem.

A test was run with 1.5 volts D.C. applied across two U-bend specimens for the duration of the test (72 hrs.). Both specimens cracked in half. The results would have been definitive only if one specimen cracked and the other did not.

CONCLUSIONS

As indicated in the previous sections, essentially all of the specific objectives of the program have been achieved. In general terms, experimental methods were developed to define the composition of N_2O_4 systems and to establish their stress corrosion cracking behavior. These developments permitted the empirical correlation of observed SCC behavior with various concentration levels of minor constituents of the system. The direct experimental evidence obtained in this work was insufficient to define the actual attack mechanism involved in the stress corrosion cracking of 6Al 4V titanium alloy. However, this was more or less anticipated, since the actual mechanism of stress corrosion cracking has been unequivocally proven in very few systems despite years of extensive experimental investigation. In the 6Al 4V Ti-N_2O_4 system, the best that can be done at the present state of knowledge is to postulate a possible mechanism that is consistent with as many observed facts as possible. Several mechanisms have been proposed by other investigators (11,12).

It is generally recognized that for an alloy to be susceptible to stress corrosion cracking, it must develop wide slip-steps when plastically deformed, a passive surface film must be ruptured, and the alloy must be exposed to an environment in which some part of the active slip-step surface is not partially repassivated within a critical time period. In modern theories of SCC, there seems to be general concurrence in the view that cracking is related to piling up of dislocations at barriers of

one kind or another, e.g., grain boundaries or complex slip planes. These aggregates of dislocations or stacking faults may accelerate diffusion and transport of impurity and alloy atoms to the imperfection arrays, causing localized segregation. The resulting inhomogeneities can cause preferential dissolution by an electrochemical mechanism, or the adsorption of specific components of the environment that can reduce the surface energy (8,21).

Fresh titanium and vanadium surfaces react very rapidly with oxygen. Andreeva (13) has reported that fresh Ti surfaces react with air at room temperature within a few seconds to form an oxide film 12-16 Å thick. Slow growth continues for ∿70 days, at which time the film is ∿50 Å thick. Film growth during this period is said to follow a direct logarithimic law. A portion of the film appears to be adsorbed rather than chemisorbed, since it can be removed by high vacuum at room temperature. It is further reported (15) that the oxide film on titanium is formed by oxygen moving inward through the oxide layer rather than by metal moving outward. In such cases it is likely that the oxide layer will be in a state of strain, particularly if the density of the oxide is less than that of the metal. Stressing the metal, or further oxidation of the surface while stressed, can transfer additional stresses to the oxide film making it more susceptible to spontaneous break-down at a critical film thickness. Such a break-down exposes highly active metal surfaces to attack by the environment.

The molecular species that are present in cracking and non-cracking N_2O_4 systems are listed below:

Cracking	Non-Cracking
N_2O_4	N_2O_4
NO_2	NO_2
HNO_3	HNO_3
O_2	N_2O_3
	HNO_2
	H_2O

This work has shown that the addition of O_2 to a reactive N_2O_4 system increases the rate and/or the extent of cracking. However, the absence of dissolved O_2 does not prevent SCC. Cracking occurs in the presence of 20-7000 ppm. HNO_3; raising the HNO_3 level to 1-2% decreases the rate and/or the extent of cracking. It thus appears that neither O_2 nor HNO_3 can be considered attacking species, despite the fact that their concentration levels affect the reaction.

In considering inorganic reactions of the liquid $N_2O_4 \rightleftharpoons 2NO_2$ system, few reaction mechanisms actually involve the molecular species themselves. The neutral NO_2 radical does participate in some inorganic and many organic reactions, but in this study, vapor phase testing showed that NO_2 itself or in mixtures with O_2 gas did not cause cracking. From many studies of the inorganic reactions involving liquid N_2O_4 (7,14,16,18), has been concluded that dissociation of N_2O_4 into NO^+ and NO_3^- ions is involved. It is postulated that on breaking the N-N bond

in N_2O_4, the bonding electrons are shared unequally to give NO_2^+ and NO_2^- ions, initially as the ion pair $[NO_2^+][NO_2^-]$. Strong electron acceptors can stop the process at this stage (19,20), but since these ions have not been identified in the pure liquid, the reaction $NO_2^+ + NO_2^- \longrightarrow NO^+ + NO_3^-$ must follow immediately and must be irreversible (7). The high oxidizing power of the nitronium ion in close proximity to the nitrite ion would probably render the two groups incompatible. The following representation of the equilibria existing in liquid N_2O_4 has therefore been proposed (7):

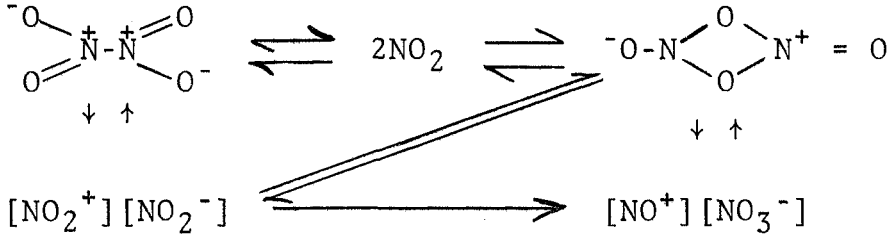

Although the majority of the reactions of liquid N_2O_4 can be correlated with the self-ionization to form NO^+ and NO_3^- ions, this does not appear to be the case in the SCC of titanium alloys. In the first place, it has been reported that pure N_2O_4 does not react with Ti metal (7). Secondly, addition of high dielectric constant solvents such as HNO_3, enhances the ionization. So also does the addition of NO, N_2O_3, or NOCl (7). This has been confirmed by the measurements of electric properties in this work. In neither of the above cases does this increase in ionization result in stress corrosion cracking. Accordingly, another attacking species must be sought.

One possibility is the nitronium ion, NO_2^+. The behavior of this strongly oxidizing ion has been studied in the reactions

of dinitrogen pentoxide, N_2O_5, which is believed to undergo self-ionization to give NO_2^+ and NO_3^- ions. The use of N_2O_5 in the preparation of the anhydrous nitrates of many metals, including those of the early transition elements, Ti, V, Cr, Zr, is of particular interest. In non-ionizing media, these anhydrous nitrates are stable, covalent compounds of rather unusual volatility. They form addition compounds, i.e., solvates, with N_2O_4 that often crystallize from solution. The metal-nitrate covalent bond is decomposed by water and other high dielectric constant compounds. In the anhydrous nitrate of titanium, $Ti(NO_3)_4$, all four NO_3 groups are bidentate and are arranged around the metal atom in two planes at right angles to each other. This compound is extremely reactive with organic compounds. It is postulated that this reactivity is due to the NO_3 radical that is released from anhydrous nitrates in cases where the metal atom has sufficient electron-withdrawing power.

$$Ti^{IV}(NO_3)_4 \longrightarrow Ti^{III}(NO_3)_3 + NO_3$$

Vanadium behaves in similar fashion to titanium. However, reaction with N_2O_5 produces $VO(NO_3)_3$ rather than $V(NO_3)_5$.

A simple mechanism for the generation of NO_2^+ ions in the 6Al 4V Ti alloy-N_2O_4 system is not readily postulated because of the great chemical complexity of the alloy surface. Some possibilities include reaction of N_2O_4 with strong Lewis acid impurities in the alloy, reaction with non-stoichiometric oxides, or by electrochemical generation. Because of the appearance of significant amounts of Ti and V in solution in N_2O_4, compounds of these metals are most highly suspect.

It has been shown in this work that the presence of HNO_2/H_2O and certain organic impurities cause complete inhibition of SCC. In the case of HNO_2/H_2O, both species co-exist whenever sufficient N_2O_3 and protons are present. These compounds could inhibit by adsorption on the active metal surface to prevent the formation of NO_2^+ ions, or to hydrolyze any anhydrous nitrates that might tend to form. It thus appears that the inhibitory action of these species most likely occurs at the metal surface rather than in the liquid phase. Surface reaction of any organic species may also be the main path of inhibition of these compounds. However, in addition, oxidation of these compounds results in the formation of N_2O_3 in sufficient concentration to produce some HNO_2/H_2O which would contribute to the inhibition.

In summary, the proposed mechanism is as follows:

(1) Stressing of the alloy causes the formation of slip-steps and/or rupture of the protective oxide layer to expose fresh metal surface.

(2) Liquid N_2O_4 reacts with the metal surface, presumably at boundaries where impurities and alloy atoms are concentrated to form nitronium, NO_2^+, ions.

(3) These ions react at their site of generation with essentially any of the metals present in the alloy to form anhydrous covalent nitrates that may dissolve in the N_2O_4 and/or precipitate from solution as N_2O_4 solvates.

$$Me^{\circ} + n[NO_2^+] \longrightarrow Me^{+n} + NO_2$$

$$Me^{+n} + n[NO_3^-] \longrightarrow Me(NO_3)_n$$

$$Me(NO_3)_n + N_2O_4 \rightleftharpoons Me(NO_3)_n \cdot N_2O_4$$

(4) Formation of the anhydrous nitrates causes crack initiation. The applied stress then helps to propagate the crack by exposing fresh reactive surface at the crack tip allowing the reaction to continue.

(5) Inhibition of the reaction occurs when the equilibrium products HNO_2/H_2O are adsorbed on the fresh metal surface thus preventing formation of NO_2^+ ions and/or hydrolyzing the anhydrous nitrates.

BIBLIOGRAPHY

(1) A. Z. Conner, et al., "A Study of the Mechanism of Chemical Reactivity of Nitrogen Tetroxide with Titanium Alloy", Final Report, Contract No. NAS 8-21207, Feb. 28, 1969.

(2) C. M. Wright, A. A. Orr, and W. J. Balling, Anal. Chem. 40, 29 (1968).

(3) A. Savitsky and M. J. E. Golay, Anal. Chem. 36, 1627 (1964).

(4) G. Herzberg, "Infrared and Raman Spectra of Polyatomic Molecules", Van Nostrand, N. Y., 1945.

(5) E. T. Chang and N. A. Gokcen, J. Phys. Chem. 70, 2394 (1966).

(6) E. D. Coon, et al., U.S. Dept. Com. Off. Tech. Service, AD 220479, 1959; CA 58, 75976 (1963).

(7) C. C. Addison, "Chemistry in Liquid Dinitrogen Tetroxide", Part 1, in "Chemistry in Nonaqueous Ionizing Solvents", G. Jander, H. Spandau, and C. C. Addison, editors, Pergamon Press, N. Y. 1967.

(8) E. N. Pugh, J. A. S. Green, and A. J. Sedriks "Current Understanding of Stress Corrosion Phenomena", March 1969, RIAS Technical Report 69-3.

(9) E. N. Pugh, "Environment-Sensitive Mechanical Behavior" A. R. C. Westwood and N. S. Stoloff, editors, Gordon and Breach, New York, 1966.

(10) J. B. Cotton, "Anodic Polarization of Titanium", Chemistry and Industry 3, 68 (1958).

(11) G. F. Kappelt and E. J. King, "Observations on the Stress Corrosion of 6Al 4V Titanium Alloy in Nitrogen Tetroxide", Bell Aerosystems Co., paper presented at AFML Conference, Denver, Colorado, 1967.

(12) P. J. Moreland and W. K. Boyd, "Stress Corrosion Cracking of Ti and Ti-6Al-4V Alloy in Dinitrogen Tetroxide", Corrosion 26, 153 (1970).

(13) V. V. Andreeva, Corrosion 20, 35t (1964).

(14) A. Z. Conner, et al., "Nitrogen Tetroxide", Hercules Incorporated, 1968.

(15) U. R. Evans, "The Corrosion and Oxidation of Metals", St. Martins Press, Inc., New York, 1960.

(16) P. Gray, "The Chemistry of Dinitrogen Tetroxide", Royal Institute of Chemistry Monograph, No. 4, 1958.

(17) H. Leidheiser, Jr., "Corrosion", Chem. & Eng. News, 78, April 15, 1965.

(18) "Mellors' Comprehensive Treatise on Inorganic and Theoretical Chemistry", Vol. VIII, Supplement 11, Nitrogen (Part 11).

(19) R. W. Sprague, "Reactions of Oxides of Nitrogen with the Boron Halides", Dissertation, The Ohio State University, 1957.

(20) R. W. Sprague, A. B. Garrett and H. H. Sisler, J. Amer. Chem. Soc., 82, 1059 (1960).

(21) H. H. Uhlig, "Stress Corrosion Cracking" in "Treatise on Fracture", H. Leibowitz, editor, Academic Press, Inc., N. Y., 1967.

APPENDIX

EXPERIMENTAL PROCEDURES

I. Spectrophotometric Analysis of N_2O_4 for NO, HNO_3, HNO_2 and H_2O. Procedures for Sample Handling and Spectral Data Acquisition

The cell is dried prior to use, by removing it from the cooling jacket and placing it in a 110°C. oven for two hours with a continuous trickle purge of nitrogen. The purge is continued while the cell cools to room temperature after removal from the oven. All valves are then closed, the cell is replaced in the cooling jacket and then placed, along with the sample bombs, into the dry box on the spectrophotometer. The cell is again purged with nitrogen as it is cooled to -10°C.

The cell is positioned in the sample compartment of the Cary 14, and while it is cooling, the instrument/cell background is obtained. This corrects for any irregularities in the baseline, and is subtracted from the sample spectrum. A header is manually punched onto the paper tape consisting of (1) the date (as an identifier), (2) the linear offset or difference between the tape punch and the instrument recorder when the latter is set at zero, (3) the starting wavelength in nanometers, and (4) the stopping wavelength in nanometers. (See Appendix V for tape format). The digital spectrum is then recorded automatically at 1 nm. intervals between 1550 and 1350 nm. at a scanning speed of 1 nm./sec. using the 0 to 0.1 absorbance slidewire. A sample bomb is then connected to the fill valve of the cell, the nitrogen line is removed and all valves are closed. A Teflon vent line is used to connect the outlet valve of the cell to a waste receptacle in the hood

at the rear of the dry box. The sample bomb valve, the fill valve and cell outlet valve are opened in order. When liquid N_2O_4 is observed in the Teflon vent line, the outlet valve is closed and the waste line transferred from the outlet valve to the gas inlet valve which is then opened until liquid N_2O_4 is observed in the line. The valves are closed in reverse order, i.e., gas inlet, sample inlet, and sample bomb. Ten minutes is allowed for the sample to attain the cell temperature of -10°C. This temperature is measured with a copper-constantan thermocouple inserted in a well in the cell block, and a potentiometer. The temperature of -10°C. was selected initially for several reasons. It was just above the freezing point of N_2O_4; it was about the limit of the refrigeration unit used without special insulation; and interfering NO_2 was at a minimum. Although later refinements in the data processing program permitted correction for NO_2 at any temperature, the fact that the band width, peak height, and wavelength of the absorption maxima of the bands of the protonated species vary with temperature, made it impractical to record routine spectra at any temperature other than -10°C. where all of the reference spectra were obtained.

Prior to punching the tape header described below, the sample is checked to determine which slidewire and wavelength pair will be used for the NO determination. The most accurate measurement will be made by using the shortest wavelength pair at which the absorbance difference between the two wavelengths of the pair is less than 1.0 (or 0.10 if the 0 to 0.1 slidewire is being used for low NO samples). The wavelength is set to 900 nm. and the

pen position adjusted to about 0.03 A using the balance control. The wavelength is then set to 700 nm. If the pen remains on scale, this pair is used, if not, the next higher wavelength pair is investigated, repeating the procedure of setting the pen to about 0.03 A at the longer wavelength of the pair and checking the shorter wavelength for an on-scale pen position. The wavelength pairs which have been calibrated and the code numbers assigned are shown in the work sheet, Appendix V. At the appropriate place in the tape header (entires 5 and 6), the spectrophotometer wavelength is set to the longer of the predetermined wavelength pair and the pen position recorded by pressing the paper tape "punch" button, then to the shorter wavelength where pen position is similarly recorded. A sample header is punched on the tape consisting of the following:

(1) Date.

(2) Sample identification number.

(3) Slidewire used for the NO measurement.

(4) Cell path used for the NO measurement.

(5) A code number indicating which wavelength pair was used as the NO measurement.

(6) The pen position at the longer wavelength of the NO measurement pair.

(7) The pen position at the shorter wavelength of the NO pair.

(8) The slidewire used to record the NIR spectrum from 1550-1350 nm.

(9) The cell pathlength used for the NIR region.

(10) The cell temperature when the spectrum is recorded.

The options available for (2) and (8) above were 0 to 0.1 absorbance and 0 to 1.0 absorbance full scale. The six options of wavelength range code for NO determination (5) make use of wavelength pairs further from the peak maximum at 700 nm. of the very broad electronic band of N_2O_3 as the NO concentration increases. The shortest wavelength pair at which both are on scale gives the best precision. Prior to the use of these ranges, all measurements were made on the 700-900 nm. pair which necessitated using a 2 mm. cell to measure NO, and the 5.85 cm. cell for the protonated species, hence the two entries for cell path (4) and (9). The sample temperature is used to correct the NO reading for interfering NO_2 whose concentration is temperature dependent. The data in the heading are used by the computer in making corrections, calculations, and scaling of the plotted output.

The digital spectrum at 1 nm. intervals is recorded as the sample is scanned from 1550 to 1350 nm. at 1 nm. per second. With the sample bomb still placed on the fill valve, and a Teflon line connecting the outlet valve to the waste receptacle, a nitrogen (5 psi.) line is connected to the gas inlet valve of the cell; the outlet valve and gas inlet valve are opened in that order, and the cell contents are flushed into the waste receiver. Cell is then ready for refilling if duplicate results are desired. If a new sample bomb is to be sampled, nitrogen flow should be maintained during removal of the old bomb and attachment of the new bomb to prevent admission of air or moisture into the cell.

II. A Documented Listing of a Fortran IV Program for Processing Digital Spectra Recorded on Perforated Paper Tape

```
C       THIS PROGRAM PROCESSES DATA TAPES FROM THE NEAR IR (CARY MODEL 14)
C       ANALYSIS OF N2O4 FOR HNO3,HNO2,AND H2O. IT CAN ALSO BE USED FOR
C       GENERAL PURPOSE SPECTRUM MANIPULATION AND PLOTTING.
        DIMENSION KORR(1020),KAB(21),KBG(400),ID(20),K(1200),IBG(10)
        DIMENSION LAB(18),K4(200),KS(10),IDATE(4),DATE(3),K3(200)
        DIMENSION K3H(200),K2H(200),K1H(200),LL(3),PPM(4),Z(3),FLG(2)
        DIMENSION AINV(3,3),DA(3),SCALE(6),ABNO(6),NM(2,6)
        COMMON KORR
        EQUIVALENCE (PPM(1),PPM3),(PPM(2),PPM3H),(PPM(3),PPM2H),
       1(PPM(4),PPM1H)
        DATA ITI,ITY,ITR,ITP,KR,LP/ 5, 6, 9, 8, 9,18/
        DATA LAB/'NM','A ','ID','UN','SM','CE','LL','PP','M ','NO','  '
       1,'HN','O3','HN','O2','H2','O ',' '/ '/
        DATA FLG(2)/' (=)'/
        DATA SCALE/3.54,0.052,0.,0.,0.,0./
        DATA ABNO/3.00,0.749,0.297,0.118,0.039,0.0174/
        DATA NM/900,700,900,850,950,920,1140,1070,1140,1110,1270,1220/
C
C       READ SPECTROPHOTOMETRIC DATA AND REFERENCE SPECTRA.
C       N2O4=1 FOR N2O4 ANALYSIS. 0 FOR GENERAL PURPOSE.
        READ(KR,1)KAB
        READ(KR,1)N2O4
    1 FORMAT(16I5)
        IF(N2O4.EQ.0) GO TO 26
        READ(KR,11)AINV
   11 FORMAT(3F10.0)
        READ(ITR,5)NN4,LAST4,IDNO4,SLWR4,PATH4,TEMP4,CONC4,(K4(I),I=1,NN4)
        READ(ITR,5)NN3,LAST3,IDNO3,SLWR3R,PATH3R,TEMP3,PPM3R,(K3(I),I=1,
       1NN3)
        READ(ITR,5)NN3H,LAST3H,IDNO3H,SLWR3H,PATH3H,TEMP3H,PPM3HR,
       1(K3H(I),I=1,NN3H)
        READ(ITR,5)NN2H,LAST2H,IDNO2H,SLWR2H,PATH2H,TEMP2H,PPM2HR,
       1(K2H(I),I=1,NN2H)
        READ(ITR,5)NN1H,LAST1H,IDNO1H,SLWR1H,PATH1H,TEMP1H,PPM1HR,
       1(K1H(I),I=1,NN1H)
    5 FORMAT(3I5,4F10.3/(20I4))
C
C       TERMINATE PLOT ROUTINE IF NECESSARY
   26 IF(IFLAG.EQ.1) CALL TMPLOT(1)
        IFLAG=0
C
C       SET SENSE SWITCH 1 FOR FAST RUN,IE. ALL TAPES LOADED,NO PAUSES
C       AFTER DATA ERROR MESSAGES. PROGRAM CONTROL FROM CARD READER.
        IF(KSS(1).EQ.0) PAUSE 'LOAD INST. BG. TAPE.'
        ITI=5
        KT=0
C
C       READ AND PROCESS HEADER DATA ON BACKGROUND SPECTRUM TAPE.
        IBG(10)=10
        CALL IRD(IBG(1),4,N,8)
        IF(N2O4.EQ.0) CALL IRD(IBG(9),4,N,2)
        NBG=IBG(1)
        INIT=1000*IBG(5)+IBG(6)/10
```

```
      LAST=1000*IBG(7)+IBG(8)/10
      NN=(INIT-LAST)/(IBG(10)/10)
C
C     CALCULATE AND INTERPOLATE ABSORBANCE SCALE CORRECTIONS.
      DO 10 I=1,20
      SETPT=50*(I-1)
      L1=KAB(I)+IBG(4)/10+1
      L2=KAB(I+1)+IBG(4)/10
      PINC=50.0/(KAB(I+1)-KAB(I))
      RM=0.0
      DO 10 J=L1,L2
      KORR(J)=SETPT+RM*PINC+0.5
   10 RM=RM+1.0
C
C     READ BACKGROUND SPECTRUM, CHECK FOR DATA ERRORS,APPLY ABSORBANCE
C     SCALE CORRECTIONS.
      CALL IRD(KBG(1),3,N,400)
      IF(N-NN)20,22,20
   20 WRITE(ITY,2)N
      IF(KSS(1).EQ.0) PAUSE
    2 FORMAT(I5,29H DATA POINTS RECORDED FOR KBG)
   22 DO 24 I=1,NN
      J=KBG(I)+1
   24 KBG(I)=KORR(J)
      IF((NN.NE.NN4.OR.LAST.NE.LAS14).AND.N204.EQ.1) WRITE(ITY,6)
    6 FORMAT(' WAVELENGTHS DO NOT CHECK.')
      IF(KSS(1).EQ.0) PAUSE 'LOAD SAMPLE TAPE. '
      IF(KSS(1).EQ.1) ITI=9
C
C     READ AND PROCESS HEADER DATA ON SAMPLE SPECTRUM TAPE.
   27 CALL IRD(IDATE(1),2,N,4)
      CALL IRD(ID(1),4,N,2)
      IF(IDATE(4).GT.0) GO TO 29
      DO 28 I=1,3
   28 DATE(I)=IDATE(I)
      IF(N204.EQ.0) GO TO 33
      CALL IRD(ID(9),4,N,6)
   29 CALL IRD(KS(1),3,N,2)
      IF(IDATE(4).GT.0) GO TO 30
   33 CALL IRD(ID(3),4,N,6)
   30 IDNO=1000*ID(1)+ID(2)/10
      ID1=-IDNO/100
      ID2=-ID1*100-IDNO
      SLWR=ID(4)/1E2
      PATH=ID(5)*10.0+ID(6)/1E3
      TEMP=ID(8)/1E2
      IF(ID(7).NE.0) TEMP=-TEMP
      IF(N204.EQ.0) GO TO 35
      SLWR3=ID(9)*100.0+ID(10)/1E2
      PATH3=ID(11)*10.0+ID(12)/1E3
      LINT=ID(14)/10
C
C     CALCULATE PPM OF NO (N203) CORRECTED FOR NO2.
```

```
      AREL=(((0.972E-6*TEMP+1.643E-5)*TEMP+8.037E-4)*TEMP+7.069E-3)/5.85
      ANO2=AREL*SCALE(LINT)
      ANO=(KS(2)-KS(1))*SLWR3/PATH3/1E3-ANO2
      IF(LINT.EQ.1) ANO=ANO-.005
      PPM3=ANO/ABNO(LINT)*1E4
      IF(PPM3.LT.0.0) PPM3=0.0
C
C     READ SAMPLE SPECTRUM AND STORE IN BOTTOM THIRD OF ARRAY K. CHECK
C     FOR DATA ERRORS AND CALCULATE CORRECTION FACTORS FOR SLIDEWIRE
C     RANGE, AND ABSORPTION DUE TO N2O3 AND N2O4.
   35 CALL IRD(K(801),3,N,400)
      IF(N-NN)31,32,31
   31 WRITE(ITY,3)N,IDNO
    3 FORMAT(I5,32H DATA POINTS RECORDED FOR SAMPLE,I5)
      IF(KSS(1).EQ.0) PAUSE
   32 BGSW=0.1/SLWR
      CORR3=0.0
      CORR4=0.0
      IF(N2O4.EQ.0) GO TO 39
      CORR3=SLWR3R/SLWR*PATH/PATH3R*PPM3/PPM3R
      CORR4=SLWR4/SLWR*PATH*(1.0-PPM3/1E6)/PATH4
C
C     CHECK INDIVIDUAL DATA POINTS OF SAMPLE AND N2O3 AND N2O4 REFERENCE
C     SPECTRA FOR OFF-SCALE CONDITION  APPLY ABSORBANCE SCALE CORRECTION
C     AND SUBTRACT BACKGROUND,N2O3 AND N2O4 CONTRIBUTIONS, STORE RESULT
C     IN UPPER THIRD OF K.
   39 DO 36 I=1,NN
      IF(K(I+800).GT.990.OR.K3(I).LT.0.OR.K4(I).LT.0) GO TO 34
      J=K(I+800)+1
      K(I)=KCRR(J)-KBG(I)*BGSW-K3(I)*CORR3-K4(I)*CORR4
      GO TO 36
   34 K(I)=30000
   36 CONTINUE
C
C     SEARCH FOR MINIMUM OF CORRECTED SPECTRUM AND SET MINIMUM=0, LABEL
C     OFF SCALE POINTS WITH -1.
      LIL=9999
      DO 38 I=1,NN
      IF(K(I).LT.LIL) LIL=K(I)
   38 CONTINUE
      DO 42 I=1,NN
      IF(K(I).GT.1000) GO TO 40
      K(I)=K(I)-LIL
      GO TO 42
   40 K(I)=-1
   42 CONTINUE
C
C     SMOOTH CORRECTED SPECTRUM USING SEVEN POINT LEAST SQUARES FIT TO
C     QUADRATIC.  STORE IN MIDDLE THIRD OF K.
      DO 44 I=1,NN
   44 K(I+400)=-1
      N=NN-6
      DO 50 I=1,N
```

```
      DO 46 J=0,6
      IJ=I+J
   46 IF(K(IJ).EQ.-1) GO TO 48
      K(I+403)=(-2*(K(I)+K(I+6))+3*(K(I+1)+K(I+5))+6*(K(I+2)+K(I+4))
     1+7*K(I+3))/21
      GO TO 50
   48 K(I+403)=-1
   50 CONTINUE
C
C     CALCULATE CONCENTRATIONS OF H2O, HNO2, AND HNO3 USING SMOOTHED
C     DATA.
      DA(1)=K(547)*SLWR*.001
      DA(2)=K(503)*SLWR*.001
      DA(3)=K(481)*SLWR*.001
      DO 53 I=2,4
   53 PPM(I)=0.0
      DO 51 I=1,3
      DO 51 J=1,3
   51 PPM(I+1)=PPM(I+1)+AINV(I,J)*DA(J)/PATH
      CALC1H=2.473E-8*PPM3H**2*PPM3
      CALC2H=6.636E-5*PPM3H*PPM3
C
C     LB AND IFLAG HELP CONTROL PLOTTING.
      IF(KSS(1).EQ.0) WRITE(ITY,7)ID1,ID2
    7 FORMAT(7H SAMPLE,I4,I3)
      IF(LB.NE.1) IFLAG=0
C
C     READ PROGRAM CONTROL PARAMETER FROM TELETYPE OR CARD READER.
   52 READ(ITI,8)KK,LL
    8 FORMAT(A1,3I1)
C
C     SET CONTROL FLAGS FOR SUBTRACTION OF SELECTED REFERENCE SPECTRA.
      DO 56 I=1,3
      Z(I)=0.0
   56 IF(LL(1).EQ.I.OR.LL(2).EQ.I.OR.LL(3).EQ.I) Z(I)=1.0
      IZ1=Z(1)
      IZ2=Z(2)
      IZ3=Z(3)
      IF(IFLAG.EQ.0.OR.KK.EQ.'= '.OR.LB.EQ.1) GO TO 54
      CALL TMPLOT(1)
      IFLAG=0
      YJP=0.0
C
C     PROGRAM CONTROL PARAMETERS: T, READ TAPE; R, RESTART; E, EXIT;
C     K, TRANSFER CONTROL TO TELETYPE; C, TRANSFER CONTROL TO CARD
C     READER; S2 OR S3, SUPRESS PLOTTING OR PRINTING; B1, SUPERIMPOSE
C     PLOTTED SPECTRA. B, STOP SUPERPOSITION; N1 OR N, SET N204 CONTROL
C     FLAG TO 1 OR 0; O,P OR 1, PRINT AND PLOT DATA IN UPPER, MIDDLE,
C     OR LOWER THIRD OF ARRAY K; =, FOLLOWED BY 1,2, OR 3 OR ANY COMB-
C     INATION OF 1,2, AND 3, PRINT AND PLOT SMOOTHED SPECTRUM MINUS
C     CONTRIBUTIONS OF 1=H2O, 2=HNO2, 3=HNO3.
   54 IF(KK.EQ.'T ') GO TO 27
      IF(KK.EQ.'R ') GO TO 26
```

```
      IF(KK.EQ.'E ') GO TO 400
      IF(KK.EQ.'K ') ITI=5
      IF(KK.EQ.'C ') ITI=9
      IF(KK.EQ.'S ') LSS=LL(1)
      IF(KK.EQ.'B ') LB=LL(1)
      IF(KK.EQ.'N ') N204=LL(1)
      M=0
      IF(KK.EQ.'O ') GO TO 80
      M=400
      IF(KK.EQ.'P ') GO TO 80
      M=800
      IF(KK.EQ.'I ') GO TO 80
      IF(KK.NE.'- ') GO TO 52
C
C     CALCULATE PROPORTIONALITY CONSTANTS AND SUBTRACT REFERENCE SPECTRA
      CORR1H=Z(1)*SLWR1H/SLWR*PATH/PATH1H*PPM1H/PPM1HR
      CORR2H=Z(2)*SLWR2H/SLWR*PATH/PATH2H*PPM2H/PPM2HR
      CORR3H=Z(3)*SLWR3H/SLWR*PATH/PATH3H*PPM3H/PPM3HR
      DO 60 I=1,NN
      IF(K(I+400).LT.0) GO TO 58
      K(I+800)=K(I+400)-CORR1H*K1H(I)-CORR2H*K2H(I)-CORR3H*K3H(I)
      GO TO 60
   58 K(I+800)=-1
   60 CONTINUE
C
C     M1 AND M2 SET RANGE IN ARRY K.  KT COUNTS SPECTRA OUTPUT.
   80 M1=M+1
      M2=M+NN
      KT=KT+1
C
C     OUTPUT TO PRINTER
      IF(KSS(3).EQ.1.OR.LSS.EQ.3) GO TO 90
      DO 81 I=1,3
   81 IDATE(I)=DATE(I)
      WRITE(LP,4)(IDATE(I),I=1,3),KT
    4 FORMAT(1H1,I2,1H/,I2,1H/,I2,I4)
      IF(ID2.EQ.0) GO TO 82
      WRITE(LP,12)ID1,ID2
   12 FORMAT(11H SAMPLE NO,,I8,I3)
      GO TO 83
   82 WRITE(LP,13)ID1
   13 FORMAT(11H SAMPLE NO,,I8)
   83 IF(N2C4.EQ.0) GO TO 84
      A1=KS(1)*.001*SLWR3
      A2=KS(2)*.001*SLWR3
      WRITE(LP,14)NBG,SLWR3,LAST,INIT,PATH3,SLWR,NM(1,LINT),A1,PATH,NM(2
     1,LINT),A2,TEMP,PPM3,PPM3H,FLG(IZ3+1),PPM2H,FLG(IZ2+1),PPM1H,FLG(IZ
     21+1),CALC2H,CALC1H
   14 FORMAT(31X,14HN2O3  ANALYSIS/12H INST, BKGD,,I9,11X,3HS/W,F10.1/
     111H SCAN RANGE,I9,1H-,I4,/X,4HCELL,F10.2/11H SAMPLE S/W,F10.1,11X,
     22HA(,I4,1H),F9.4/12H SAMPLE CELL,F10.2,10X,2HA(,I4,1H),F9.4/13H SA
     3MPLE TEMP,,F8.1,11X,3HPPM,F12.0//F10.0,10H  PPM HNO3,A4/F10.0,10H
     4 PPM HNO2,A4/F10.0,9H  PPM H2O,A4/F10.0,29H  PPM HNO2 FROM EQUIL.
```

```
     5CONST,/F10.0,29H  PPM H2O  FROM EQUIL, CONST.//)
      GO TO 86
   84 WRITE(LP,15)NBG,LAST,INIT,SLWR,PATH,TEMP
   15 FORMAT(12H INST, BKGD,,I9/11H SCAN RANGE,I9,1H-,I4/11H SAMPLE S/W,
     1F10.1/12H SAMPLE CELL,F10.2/13H SAMPLE TEMP,,F8.1///)
   86 IF(KK,EQ,'O ') WRITE(LP,87)
      IF(KK,EQ,'I ') WRITE(LP,88)
   87 FORMAT(11H UNSMOOTHED/)
   88 FORMAT(9H RAW DATA/)
      WRITE(LP,16)(K(I),I=M1,M2)
   16 FORMAT(10I5/)
C
C     OUTPUT TO PAPER TAPE PUNCH,
   90 IF(KSS(4),EQ,0) GO TO 100
      WRITE(ITP,5)NN,LAST,IDNO,SLWR,PATH,TEMP,PPM3,(K(I),I=M1,M2)
C
C
C     OUTPUT TO PLOTTER,
  100 IF(KSS(2),EQ,1,OR,LSS,EQ,2) GO TO 52
      IF(IFLAG,EQ,1,AND,(KK,EQ,'= ',OR,LB,EQ,1)) GO TO 212
      IXL=(NN+19)/20
      CALL INPLOT(1,=1,,IXL+1,,IXL+2,,=,58,10,42)
      IFLAG=1
      DO 170 I=0,IXL
      CALL NUMBER(I=,22,=,30,,14,2,*ING(10)*I+LAST,0,,=1)
  170 IF(I,EQ,IXL/2) CALL SYMBOL(I+,36,=,49,,21,LAB(1),0,,2)
      CALL DOPLOT(1,FLOAT(IXL),0,)
      DO 180 I=0,IXL
      X=IXL-I
      CALL DOPLOT(0,X,0,00)
      CALL DOPLOT(0,X,0,07)
  180 CALL DOPLOT(0,X,0,00)
      DO 200 I=1,10
      CALL NUMBER(=,37,I=,07,,14,SLWR*I/10,,0,,2)
  200 IF(I,EQ,5) CALL SYMBOL(=,50,5,36,,28,LAB(2),0,,2)
      CALL SYMBOL(,50,9,5,,14,LAB(3),0,,2)
      CALL NUMBER(1,25,9,5,,14,FLOAT(ID1),0,,=1)
      IF(ID2,EQ,0) GO TO 201
      CALL NUMBER(1,61,9,5,,14,FLOAT(ID2),0,,=1)
  201 IF(M,EQ,0) CALL SYMBOL(2,10,9,5,,14,LAB(4),0,,4)
      CALL SYMBOL(,50,9,25,,14,LAB(5),0,,4)
      CALL NUMBER(1,25,9,25,,14,PATH,0,,2)
      X=0,50
      DO 202 I=1,3
      CALL NUMBER(X,9,0,,14,DATE(I),0,,=1)
      X=X+,12
      IF(I,EQ,3) GO TO 204
      IF(DATE(I),GT,9,0) X=X+,12
      CALL SYMBOL(X,9,0,,14,LAB(18),0,,2)
  202 X=X+,12
  204 IF(N204,EQ,0) GO TO 208
      CALL SYMBOL(1,20,8,52,,14,LAB(6),0,,4)
      CALL DOPLOT(1,1,10,8,50)
```

```
      CALL DUPLOT(0.1,64.8,50)
      DO 206 I=0,3
      CALL SYMBOL(0.50,8,25-I*0.25,.14,LAB(2*I+10),0.,4)
  206 CALL NUMBER(1.20,8.25-I*0.25,.14,PPM(I+1),0.,-1)
  208 CALL DUPLOT(1.0,.10,)
      DO 210 I=0,10
      Y=10-I
      CALL DUPLOT(0.0,00,Y)
      CALL DUPLOT(0.0,07,Y)
  210 CALL DUPLOT(0.0,00,Y)
  212 IC=1
      DO 220 J=1,NN
      I=NN+1-J+M
      IF(K(I),NE,-1) GO TO 216
  215 IC=1
      GO TO 220
  216 CALL DUPLOT(IC,J/20,,K(I)/100,)
      IC=0
  220 CONTINUE
      IF(LB,LG,1) GO TO 52
      Y=0,80-0.20*YJP
      CALL NUMBER(FLOAT(IXL),Y,,14,FLOAT(KT),0.,-1)
      CALL SYMBOL(IXL+,25,Y,,14,KK,0,,2)
      DO 230 I=1,J
  230 IF(LL(I),GT,0) CALL NUMBER(IXL+,25+,12*I,Y,,14,FLOAT(LL(I)),0,,-1)
      YJP=YJP+1,0
      GO TO 52
  400 IF(IFLAG,EQ,1) CALL TMPLOT(1)
      CALL EXIT
      END
      EOF
```

III. A Computer Program for Calculating Absorptivities from Relative Absorbances Measured in a Closed System

The computer program described herein is written in General Electric time-sharing BASIC. The documentation which precedes it contains numbers enclosed in [ ] which refer to the line numbers in the program list.

Lines [10 thru 39] represent typical input data. Line [10] contains the number of sets of spectral data to follow, and the concentration (ppm.) of HNO_3 in the oxygenated sample. Line [20] contains the matrix of relative absorbances of the three standard reference spectra. Lines [31 thru 39] contain the nine sets of data, each consisting of ppm. of NO and the absorbances (x 10^3) at the analytical wavelengths, 1404, 1448, and 1470 nm.

Lines [120-150] read and compute the inverse of the matrix of relative absorbances. The loop [160-290] reads a set of spectral data, computes the specific absorbances, B(I), and then multiplies by the inverse matrix to get the a·c values which are stored in the array K(L,I). Line [300] permits the operator to choose any combination of three of the sets of input data which are then used to compute a set of absorptivities in lines [310-450]. Loop [310-360] sets up the matrix of coefficients, the A's, and constant vectors, B(I). These simultaneous equations are inverted in [380] and the values of the three absorptivities are calculated and printed in loops [400-450]. This process is repeated for as many ternary combinations as desired.

```
N204          08:56       02/12/70

10 DATA 9,9161
20 DATA 1,0,.006,.006,1,.118,0,.043,1
31 DATA 7,5,106,863
32 DATA 748,183,73,486
33 DATA 1524,215,71,406
34 DATA 2805,251,87,270
35 DATA 19838,245,146,187
36 DATA 35071,215,172,150
37 DATA 55081,187,200,136
38 DATA 76062,156,213,130
39 DATA 100964,114,211,126
100 DIM K(10,3),D(3)
110 READ P,Q
120 MAT K=ZER(P,3)
130 MATREAD A(3,3)
140 MAT C=ZER(3,3)
150 MAT C=INV(A)
160 FOR L=1 TO P
170 READ N(L)
180 FOR I=1 TO 3
190 READ B(I)
200 LET B(I)=B(I)/5850*(1-N(L)/1E6)
210 NEXT I
220 MAT D=ZER
230 FOR I=1 TO 3
240 FOR J=1 TO 3
250 LET D(I)=D(I)+C(I,J)*B(J)
260 NEXT J
270 LET K(L,I)=D(I)
280 NEXT I
290 NEXT L
300 INPUT M(1),M(2),M(3)
310 FOR I=1 TO 3
320 LET B(I)=Q*(1-N(M(I))/1E6)/63
330 LET A(I,1)=K(M(I),1)*2
340 LET A(I,2)=K(M(I),2)
350 LET A(I,3)=K(M(I),3)
360 NEXT I
370 MAT C=ZER(3,3)
380 MAT C=INV(A)
390 MAT D=ZER
400 FOR I=1 TO 3
410 FOR J=1 TO 3
420 LET D(I)=D(I)+C(I,J)*B(J)
430 NEXT J
440 PRINT 1/D(I)
450 NEXT I
460 PRINT
470 GO TO 300
480 END

READY
```

IV. Composition of the System N_2O_4-N_2O_3-HNO_3-HNO_2-H_2O as a Function of Temperature. A Computational Algorithm and Computer Program

The concentrations in ppm. of N_2O_4, HNO_2, and H_2O at -10° and of N_2O_4, N_2O_3, HNO_3, HNO_2, and H_2O at some other temperature (e.g., 70°) can be calculated from the ppm. of N_2O_3 (as NO) and HNO_3 at -10° in the following manner. The square brackets enclose line numbers or other references to the computer program (at the end of this appendix) which performs the computations described in the text. The program is written in General Electric time-sharing BASIC.

Let P_2 and P_3 be the ppm. of NO and HNO_3 and t the temperature (°C.) for which the composition of the system is to be predicted [160-170].

In general, let P_i and N_i be ppm. and moles/liter, respectively, of all components, where:

1 = N_2O_4

2 = NO

3 = HNO_3

4 = HNO_2

5 = H_2O

$N_1 \sim (10^6-P_2-P_3)$ x density x $10^{-3}/92$, where 92 is molecular weight of N_2O_4 and density is computed from the empirical relationship

$$d = 1.4927 - 2.235 \times 10^{-3} \times t - 2.75 \times 10^{-6} \times t^2 \qquad [150]$$

for a temperature of -10° [180]. Similarly,

$$N_2 = P_2 \times d \times 10^{-3}/30 \qquad [200]$$

$$N_3 = P_3 \times d \times 10^{-3}/63 \qquad [210]$$

The number of moles/liter of H_2O and HNO_2 are calculated from the -10° equilibrium constants

$$N_5 = \frac{N_3^2 \times N_2}{K_3 \times N_1^{1.5}} \qquad [220]$$

where equilibrium constant K_3 at -10° is 4.70×10^{-4}.

$$N_4 = \frac{K_1 \times N_1 \times N_5}{N_3} \qquad [230]$$

where $K_1 = 2.93 \times 10^{-3}$

The ppm. at -10° of HNO_2, H_2O, and N_2O_4 are

$$P_4 = N_4 \times 47 \times 10^3/d$$

$$P_5 = N_5 \times 18 \times 10^3/d$$

$$P_1 = 10^6 - \text{sum of } P_{2-5} \qquad [240\text{-}260]$$

Initial values for the calculation of composition at temperature t are derived from the P_i above. Moles/liter are calculated using the density at t [270-320]. The equilibrium constants at t are calculated from:

$$K_1 = \exp. \left(\frac{-3204}{273.16 + t} + 6.34314 \right)$$

$$K_2 = \exp. \left(\frac{407}{273.16 + t} + 0.618657 \right) \qquad [330,340]$$

Let X = No. of moles/liter of reactants which are transferred as the equilibrium shifts. Then

$$E_1 = \frac{(N_3 + X)\ (N_4 + X)}{(N_1 - X)\ (N_5 - X)}$$

X must fall in the range 0 to N_5 because N_5 decreases with increasing temperature. [350,360, Note: X(1) and X(3) are the limits of the iterative search] X is set initially at the upper limit and E_1 is calculated and compared to K_1. The next guess for X is

$$X = \frac{X(1) + X(3)}{2}$$

For successive guesses, either the upper or the lower limit is set equal to X before the new X is calculated. The choice of which limit is changed is determined by the sign of $E_1 - K_1$ so as to keep the true X inside the new half interval. [510, 520, Note: the use of X(1) and X(3) is dictated by programming considerations in these lines.] The process is repeated until

$$\left|\frac{E_1 - K_1}{K_1}\right| < 0.01$$

The new found composition is used as initial values [430-460] in the second equilibrium represented by

$$E_2 = \frac{(N_3 + X/3)\ (N_2 + 2X/3)^2\ (N_5 + X/3)}{(N_4 - X)^3}$$

X must be in the range 0 to N_4. A procedure strictly analogous to that above is used to find a new X [470-530]. Now the new composition [550-580] is used as initial values in the first equilibrium. This alternation is continued until X is found to be less than 10^{-6} moles/liter [420,540] at which point the iteration is halted and the concentrations in moles/liter are again converted to ppm. [The computer program prints the original -10° composition in line 670 and the predicted composition in line 810. Lines 600 to 820 also include the conversion functions and appropriate decimal fraction truncation for the printed output.]

Input format for the program is as follows:

10 DATA t, label, P_2, P_3, ---

where t = temperature (C.), label is a sample identifier, and P_2 and P_3 are ppm. of NO and HNO_3. Additional sets of "label, P_2, P_3" data may be appended. Line numbers up to 99 may be used.

```
100 PRINT"PPM OF:       N2O4          NO          HNO3       HNO2          H2O"
110 PRINT
120 LET R1=0.01
130 LET R2=0.01
140 LET R3=1E-6
150 DEF FND(T)=1.4927-2.235E-3*T-2.75E-6*T↑2
160 READ T
170 READ D$,P2,P3
180 LET D=FND(-10)
190 LET N1=(1E6-P2-P3)*D/92E3
200 LET N2=P2*D/30E3
210 LET N3=P3*D/63E3
220 LET N5=N3↑2*N2/(4.6978E-4*N1↑1.5)
230 LET N4=2.9323E-3*N1*N5/N3
240 LET P4=N4*47E3/D
250 LET P5=N5*18E3/D
260 LET P1=INT(1E6-P2-P3-P4-P5+0.5)
270 LET D=FND(T)
280 LET N1=P1*D/92E3
290 LET N2=P2*D/30E3
300 LET N3=P3*D/63E3
310 LET N4=P4*D/47E3
320 LET N5=P5*D/18E3
330 LET K1=EXP(-3204/(273.16+T)+6.34314)
340 LET K2=EXP(  407/(273.166+T)+0.618657)
350 LET X(1)=0
360 LET X=X(3)=N5-1E-20
370 LET E1=(N3+X)*(N4+X)/((N1-X)*(N5-X))
380 IF ABS(E1-K1)/K1 <R1 THEN 420
390 LET X(SGN(E1-K1)+2)=X
400 LET X=(X(1)+X(3))/2
410 GO TO 370
420 IF X<R3 THEN 600
430 LET N4=N4+X
440 LET N1=N1-X
450 LET N5=N5-X
460 LET N3=N3+X
470 LET X(1)=0
480 LET X=X(3)=N4-1E-20
490 LET E2=(N3+X/3)*(N2+2*X/3)↑2*(N5+X/3)/(N4-X)↑3
500 IF ABS(E2-K2)/K2 <R2 THEN 540
510 LET X(SGN(E2-K2)+2)=X
520 LET X=(X(1)+X(3))/2
530 GO TO 490
540 IF X<R3 THEN 600
550 LET N3=N3+X/3
560 LET N2=N2+2*X/3
570 LET N5=N5+X/3
580 LET N4=N4-X
590 GO TO 350
```

```
600 PRINT D$
610 LET P4=INT(P4*100+0.5)/100
620 IF P4<10 THEN 640
630 LET P4=INT(P4+0.5)
640 LET P5=INT(P5*100+0.5)/100
650 IF P5<10 THEN 670
660 LET P5=INT(P5+0.5)
670 PRINT"AT -10";TAB(11);P1;TAB(23);P2;TAB(33);P3;TAB(43);P4;TAB(53);P5
680 LET P1=INT(N1*92E3/D+0.5)
690 LET P2=INT(N2*30E5/D+0.5)/100
700 IF P2<10 THEN 720
710 LET P2=INT(P2+0.5)
720 LET P3=INT(N3*63E5/D+0.5)/100
730 IF P3<10 THEN 750
740 LET P3=INT(P3+0.5)
750 LET P4=INT(N4*47E5/D+0.5)/100
760 IF P4<10 THEN 780
770 LET P4=INT(P4+0.5)
780 LET P5=INT(N5*18E5/D+0.5)/100
790 IF P5<10 THEN 810
800 LET P5=INT(P5+0.5)
810 PRINT"AT ";T;TAB(11);P1;TAB(23);P2;TAB(33);P3;TAB(43);P4;TAB(53);P5
820 PRINT
830 GO TO 170
9999 END
```

V. Tape Format Work Sheets

SET PEN TO 0.000, PUNCH. TAPE SHOULD READ .002 TO .004
SET PEN TO 0.990, PUNCH. TAPE SHOULD READ .992 TO .994 (LAST DIGIT SHOULD BE WITHIN .001 OF LAST DIGIT OF ZERO PUNCH.)
ADJUSTMENTS ARE MADE WITH "HI" & "LO" POTS ON CARY RECORDER
RECHECK BOTH .000 AND .990 READINGS AFTER ADJUSTING EITHER POT

INSTRUMENT/CELL BACKGROUND

MANUAL (+)

BACKGROUND NUMBER (DATE MO/DA/YR)	X X/X X/X X/0
ZERO POINT (DIFFERENCE FROM 0.000	0 0 0 0.0 0 X
STARTING WAVELENGTH (IN NANOMETERS)	0 0 0 X X X X
STOPPING WAVELENGTH (IN NANOMETERS)	0 0 0 X X X X

TAPE FEED

AUTO (A)

DATA POINTS (BACKGROUND MUST BE RUN USING 0.1 SLIDEWIRE)

TAPE FEED

SAMPLE

MAN (+)	DATE (MO/DA/YR)	XXX/X X/X X/0
MAN (+)	ID NO. (NOTEBOOK PAGE AND NUMBER)	0 0 X X X-X X
MAN (+)	N203 SLIDEWIRE (1.0 OR 0.1)	0 0 0 0 0 X.X
MAN (+)	N203 CELL PATH IN CM	0 0 0 X X.X X
MAN (+)	N203 WAVELENGTH RANGE CODE*	0 0 0 0 0 0 X
AUTO (A)	N203 ABSORBANCE (LONG WAVELENGTH)	----------
AUTO (A)	N203 ABSORBANCE (SHORT WAVELENGTH)	----------
MAN (+)	NIR SLIDEWIRE (1.0 OR 0.1)	0 0 0 0 0 X.X
MAN (+)	NIR CELL PATHLENGTH IN CM	0 0 0 X X.X X
MAN (+)	TEMP IN DEG. C (PLACE "1" IN LEFT COL. FOR NEGATIVE TEMPS)	X 0 0 0 X X.X

TAPE FEED

AUTO (A)

DATA POINTS

TAPE FEED

FOR SAMPLE SERIES WHERE ONLY ID AND N203 ABSORBANCES CHANGE, THE FOLLOWING SAMPLE FORMAT CAN BE USED AFTER THE FIRST SAMPLE COMPLETE HEADING ABOVE HAS BEEN ENTERED.

MAN (+)	NEW FORMAT CODE	0 0 0 0 0 0 1
MAN (+)	ID NO. (NOTEBOOK PAGE AND NUMBER)	0 0 X X X-X X
AUTO (A)	N203 ABSORBANCE (LONG WAVELENGTH)	----------
AUTO (A)	N203 ABSORBANCE (SHORT WAVELENGTH)	----------

TAPE FEED

AUTO (A)

DATA POINTS

TAPE FEED

N203 WAVELENGTH RANGE		CODE *
LONG	SHORT	
900	700	1
900	850	2
950	920	3
1140	1070	4
1140	1110	5
1270	1220	6

THE N204 COMPUTER PROGRAM CAN BE USED TO SUBTRACT ANY DIGITIZED SPECTRUM FROM ANY OTHER OVER ANY WAVELENGTH RANGE AT PUNCH INTERVALS OF 1 PUNCH PER 1, 2, 5, OR 10 NANOMETERS PROVIDING THE TOTAL NUMBER OF DATA PUNCHES DOES NOT EXCEED 400

ALIGN TAPE PUNCH WITH PEN SETTINGS AT 0.000 AND 0.990 AS DESCRIBED ON REVERSE SIDE OF INSTRUCTION SHEET.

USE THE FOLLOWING FORMAT AS HEADING FOR THE DIGITIZED SPECTRUM WHICH IS TO BE SUBTRACTED FROM ANOTHER SPECTRUM.

MANUAL (+)

DATE (MO/DA/YR)	X X/X X/X X 0
ZERO POINT (DIFFERENCE FROM 0.000)	0 0 0 0.0 0 X
STARTING WAVELENGTH (IN NANOMETERS)	0 0 0 X X X X
STOPPING WAVELENGTH (IN NANOMETERS)	0 0 0 X X X X
PUNCH INTERVAL (1 PUNCH PER 1, 2, 5, OR 10 NM)	0 0 0 0 0 X X

TAPE FEED

AUTO (A)

DATA POINTS

TAPE FEED

USE THE FOLLOWING FORMAT AS HEADING FOR ALL DIGITIZED SPECTRA FROM WHICH THE ORIGINAL SPECTRUM IS TO BE SUBTRACTED.

MANUAL (+)

DATE (MO/DA/YR)	X X/X X/X X 0
ID NO. (NOTEBOOK PAGE AND NUMBER)	0 0 X X X-X X
SLIDEWIRE (1.0 OR 0.1)	0 0 0 0 0 X.X
PATHLENGTH (IN CM)	0 0 0 X X.X X
TEMPERATURE IN DEG. C (PLACE "1" IN LEFT COL FOR -)	X 0 0 0 X X.X

TAPE FEED

AUTO (A)

DATA POINTS

TAPE FEED

VI. Thermal Dissociation Study Procedures

The procedures used in this work on the NO_2 dissociation were essentially the same as those used in previous work on the determination of dissolved oxygen in N_2O_4 by gas chromatography (1).

Apparatus

With the exception of the items noted below, the arrangement of major components and the other auxiliary equipment was the same as in previous work.

(1) The plastic glove bag was replaced by a Plexiglas dry box 36" x 24" x 20", Greiner Scientific Corporation, Cat. No. 41-905 with accessories (Bellows Gloves - 41-907-31, Clamping Rings - 41-907-32, Air Lock - 41-905-02, and Interior Cover - 41-905-04). The box was fitted with a two-outlet receptacle for internal power.

(2) Gas Chromatograph Inlet - The center top of the 1/4 in. O.D. stainless "Tee" (400-3TTM) was connected on the external side of the dry box to a 400-71-4 bulkhead female connector. The Swagelok side of the connector was located inside the dry box and the nut fitted with a silicone septum.

(3) Sample Syringe, Gas - 2 ml. capacity - Pressure-Lok available from Precision Sampling Corporation, P.O. Box 15119, Baton Rouge, Louisiana, 70815, Cat. No. 010034. The barrel was wrapped with a heater constructed of 18-gauge Nichrome insulated wire. The heating wire was then wrapped with glass tape in which was imbedded an iron-constantan thermocouple. The heater was connected to a variable voltage supply located inside the

dry box; the thermocouple was connected to a Fisher 0° to 500°C. pyrometer, Model 32-J.

(4) Needles - 6 inch to fit 010034 2 cc. gas syringe Cat. No. 913055 (0.028 in. O.D., 0.008 in. I.D.). The length must be specified in the order.

(5) Valve - Ball - Whitey Cat. No. 4354. Specify stainless steel body.

(6) Valve - Forged Body - Whitey Cat. No. IRS4. Specify stainless steel body.

(7) Heating Mantle - Cylindrical - A. H. Thomas, Philadelphia, Pa., Cat. No. 6136-A50.

(8) Temperature Controller - West Guardsman - Model J 0-300°C.

(9) Pressure Vessel - The pressure vessel with constant temperature jacket is diagrammed in Figure 24. Construction of the inner vessel (volume 537 $cm.^3$) was of 304L stainless steel; the outer jacket of aluminum. The outer jacket was removed when installing the heating mantle. The cap was threaded and could be removed from the cell body so that test U-bend specimens could be inserted. The pressure plate top was sealed with a Teflon gasket, pressed into place by means of eight screws. The ball valve (#4354) was connected to the 1/4-inch O.D. stainless tube in the top of the pressure vessel. A septum was attached to the other end of the ball valve by means of a 1/4 inch to 3/16 inch Swagelok reducer (300-R-4).

A forged body needle valve (IRS4) was attached to one of the 1/4 inch O.D. tubes projecting from the bottom. The other was plugged. The 1/8 inch NPT hole in the top cover was fitted with a 1/8 inch NPT pipe to 1/8 inch Swagelok BT fitting. The thermocouple (item 10 below) was positioned so that the tip was somewhat less than half-way into the vessel cavity.

(10) Thermocouple - Thermoelectric Ceramocouple Type 5J-1120L for temperature range 70 to 100°C. Calibrated versus NBS thermometers at ice, room, and boiling temperatures using a L&N portable potentiometer.

(11) Septa - Teflon backed silicone - Sheet stock F-138, from Canton Bio-Medical Products, P.O. Box 154, Swarthmore, Pa. 19801. Septa were cut with a No. 4 cork borer to fit the 3/16 inch nut of the sampling port.

(12) Dropping funnel - 250 ml. with Teflon stopcock - Kontes No. K-632280. Drip tip was cut off so that the end fitted snuggly into the 3/8 inch end of a 3/8 to 1/4 inch Swagelok reducing union. The glass to metal seal was made with 3/8 inch Teflon front and back ferrules. This assembly was fitted with a "cardboard box condenser" and attached to the pressure vessel filling apparatus as shown in Figure 23.

(13) Magnetic stirrer.

Reagents

For all the described work, RR N_2O_4 (Mil-O-26539B) from the one-ton cylinder was loaded into a 2-liter pressure bomb equipped with bottom dip tube and vent. Hercules designation X15927-12-2.

Gas Chromatographic Conditions

Temperatures: Column, injection port, and detector all at ambient (24-27°C.).

Filament Current: 350 milliamperes

Carrier Gas: Helium at 40 milliliters/minute

Cylinder Pressure: 40 psi.

Recorder: Brown, 1 mv., 1 sec. full scale

Chart Speed: 40 inches/hour

Cold Trap: Dry ice - isopropanol (∿-72°C.)

Calibration

The method for oxygen calibration was the same as used in previous work (1). Recalibration with the current equipment yielded a response factor, F, of 0.358 ± 0.021 micrograms $O_2/cm.^2$ over the range of 1.4 to 13.9 micrograms of oxygen. A value of 0.334 $\mu g./cm.^2$ was obtained previously. And

$$F = \frac{\mu g.\ O_2}{O_2 \text{ Peak Area } (cm.^2)} = \frac{\mu l.\ (air) \times 81.81}{\text{Area} \times T\ ^\circ K} \qquad (1)$$

Procedure

Connect the 250 ml. dropping funnel and the pressure vessel to the vacuum flushing system as shown in Figure 22. With valve A closed, precool the dropping funnel by placing dry ice in the cardboard box condenser. Begin eliminating air from the cell and adjoining parts by alternately flushing with helium (open valve C) and evacuating. (Close valve (C) and stopcock (A).) Repeat the evacuation and purging operations five times, ending with the system filled with helium.

From the N_2O_4 reservoir, add about 250 ml. to the cool dropping funnel. Open valve (B) and crack valve (C) to equalize the pressure. Open stopcock (A) and allow the N_2O_4 to slowly enter the cell. When the funnel is empty close valves (B) and (C) and disconnect the cell from the filling system. CAUTION: N_2O_4 remains in the lines to the cell. Loosen the connection only enough so that the excess liquid can be caught in a container. After the excess liquid N_2O_4 has drained off, purge the filling lines by slowly admitting a flow of purge gas.

Place the loaded pressure vessel onto a magnetic stirrer located inside the dry box and begin stirring the cell contents. Set the temperature controller at 25°C. Load the dry box with syringes, tools, fittings, and other accessories necessary for sampling and other operations.

Close the open end of the dry box and begin purging the box with nitrogen. This operation requires 3 to 5 hours or at least until the level has reached a value of about 0.05 to 0.02% where

$$\% O_2 = \frac{\text{Partial Pressure of Oxygen, } P_{O_2}}{\text{Total Pressure, } P_T} \qquad (2)$$

or $\% O_2 = P_{O_2} \times 100$

where P_T is 1 atmosphere, and PO_2 is given by equation 3 below.

When the desired level of oxygen has been reached, attach the 1/4" to 3/16" reducer to the exit end of the ball valve (C) on the pressure vessel. Loosely attach the 3/16" nut containing a Teflon-backed septum. Vent a small amount of N_2O_4 to purge the fitting and turn the nut finger tight.

With the gas chromatograph set at the proper operating conditions, and with the syringe heater set at the internal temperature of the pressure vessel, sample the vapor phase over the N_2O_4 by opening the ball valve (C) and inserting a 6-inch needle attached to a Pressure Lok gas syringe through the septum so that the needle penetrates below the top of the pressure vessel. Flush the syringe several times with N_2O_4 vapor and then withdraw the desired sample size. Isolate the sample in the syringe barrel with the nosepiece valve of the syringe. Withdraw the needle and insert it into the back of the gas chromatograph inlet. Compress the sample slightly and then open the nosepiece valve. Inject the sample. Close valve C.

Obtain the chromatogram and measure the oxygen peak area by triangulation. Calculate the partial pressure of oxygen, P_{O_2}, in atmosphere above the liquid N_2O_4 from

$$P_{O_2} \quad \frac{F \times A_{O_2} \times R \times T \times 10^{-6} \text{ (atm.)}}{M \times V'} \tag{3}$$

where A_{O_2} = area of the oxygen peak in $cm.^2$

R = gas constant = 0.0821 l-atm./°K-mole

T = absolute temperature, °K

M = molecular weight of oxygen = 32

V' = sample or aliquot size in liters

Relate the oxygen in the gas phase, P_{O_2}, to the concentration in liquid phase through the equation

$$\text{ppm. } O_2 \text{ (liquid)} = \frac{K \times 32 \text{ g. } O_2/\text{mole}}{92 \text{ g. } N_2O_4/\text{mole}} \times 10^6 \frac{\mu\text{g.}}{\text{g.}} \times P_{O_2} \qquad (4)$$

where K is the reciprocal Henry's Law constant. Now K varies with temperature and may be calculated as a function of such change from the relation (2).

$$-2.303\ RT \log K = 664 + 11.46T \qquad (5)$$

where R is given as 1.97 cal./°K-mole.

VII. Measurement of Electrical Properties

A. Volume Resistivity

1. Equipment

a. Cary Model 31 Vibrating Reed Electrometer

b. Keithley Model 241 Regulated High Voltage Supply

c. Balsbaugh 2TN50 Liquid Measuring Cell

2. Conditions

a. Applied voltage: 100 volts D.C.

b. Electrification time: 60 sec.

c. Temperature: 24°C.

d. Relative humidity: 50%

3. Procedure

ASTM D 257

B. Dielectric Constant and Dissipation Factor

1. Equipment

a. General Radio 716C Bridge - Freq. 100 H_z to 100K H_z

b. General Radio 716 CSI Bridge - Freq. 1 meg. H_z

c. Balsbaugh 2TN50 Liquid Measuring Cell

2. Conditions

a. Temperature: 24°C.

b. Relative humidity: 50%

3. Procedure

ASTM D 150 (substitution method)

VIII. Stress Corrosion Cracking Tests with Additives

A number of SCC runs were made with RR N_2O_4 (X15927-12-2) containing varying amounts of selected additives. Test media (RR N_2O_4 + additive) were prepared as follows:

(1) Test Medium Mix Tank (TMM), ca. 1750 ml. capacity, was partially filled with RR N_2O_4, shaken and emptied.

(2) Emptied TMM Tank was purged with N_2 for ca. 1 minute at 5 psig.

(3) Dip tube assembly was removed.

(4) Desired amount of additive was weighed and transferred to TMM Tank.

(5) Replaced dip tube assembly immediately after the additive was charged to TMM Tank.

(6) Filled TMM Tank completely with RR N_2O_4 (2300-2400 g.).

(7) TMM Tank and contents were shaken and allowed to stand overnight.

The following SCC test procedure was utilized for all additive runs:

(1) Specimens were prepared as described in the First Quarterly Report.

(2) Specimens were inserted into the new 6" test cell, sealed, and cell pressure tested with 130 psig. N_2.

(3) The test cell was filled from a TMM Tank, shaken slightly and emptied.

(4) The test cell was filled again from the same TMM Tank and then disconnected.

(5) Approximately 80-100 ml. of test medium was removed from the cell.

(6) Test cell was sealed and inserted in an oven at 165-170°F. for ca. 72 hrs.

(7) After exposure cells were cooled down in the oven (1-2 hours).

(8) Content was purged from the cool test cells directly into analytical sample bulbs and/or directly into the waste N_2O_4 hold tank.

(9) Test cell was purged for ca. 1 minute with N_2.

(10) Test cell was opened, specimens removed and washed with water before examination for cracking both visually and with the aid of a microscope.

IX. Standard Procedure for Filling SCC Test Cell with RR N_2O_4 or G8 N_2O_4

General

(1) Check all valves to make sure they are turned off.

(2) Nitrogen valve at the cylinder, (14) should be on at all times with ca. 2-6 psig.

(3) See Figure 31 for line and piping schematic.

(4) Open valves (1), (4) and (6).

Procedure

(1) If MIL-SPEC N_2 is desired, close (14) and open (15).

(2) Connect lower valve on cell to the desired N_2O_4 system, and higher valve to the waste line.

(3) Open valves (23), (24), (10), (30) in the waste line and the higher valve on the test cell in the order listed to vent the N_2 from the cell.

(4) If connected to the RR N_2O_4 delivery system:

a. Open lower valve of the test cell.

b. Open valves (25), (12), (29). Blow N_2 through the test cell (T.C.) for ca. 15 seconds.

c. Close lower valve on T.C. for 15 seconds.

d. Open lower valve on T.C. for 15 seconds.

e. Close valves (25), (12) and (29).

If connected to the G8 N_2O_4 delivery system:

a. Open lower valve on T.C.

b. Open valves (7) and (28). Blow N_2 through the T.C. for ca. 15 seconds.

c. Close lower valve on T.C. for 15 seconds.

d. Open lower valve on T.C. for 15 seconds.

e. Close valves (7) and (28).

(5) Filling of the Test Cell.

a. Open valves (13) and (29) for RR N_2O_4 or open (8) and (28) for G8 N_2O_4. Let the delivery valve remain open until liquid N_2O_4 can be seen running down the sight glass of the waste receiver.

b. Close valves (13) and (29) (RR) or valves (8) and (28) (G8).

c. Close both T.C. valves - gently rock the T.C. several times.

d. Close valve (10).

e. Open - both T.C. valves, either (21) and (29) (RR) or (18) and (28) (G8), also (9). This will empty the T.C. under N_2 pressure. Allow these valves to remain open until no N_2O_4 can be seen running down the sight glass of the waste receiver.

f. Close valves (21) and (29) (RR) or valves (18) and (28) (G8), also close (9).

g. Open valves (10), (13), (29) (RR) or (8), (28) (G8). Remain open until liquid N_2O_4 can be seen running down the sight glass of the waste receiver.

h. Close valves (13) (RR) or (8) (G8), both T.C. valves. Gently rock T.C. back and forth several times.

i. Close valve (10).

j. Open both T.C. valves, (21) and (29) (RR) or valves (18) and (28) (G8), (9). Remain open until liquid N_2O_4 stops running down the sight glass on the waste receiver.

k. Close valves (21) (RR) or (18) (G8) and (9).

l. Open valves (10). Then open either valve (13) (RR) or (8) (G8). Remain open until liquid N_2O_4 can be seen running down the sight glass of the waste receiver.

m. Close either (13) and (29) (RR) or (8) and (28) (G8), and both valves of the T.C.

n. Disconnect at both valves of the T.C. Cell is now full.

(6) After experiments are completed, all valves, except the waste receiver vent valve (23) must be turned off.

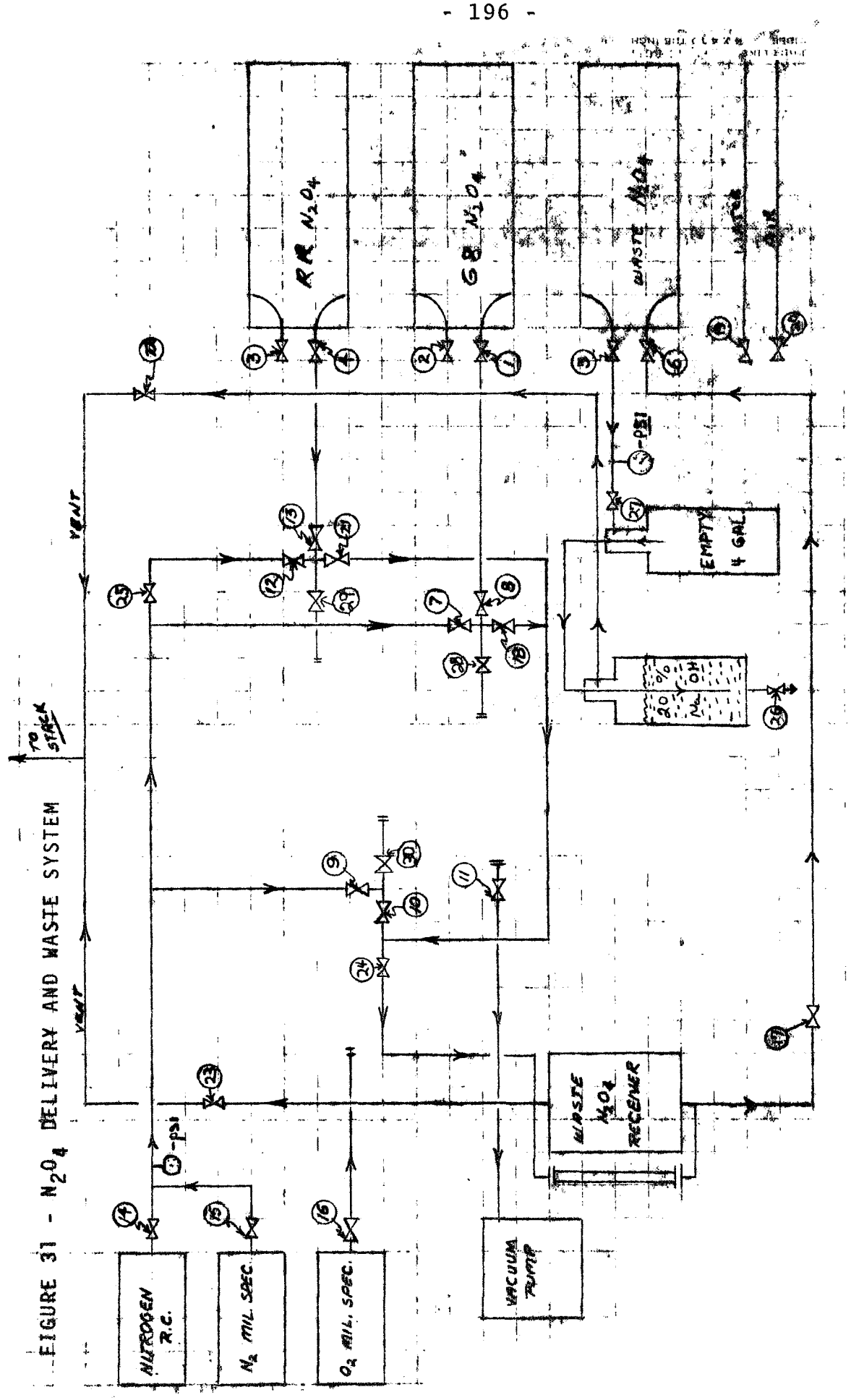

FIGURE 31 - N_2O_4 DELIVERY AND WASTE SYSTEM

Designations - Figure 31

(1) RR N_2O_4 discharge

(2) RR N_2O_4 vent

(3) G8 N_2O_4 vent

(4) G8 N_2O_4 discharge

(5) Waste N_2O_4 vent

(6) Waste N_2O_4 charging

(7) Nitrogen - G8 delivery system

(8) G8 N_2O_4 delivery

(9) Nitrogen - waste receiving line

(10) Waste N_2O_4 - receiving line

(11) Vacuum line to vacuum pump

(12) Nitrogen - RR delivery system

(13) RR N_2O_4 delivery

(14) R.C. nitrogen source

(15) Mil. Spec. nitrogen source (supply has been depleted)

(16) Mil. Spec. oxygen source (supply has been depleted)

(17) Waste line - between waste receiver and pump

(18) Waste line - from G8 system

(19) R.C. tap water

(20) R.C. air

(21) Waste line from RR delivery system

(22) Waste cylinder vent line

(23) Waste receiver vent

(24) Waste line to waste receiver

(25) Nitrogen - By-pass control

(26) Caustic scrubber, discharge

(27) Waste cylinder vent line

(28) Cell connecting valve

(29) Cell connecting valve

(30) Cell connecting valve

X. Standard Procedure for Filling SCC Test Cell and Sampling Test Medium from 1.7 Liter Test Medium Mix Tank

General

(1) Check all valves to make sure they are closed.

(2) Connect test cell, TMM tank and sample cylinder as shown in Figure 32.

Procedure

(1) Open valves (U) and (42). This will vent the N_2 in the test cell down to atmospheric temperature.

(2) Close valves (U) and (42).

(3) Using a heat gun, warm the 1.7 liter TMM tank.

(4) Open valves (38), (43), (L), (U), (40), and (41).

(5) As soon as liquid N_2O_4 appears at the opening of valve (41), close valve (41) and open (42).

(6) As soon as liquid N_2O_4 can be seen flowing through the Teflon tubing between valves (U) and (42), close valves (42), (U), (L), (40), (43), and (38).

(7) Disconnect Teflon tubing at valve (38) and connect to valve (37).

(8) Warm the test cell and the 90 ml. sampling bomb with a heat gun for 2-3 minutes (just above 72°F.).

(9) Open valves (L), (40), (43) and (37); this will permit the test cell and the sampling to discharge all the liquid N_2O_4 into the waste hold tank.

(10) When liquid N_2O_4 is no longer flowing down the sight glass of the waste hold tank, close valves (L), (40), (43), and (37).

(11) Disconnect Teflon tubing at valve (37) and connect at valve (38).

(12) Warm the 1.7 ml. TMM tank using a heat gun.

(13) As soon as liquid N_2O_4 can be seen flowing through the Teflon tubing between valves (U) and (42), close (42), (U), (L), (43), and (38).

(14) Warm the test cell with a heat gun and open valves (L), (40) and (41).

(15) As soon as liquid N_2O_4 starts flowing out of valve (41), close valves (41), (40) and (L). The sampling bomb is now full of the test medium.

(16) Disconnect sample cylinder at valve (40).

(17) Disconnect the test cell at valves (U), and (L). The test cell is now ready to be put in the oven; it has vapor space of 90 ml.

(18) If a vapor space is desired in the sample cylinder, warm with a heat gun, while holding the cylinder perpendicular to a 316 SS beaker, open the lower valve and drain off desired volume of N_2O_4.

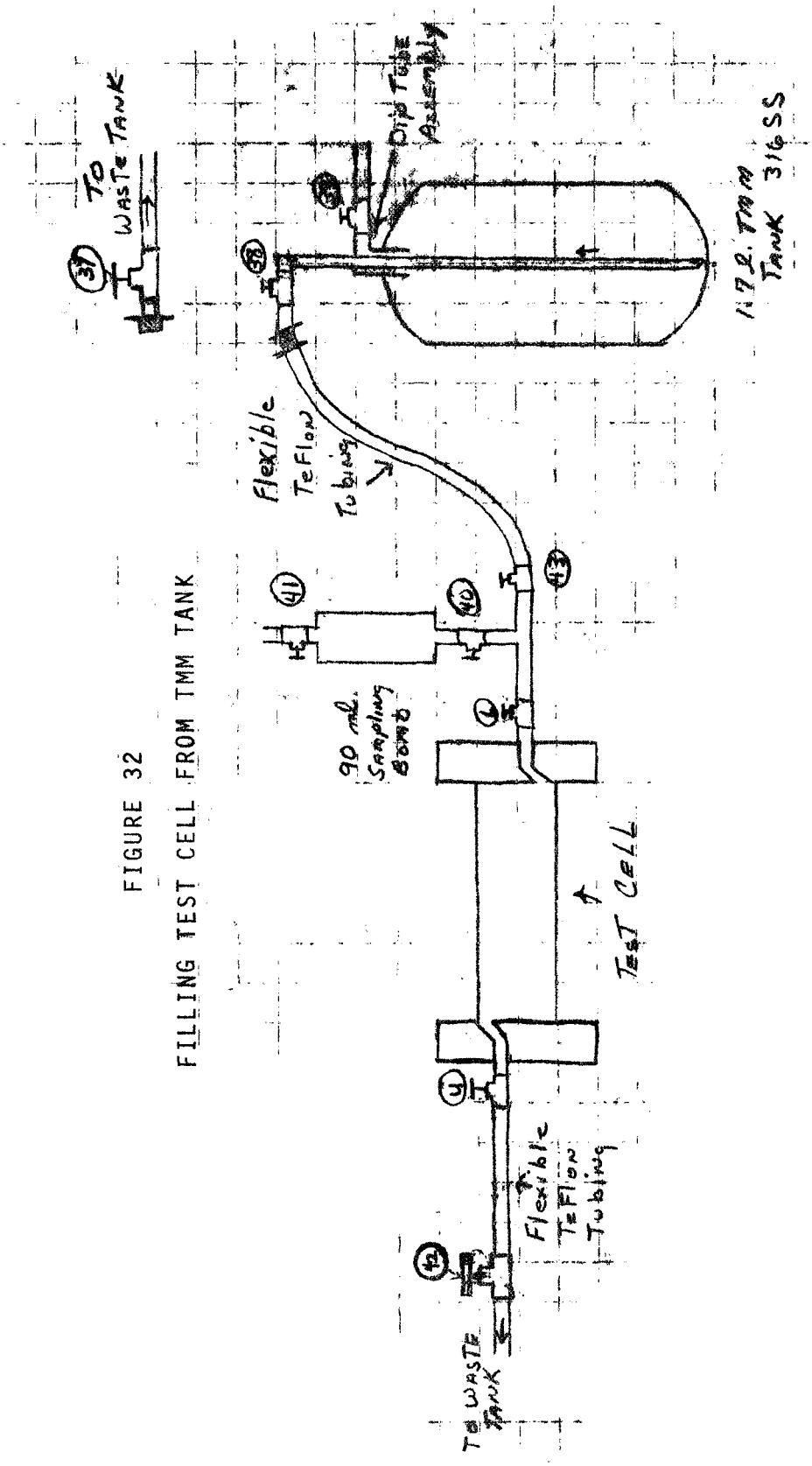

FIGURE 32

FILLING TEST CELL FROM TMM TANK

Designations - Figure 32

(U) Upper valve - test cell

(L) Lower valve - test cell

(37) N_2O_4 waste receiving line

(38) N_2O_4 delivery valve - dip tube assembly

(39) Purging and venting valve - dip tube assembly

(40) Lower valve - sample cylinder

(41) Upper valve - sample cylinder

(42) N_2O_4 waste receiving line

(43) N_2O_4 delivery valve - delivery line

All valves are 316 stainless steel Swagelok Hoke valves.

XI. Standard Procedure for Filling SCC Test Cell with Deprotonated N_2O_4 from a Nine (9) Gallon Bomb

General

(1) Check all valves to be sure they are closed.

(2) Insert fresh filter (Gelman Type A, glass fiber, 25 mm.) in holder.

(3) Double check all Swagelok connections.

Procedure

(1) Pressurize 9-gal. bomb by connecting valve (35) to a nitrogen source and pressurizing to 30-40 psig.

(2) Disconnect nitrogen source from valve (35) after pressurization.

(3) Connect test cell as shown in Figure 33.

(4) Open valve (U) to vent test cell nitrogen pressure to atmosphere.

(5) Open valves (34), (32), and (L).

(6) Close valve (U) when liquid N_2O_4 appears at this valve. All waste from this valve can be caught in a 316 stainless steel beaker.

(7) Close valves (32), (34), and (L).

(8) Open valves (31) and (L). Warm test cell with a heat gun until the N_2O_4 stops flowing down the sight glass of the waste receiver (see Fig. 31).

(9) Close valve (31).

(10) Open valves (34), (32), and (U), and repeat steps F and G.

(11) Open valves (31), (32), and (33). This will force N_2 through the Millipore filter to clear out excess N_2O_4.

(12) Disconnect test cell at valve (L).

(13) Cell is now full of N_2O_4 mixture that was in the nine (9) gallon bomb.

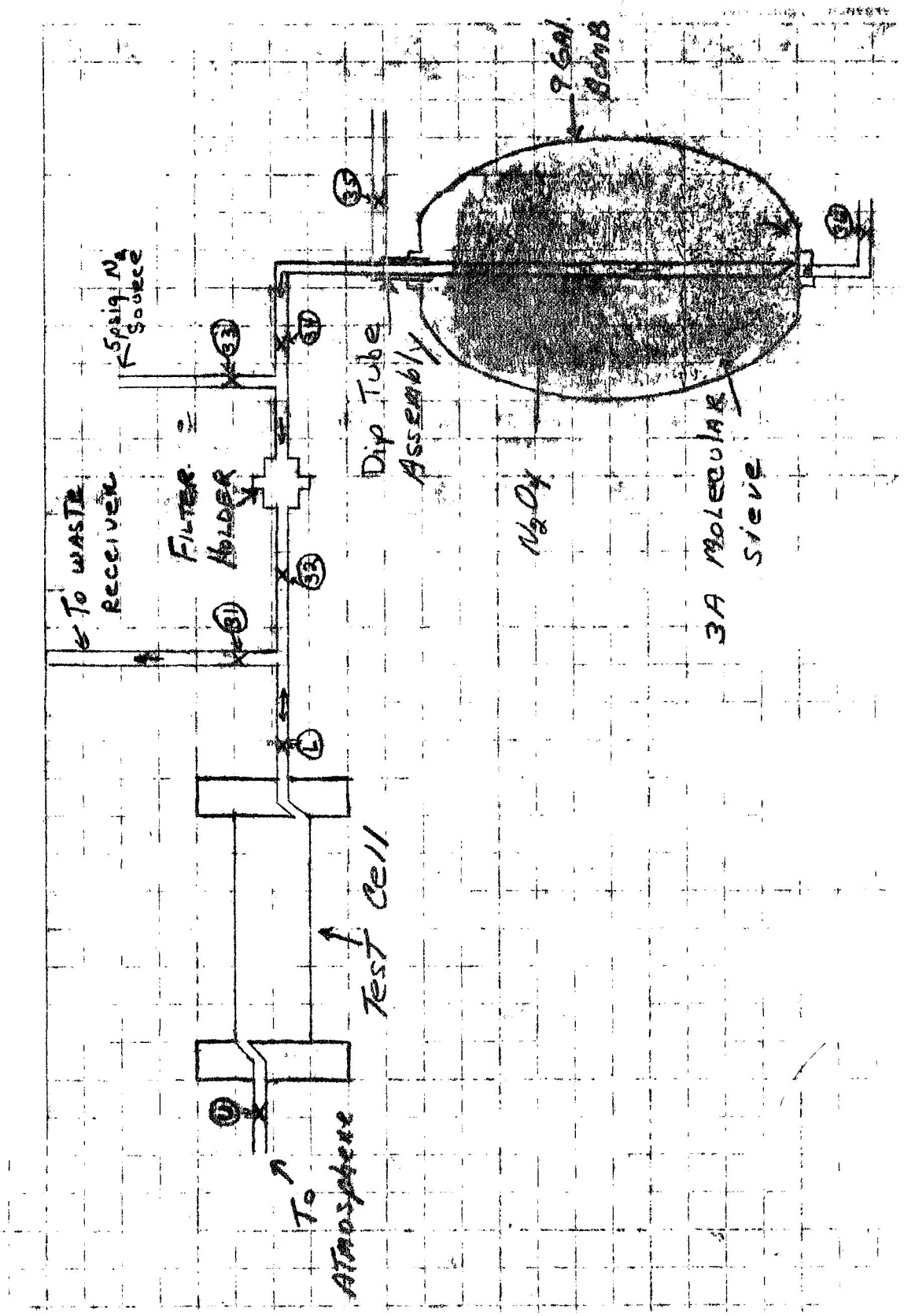

FIGURE 33 - FILLING TEST CELL FROM 9-GALLON BOMB

Designations - Figure 33

(U) Upper valve - test cell

(L) Lower valve - test cell

(31) N_2O_4 waste receiving line

(32) N_2O_4 delivery valve

(33) Nitrogen purging valve - 5 psig.

(34) N_2O_4 delivery valve - dip tube assembly

(35) Purging and venting valve - dip tube assembly

(36) 9-Gallon bomb drain

All valves are 316 stainless steel Hoke valves, Type 3212G6Y.